Technische Universität München
Fakultät für Medizin

Novel Therapeutic Strategies to Treat Hutchinson-Gilford Progeria Syndrome (HGPS)

Rouven Jakob Arnold

Vollständiger Abdruck der von der Fakultät für Medizin der Technischen Universität München zur Erlangung des akademischen Grades eines Doktors der Naturwissenschaften (Dr. rer. nat.) genehmigten Dissertation.

Vorsitz:	Prof. Dr. Carsten Schmid-Weber
Prüfer*innen der Dissertation:	1. Prof. Dr. Karima Djabali
	2. apl. Prof. Dr. Johannes Beckers

Die Dissertattion wurde am 15.12.2021 bei der Technischen Universität München eingereicht und durch die Fakultät für Medizin am 12.07.2022 angenommen.

Everything is theoretically impossible, until it is done.

Robert A. Heinlein

Abstract

Hutchinson-Gilford progeria syndrome (HGPS) is an ultra-rare pediatric premature aging disorder caused by a heterozygous *de novo* point mutation in the *LMNA* gene. Most cases carry the G608G mutation within exon 11, leading to aberrant splicing and production of a truncated prelamin A protein called progerin. Accumulation of progerin causes various toxic effects in HGPS cells and induces premature senescence at the cellular and organismal level. Tragically, children that suffer from this condition develop many age-associated diseases as well, including atherosclerosis, arthritis, alopecia and lipodystrophy. By performing a text mining analysis of the scientific literature, we found 17 genes associated with all conditions mentioned above. 14 of these were linked to the JAK-STAT signaling pathway, which was overactivated in senescent HGPS and control cultures. Inhibition of JAK1/2-STAT1/3 signaling with baricitinib restored cellular homeostasis, delayed senescence and decreased proinflammatory markers. In addition, we combined baricitinib with the farnesyltransferase inhibitor (FTI) lonafarnib, the only Food and Drug Administration-approved drug for HGPS. Although lonafarnib irrefutably ameliorates HGPS and extends patients' lifespan, it is not a cure. In this study, we found several FTI-induced cellular side effects, including genomic instability that causes binucleated and donut-shaped nuclei. Furthermore, we identified cytosolic DNA fragments caused by FTI and linked these fragments to an activated cGAS-STING-STAT1 signaling axis. Combination treatment not only prevented the activation of this inflammatory pathway, but also reduced progerin levels and improved nuclear shape, proteostasis as well as mitochondrial function. Thus, our findings support the combination of baricitinib and lonafarnib that might provide an opportunity to reduce FTI-induced cellular toxicity and is a valuable therapeutic strategy for children with HGPS and possibly other age-related conditions.

Zusammenfassung

Das Hutchinson-Gilford-Progerie-Syndrom (HGPS) ist eine äußerst seltene pädiatrische Erkrankung des vorzeitigen Alterns, die durch eine heterozygote *de novo*-Punktmutation im *LMNA*-Gen verursacht wird. In den meisten Fällen liegt eine G608G-Mutation im Exon 11 vor, die zu verändertem Spleißen und zur Produktion eines verkürzten Prelamin-A-Proteins namens Progerin führt. Die Anhäufung von Progerin verursacht toxische Wirkungen in HGPS-Zellen und führt zu vorzeitiger Seneszenz auf zellulärer und organismischer Ebene. Tragischerweise entwickeln Kinder mit HGPS viele altersbedingte Krankheiten, darunter Atherosklerose, Arthritis, Alopezie und Lipodystrophie. Durch eine Text-Mining-Analyse der wissenschaftlichen Literatur fanden wir 17 Gene, die mit allen oben genannten Krankheiten in Verbindung stehen. 14 davon waren mit dem JAK-STAT-Signalweg assoziiert, der in seneszenten HGPS- und Kontrollkulturen eine deutlich erhöhte Aktivität zeigte. Die Hemmung des JAK1/2-STAT1/3-Signalwegs mit Baricitinib stellte die zelluläre Homöostase wieder her, verzögerte die Seneszenz und verringerte proinflammatorische Marker. Darüber hinaus kombinierten wir Baricitinib mit dem Farnesyltransferase-Inhibitor (FTI) Lonafarnib, dem einzigen von der Food and Drug Administration zugelassenen Medikament für HGPS. Obwohl Lonafarnib HGPS unwiderlegbar verbessert und die Lebenserwartung der Patienten verlängert, ist es keine Heilung. In dieser Studie fanden wir mehrere FTI-induzierte zelluläre Nebenwirkungen, darunter genomische Instabilität, die zu zweikernigen und donutförmigen Zellkernen führt. Außerdem identifizierten wir durch FTI verursachte zytosolische DNA-Fragmente und brachten diese Fragmente mit einer aktivierten cGAS-STING-STAT1-Signalachse in Verbindung. Die Kombinationsbehandlung verhinderte nicht nur die Aktivierung dieses Entzündungsweges, sondern verringerte auch den Progerinspiegel und verbesserte die Kernform, die Proteostase sowie die Mitochondrienfunktion. Somit unterstützen unsere Ergebnisse die Kombination von Baricitinib und Lonafarnib, die eine Möglichkeit zur Verringerung der FTI-induzierten zellulären Toxizität bieten könnte und eine wertvolle therapeutische Strategie für Kinder mit HGPS und möglicherweise anderen altersbedingten Erkrankungen darstellt.

ACKNOWLEDGEMENTS

First and foremost, I would like to thank Professor Dr. Djabali for giving me the opportunity to do this research project in her lab. She had excellent ideas and tips regarding my research and I am very thankful for her professional and personal support. Without her outstanding guidance this work would not have been possible. In our inspiring discussions, your insightful feedback pushed me to be a better scientist.

A special gratitude to Professor Dr. Beckers from the institute of experimental genetics at the Helmholtz Zentrum for supervising me. Our discussions helped greatly in the planning of my project.

I am also very grateful to Professor Dr. Görlach, who was an excellent mentor. During my master studies and until today, I could rely on her guidance, advice and kind support that motivated me to pursue an academic career. I will not forget her encouraging way of thinking about research and, of course, our ski field trips.

Many thanks to the Progeria Research Foundation, patients and their families that provided the foundation for our research and helped broaden my knowledge about progeria by hosting a fantastic progeria meeting.

In addition, I appreciate the help of all our collaborators, without whom this work would not be possible. Many thanks to the group of Vicente Andrés García at CNIC. Thanks to Beatriz Julia Dorado de la Corte, Rosa María Nevado García, María Jesús Andrés Manzano, Cristina González Gómez and all other members for their warm hospitality during my research visit. I also want to thank all members of the institute of experimental genetics at the Helmholtz Zentrum, especially Lore Becker and Gerhard Przemeck for their kind help.

I would also like to acknowledge the never-ending patience and helpful hints of the whole epigenetics of aging team. I had a great time in the laboratory. With a special mention to Chang Liu, Jennifer Röhrl, Elena Vehns, Farah Najdi, Hannah Randl, Peter Krüger, Eva Lederer, Xiang Lu and Leithe Budel. Thank you for this good atmosphere, which always motivated me very much in everyday laboratory practice. Thanks for your great support!

I am also thankful to all my friends for their encouragement, especially Oli and Nina for their effort in helping me and finalizing this work.

Furthermore, I must express my very profound gratitude to my parents Ingrid and Walter, as well as to my brothers Daniel and Benjamin for providing me with unfailing support and continuous encouragement throughout my years of study and through the process of researching and writing this thesis. This accomplishment would not have been possible without them. Thank you.

Last but not least, I would like to express my most immense gratitude to my wife Sonja. Thank you that you are there for me every single day. I can’t imagine how I could have done this work without you. Thank you for always believing in me!

Thanks for all your encouragement.

Publication list

The following publications were published during the doctoral studies and are partly included in this thesis:

1. Liu C, Arnold R, Henriques G, Djabali K. Inhibition of JAK-STAT Signaling with Baricitinib Reduces Inflammation and Improves Cellular Homeostasis in Progeria Cells. Cells. 2019; 8(10):1276. https://doi.org/10.3390/cells8101276
2. Röhrl JM, Arnold R, Djabali K. Nuclear Pore Complexes Cluster in Dysmorphic Nuclei of Normal and Progeria Cells during Replicative Senescence. Cells. 2021; 10(1):153. https://doi.org/10.3390/cells10010153
3. Arnold R, Vehns E, Randl H, Djabali K. Baricitinib, a JAK-STAT Inhibitor, Reduces the Cellular Toxicity of the Farnesyltransferase Inhibitor Lonafarnib in Progeria Cells. International Journal of Molecular Sciences. 2021; 22(14):7474. https://doi.org/10.3390/ijms22147474

Table of Contents

1 INTRODUCTION

1.1 Aging Research

In our modern society with its increasing proportion of elderly citizens, the latest developments in aging research and the battle against age-related diseases are rapidly gaining importance. A long and high-quality life has always been strived for and is continuously pushed into new spheres, especially in this current era with the latest technology and new medical approaches. For centuries, the life expectancy of humankind remained almost the same until, since the beginning of industrialization and the associated advances in hygiene and medicine, it has continued to rise. On average, people today live to be between 77.91 years (male children) and 82.81 years (female children) in Germany (Kontis et al. 2017). The development towards longevity inevitably leads to new challenges in medicine. For instance, various diseases promote premature aging, such as Hutchinson-Gilford progeria syndrome (HGPS, OMIN 176670), mandibuloacral dysplasia (MAD, OMIN 248370), restrictive dermopathy (RD, OMIN 275210) or Malouf syndrome (OMIN 212112) (Eriksson et al. 2003; Motegi et al. 2014; Novelli et al. 2002). These genetic diseases show different aspects of the aging phenotype and thus contrast with unimodal age-related diseases that primarily display only one aspect, such as Alzheimer's disease (OMIN 104300). In particular, the HGPS syndrome has recently gained a leading role as a model for early aging (Harhouri et al. 2018; Coutinho et al. 2009).

The process of aging, which is often defined as time-dependent functional decline, is thought to be one of the most complex mechanisms to be observed in the human body as well as in all other living organisms. Although aging research has been conducted for centuries, a new phase can be recognized since the 1970s when long-lived strains

of Caenorhabditis elegans were isolated for the first time, based on the tremendous increase in knowledge of molecular biology (Klass 1983). Today, there are many theories on the origin and course of aging, which ultimately led to the *Hallmarks of Aging* in 2013 (López-Otín et al. 2013). In total, nine hallmarks were defined: 1. Altered intercellular communication, 2. Stem cell exhaustion, 3. Cellular senescence, 4. Mitochondrial dysfunction, 5. Deregulated nutrient sensing, 6. Loss of proteostasis, 7. Epigenetic alterations, 8. Telomere attrition, and 9. Genomic instability. It is important to note that all hallmarks are linked by extensive interactions and that improvements of one can affect others (López-Otín et al. 2013). Undoubtedly, further insights will be gained in the near future by the tremendous development of next-generation sequencing and *in vivo* studies such as the *International Mouse Phenotyping Consortium (IMPC)* (Gundry und Vijg 2012; Magalhães et al. 2010; Dickinson et al. 2016). Systems biology approaches are likely to become increasingly important, since the interconnectivity is crucial to the hallmarks and different micro and macro environments extending to the whole organism.

1.2 Cellular Senescence

Senescence is a state of permanent cell cycle arrest. Initially, it was considered a tumor suppressor mechanism that occurs when cells experience oncogenic stress (Campisi und Di d'Adda Fagagna 2007). However, today, the causes and phenotypes of senescence are highly variable and heterogeneous, and contrary to the idea of growth arrest, they are associated with both degenerative and hyperplastic pathologies of aging, including cancer (Campisi 2013). Accompanied by an excessive accumulation of senescent cells is a proinflammatory milieu that ultimately leads to the cells' deleterious functions (Campisi 2013). Stimuli that lead to senescence include

replicative senescence, DNA damage-induced senescence, oncogene-induced senescence, oxidative stress-induced senescence, chemotherapy-induced senescence, mitochondrial dysfunction-associated senescence, epigenetically induced senescence and paracrine senescence (Muñoz-Espín und Serrano 2014). Despite these multi-factorial causes, two major pathways have been identified to establish and maintain senescence: The p53/p21 and the p16 pathways, both leading to downstream activation of the RB protein and subsequent cell cycle arrest (Kumari und Jat 2021). In aging research, p16 and p21 are commonly used as senescence markers, but as described above, no characteristic is exclusive to the senescent state. In general, the presence of senescence is identified by several markers. An enlarged cell body and flattened morphology is a characteristic, which can easily be evaluated by standard bright-field microscopy. Another hallmark of senescence is an increased lysosomal content and a pH-dependent ß-galactosidase activity, which, along with morphology, led to one of the first histochemical tests (Lee et al. 2006). Among all features, the senescence-associated secretory phenotype (SASP) is probably the most striking, as it has the potential to explain the role of senescence in aging and age-related pathologies (Campisi et al. 2011). The secretion of cytokines, chemokines and proteases is well defined, although its' expression can be heterogeneous (Hernandez-Segura et al. 2017). SASP factors can lead to negative consequences as well as being beneficial. It is hypothesized that short-term or sub-threshold occurrence of SASP results in stimulation of cell proliferation by different growth-regulated oncogenes (Yang et al. 2006a), amphiregulin (Bavik et al. 2006) or the WNT modulator secreted frizzled related protein 1 (SFRP1) (Elzi et al. 2012). Depending on the physiological context, it can also lead to angiogenesis (Coppé et al. 2006), epithelial-to-mesenchymal transition (Laberge et al. 2012), stem cell differentiation (Brack et al. 2007; Krtolica et al. 2011; Pricola et al. 2009; Zhang et al. 2011) and is probably

involved in many more cellular processes. However, when SASP signaling persists, many factors promote inflammation and become destructive to tissues and organs (Faget et al. 2019). Molecules such as IL-1α, CCL2, IL-6, IL-8, and IFN-ß contribute to this process, ultimately leading to a chronic inflammation state called ‘inflammaging’ (Franceschi und Campisi 2014). Given the harmful consequences of senescent cells, many therapies have now been developed to either delay senescence or remove the affected cells (Soto-Gamez und Demaria 2017).

1.3 Hutchinson-Gilford Progeria Syndrome (HGPS)

The Hutchinson-Gilford progeria syndrome (HGPS) is an extremely rare pediatric disease and serves as a model for rapid aging. It was first described by Jonathan Hutchinson in 1886 and independently by Hastings Gilford in 1904 (Hutchinson 1886; Gilford 1904). Only one in 2 million children are affected by this severe condition, which leads to an average death at ~14.7 years (Ullrich und Gordon 2015). Currently, there are approximately 150 known cases worldwide. The affected children are born healthy and develop first symptoms within the first year of life. These include typical signs of aging such as joint pain and stiffness (arthritis), loss of subcutaneous fat (lipodystrophy), progressive hair loss (alopecia) and vascular disease (Hennekam 2006). However, especially in non-industrialized countries, the syndrome is recognized at a very late stage or not at all. About 90% of HGPS subjects die from progressive atherosclerosis of the coronary and cerebrovascular arteries (Baker et al. 1981). Despite the presence of multifaceted premature aging, patients do not show cognitive deterioration, cancer, cataracts or Alzheimer’s disease (Ullrich und Gordon 2015). This can be explained by the fact that neurons do not undergo mitosis in later life, except for a few exceptions, and possibly also by the presence of a protective microRNA (miR-

9) (Nissan et al. 2012). In the majority of cases, the genetic cause of HGPS is linked to a *de novo* heterogeneous point mutation G608G in the *LMNA* gene (c1824C > T; GGC > GCT) (Eriksson et al. 2003; Sandre-Giovannoli et al. 2003). Inheritance of this mutation does not usually occur, as patients often do not reach the age of sexual maturity. Nevertheless, there are known cases of women with progeria who delivered healthy offspring (Corcoy et al. 1989). On the molecular level, the mutation leads to the production of a truncated prelamin A protein called progerin (Ullrich und Gordon 2015). This protein accumulates over time in HGPS cells but was also found in smaller quantaties in senescent cells of healthy individuals (McClintock et al. 2007; Scaffidi und Misteli 2006). Naturally, the *LMNA* gene translates into two lamin isoforms; prelamin A and lamin C. While prelamin A still undergoes several post-translational modifications to become functional, lamin C is already a mature protein (Adam und Goldman 2012) (Figure 1).

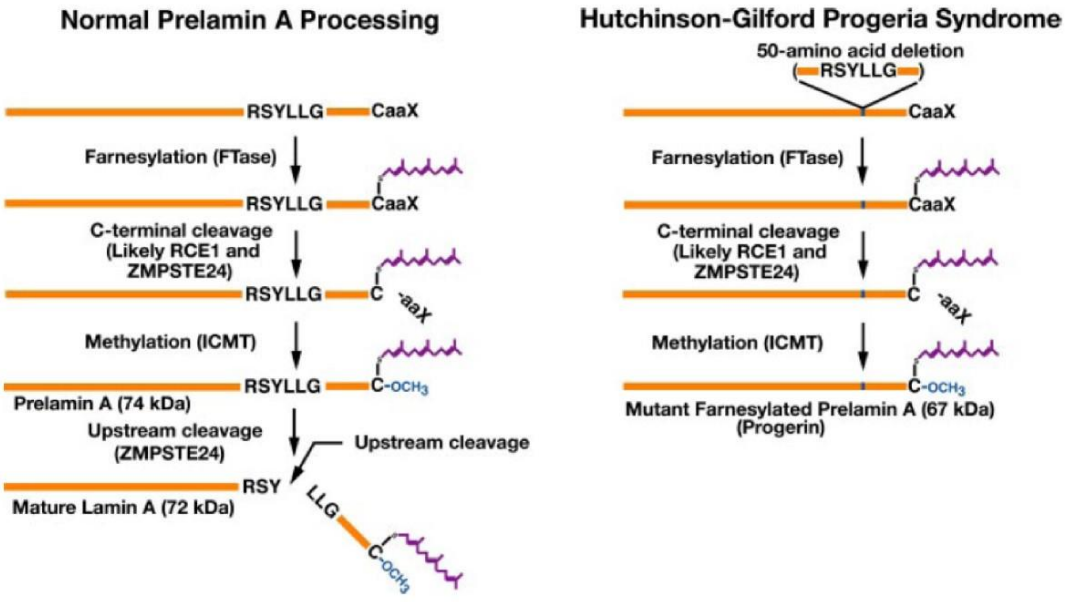

Figure 1: Prelamin A processing in normal and HGPS cells. Normal processing of prelamin A consisting of four steps and resulting in the final of mature lamin A. In HGPS, due to the 50-amino acid deletion, the cleavage site for ZMPSTE24 is missing, leading to progerin. (Coutinho et al. 2009)

First, prelamin A is farnesylated at the cysteine of the C-terminal CAAX motif, followed by proteolytic removal of the terminal tripeptide by RCE1 or Zmpste24. Subsequently, the terminal cysteine is carboxy-methylated and another internal proteolytic cleavage occurs, removing the last 15 coding amino acids that contain the two modifications by metallopeptidase ZMPSTE24 (Coutinho et al. 2009). Progerin lacks the endoproteolytic cleavage site and thus remains permanently farnesylated (Gordon et al. 2014a). In general, lamins are essential architectural proteins of the cell nucleus and act as intermediate filaments incorporated into the nuclear envelope (Dittmer und Misteli 2011). Three lamins (A, B and C) develop a protein network called lamina that is 20-50 nm wide and interacts with various proteins and chromatin (Aebi et al. 1986). Progerin disrupts the nuclear meshwork and triggers cellular alterations, including abnormal gene expression, DNA damage, mitochondrial dysfunction and premature senescence (Andrés und González 2009; Liu et al. 2019).

Nowadays, scientists have various *in vitro* and *in vivo* models available to investigate HGPS. Patient-derived cell lines such as fibroblasts, lymphoblasts or induced pluripotent stem cells (iPSCs), accessible through the Progeria Research Foundation, are crucial, as procurement is difficult due to the small number of patients (progeriaresearch.org). Cell cultures, however, are limited in their informative value, as they cannot determine the pharmacological profile of a drug for humans (Ghanemi 2015). Consequently, several *in vivo* models have been developed, including mouse and minipig models (Carrero et al. 2016; Dorado et al. 2019). Even though these models have different genetic backgrounds, they all show progerin expression, nuclear shape alterations and ultimately age prematurely (Piekarowicz et al. 2019). The first HGPS mouse model was generated by deletion of the endoprotease ZMPSTE24, leaving the carboxyl-terminal 15 amino acids attached, including the farnesyl moiety

(Pendás et al. 2002; Bergo et al. 2002). Although this approach does not accurately reflect the molecular mechanisms of HGPS, these mice exhibited many of the main symptoms of the disease, such as growth retardation, alopecia, cardiomyopathy, muscular weakness, bone fractures, lipodystrophy and premature death (Pendás et al. 2002; Bergo et al. 2002). Yang et al. created a different gene-targeted mouse model ($LMNA^{HG}$) that expresses only progerin, but not lamin A or C in homozygous mice (Yang et al. 2005; Yang et al. 2008a). Since the metallopeptidase ZMPSTE24 has other functions in the organism and the correct expression of 'normal' lamin A and C is also crucial, an alternative HGPS knock-in mouse model was generated to study the aberrant splicing of *LMNA* accurately, carrying the HGPS point mutation ($LMNA^{G608G}$) (Osorio et al. 2011). Similar to patients, these mice accumulate progerin during their lifetime, resulting in the main clinical manifestations of human HGPS (Osorio et al. 2011; Zaghini et al. 2020). Given the precise representation of the clinical picture, this model has proven to be the gold standard for drug development. Besides these three mouse models, others have been established but are not commonly used by researchers (Saxena und Kumar 2020). Recently, there has been a development that also pushes the research of HGPS much further; the production of the first large animal model of HGPS, namely a Yucatan minipig (Dorado et al. 2019). These minipigs were generated by CRISPR-Cas9 gene editing and have a knock-in mutation at *LMNA* c.1824C > T. Therefore, co-expression of progerin and lamin A/C can be observed. These animals exhibit severe growth retardation, lipodystrophy, skin and bone alterations, vascular disease, and die around puberty (Dorado et al. 2019). The vascular alterations are particularly relevant and can thus optimize preclinical research, as the system is much more similar to humans.

1.4 Therapeutic Strategies for HGPS Patients

Currently, there is no cure for HGPS. Following the identification of the gene responsible for HGPS in 2003, therapeutic approaches were rapidly developed (Eriksson et al. 2003; Sandre-Giovannoli et al. 2003). The first attempt was based on preventing the farnesylation step during post-translational modification of prelamin A, as it is the permanently attached farnesyl moiety that leads to defective incorporation into the nuclear envelope and consequently nuclear dysmorphism. Farnesyltransferase inhibitors (FTIs) were initially developed to treat cancer, as they inhibit the farnesylation of the oncogene Ras but also showed efficacy when treating HGPS fibroblasts (Wang et al. 2017a; Toth et al. 2005; Mallampalli et al. 2005; Glynn und Glover 2005; Capell et al. 2005). A detailed analysis about the use of FTIs in HGPS can be found in the next section. At the same time, it became clear that although FTIs therapeutic intervention showed some ameliorations, it does not cure the disease. Up until today, a broad spectrum of treatment strategies has been proposed and evaluated in progeria patient cells, mouse models and some even in clinical trials. These can be generally classified in strategies directly targeting the HGPS mutation, intervene with the different lamin A post-translational processing steps or progerin function and turnover (Strandgren et al. 2017). A frequently chosen approach in aging research is drug repurposing, which tests the efficacy of an established drug in other indications. This has the advantage that the safety of the application has already been demonstrated so that in any clinical trial, only the efficacy in the new indication needs to be proven. Figure 2 shows an overview of previous therapies and the mechanism of action (Saxena und Kumar 2020).

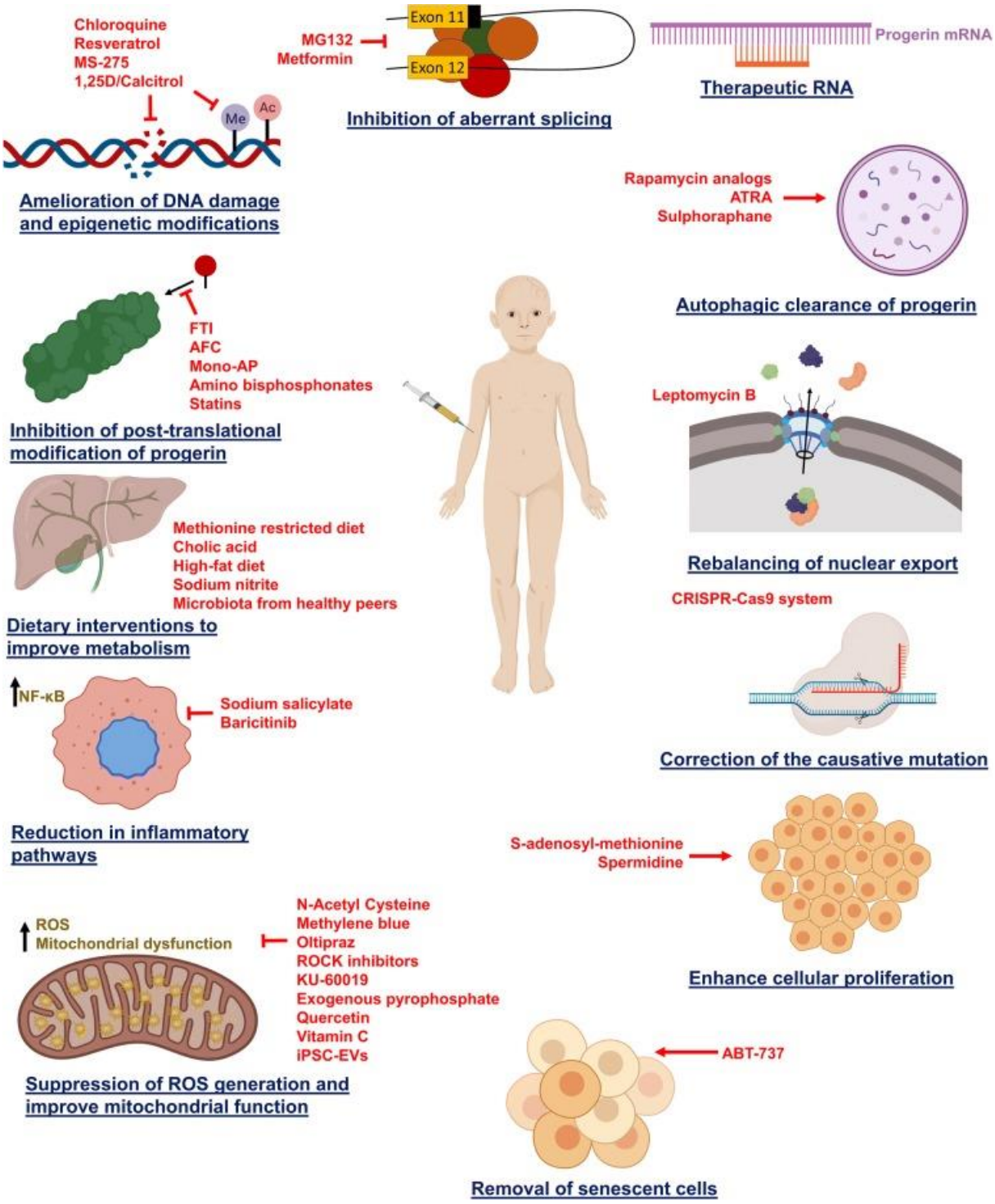

Figure 2: Therapeutic approaches for HGPS patients (Saxena und Kumar 2020)

Many of these therapies are still in a stage of intensive research with preliminary data only at the cellular level. However, three therapies reached the clinical phase, including FTI (lonafarnib), FTI (lonafarnib) + everolimus (rapamycin analog) and a ‘triple trial’

using FTI (lonafarnib), pravastatin and zoledronate (ClinicalTrials.gov, NCT03895528, NCT00879034, NCT02579044). In November 2020, lonafarnib, the first-ever progeria treatment, was granted FDA approval (Dhillon 2021). As illustrated in figure 2, the approaches are very diverse but can often improve only part of the clinical picture. It is therefore important to consider their advantages and disadvantages carefully. With regard to the multifactorial aging process, combination therapies are becoming more and more likely as they combine different mechanisms of action and thus can be more effective. Studies must clearly refute legitimate concerns such as incompatible pharmacokinetics or increased toxicity. Often, other positive characteristics such as increased compliance, synergy, reduced side effects and cost can be identified in this way.

1.4.1 Farnesyltransferase Inhibitor

Inhibiting the farnesyltransferase enzyme that adds the 15-carbon farnesyl lipid to prelamin A was the first step towards a successful treatment after the progerin protein had been identified. The concept of interfering with farnesylated prelamin A in HGPS cells gained support from studies of ZMPSTE24-/- mice carrying a single LMNA knockout allele (Fong et al. 2004). As expected, ZMPSTE24-/- mice accumulated toxic prelamin A responsible for the disease phenotypes shared with HGPS patients. Heterozygosity in the LMNA gene reduced prelamin A levels significantly. However, the intriguing result of this study was that the LMNA knockout allele abolished the disease phenotypes and misshapen nuclei typically found in ZMPSTE24-/- mice. In conclusion, the authors did not only suggest that the farnesylated prelamin A is toxic, but also that prelamin A-associated progeroid disorders might be ameliorated by blocking the farnesylation or lowering farnesylated prelamin A levels. So far, in all

studies, FTI resulted in less progerin being incorporated into the nuclear envelope, consequently ameliorating the nuclear envelopes' morphology (Capell et al. 2005; Capell und Collins 2006). Studies at the cellular and organismic level in HGPS models have shown significant improvements (Gordon et al. 2014a; Capell et al. 2005; Capell und Collins 2006; Glynn und Glover 2005; Toth et al. 2005; Yang et al. 2005; Mallampalli et al. 2005; Liu et al. 2006; Blondel et al. 2014; Constantinescu et al. 2010; Noda et al. 2015; Rivera-Torres et al. 2013; Gabriel et al. 2017; Bikkul et al. 2018; Verstraeten et al. 2011; Wang et al. 2012; Yang et al. 2006b; Yang et al. 2008a; Fong et al. 2006; Capell et al. 2008; Gordon et al. 2012; Gordon et al. 2018; Adam et al. 2013). In transiently transfected HeLa, HEK293, NIH 3T3 and human HGPS fibroblasts inhibiting farnesylation most notably restored nuclear shape, reduced nuclear blebbing and decreased progerin levels (Capell et al. 2005; Glynn und Glover 2005; Toth et al. 2005; Yang et al. 2005; Mallampalli et al. 2005; Liu et al. 2006). In addition, there were other positive indirect cellular effects of FTI, such as reduced osteogenic differentiation of HGPS-induced pluripotent stem cells (Blondel et al. 2014), enhanced DNA damage response (Constantinescu et al. 2010; Noda et al. 2015), amelioration of the mitochondrial function (Rivera-Torres et al. 2013), improved autophagy (Gabriel et al. 2017) and correction of the chromosome positioning in interphase HGPS cells (Bikkul et al. 2018). Nevertheless, prenylation is an important mechanism in cells that affects not only prelamin A but also the activity of other proteins such as lamin B, Rheb, rhodopsin kinase, Ras and others (Inglese et al. 1992; Wang und Casey 2016). In cancer therapy, for example, blocking farnesylation of the oncogene Ras was hoped to block the binding of activated Ras to the plasma membrane and thus stop the constitutive signaling activity responsible for uncontrolled cell division. It is therefore understandable that different deleterious effects of FTI have also been observed, such as induction of binucleated cells and abnormal donut-shaped nuclei (Verstraeten et al.

2011), delocalization of A- and B-type lamins away from the inner nuclear envelope (Wang et al. 2012; Adam et al. 2013), and a reduction in the proliferation rate (Gabriel et al. 2017). The advantages of the therapy were nonetheless dominant and FTI treatment in several HGPS mouse models has shown substantial improvements, including lifespan extension, improvement in bone mineralization and body weight, and reduction in cardiovascular defects (Yang et al. 2006b; Yang et al. 2008a; Fong et al. 2006; Capell et al. 2008). The promising results of the mouse studies strongly supported the use of the FTI lonafarnib for HGPS patients in the first clinical trial in 2007 (ClinicalTrials.gov, NCT00425607). In brief, patients showed prolonged mean survival time by 1.6 years, a modest increase in body weight, reduction in vascular stiffness, increased skeletal rigidity and some amelioration in sensorineural hearing and bone mineral density (Gordon et al. 2014a; Gordon et al. 2012; Gordon et al. 2018). In November 2020, lonafarnib became the first drug approved by the Food and Drug Administration (FDA) to treat progeria and progeroid laminopathies. However, in all models and under all treatment conditions, nonfarnesylated prelamin A and nonfarnesylated progerin accumulate and remain in the nucleus. Both proteins have been reported to be toxic and induce cardiomyopathy in mice (Yang et al. 2008b; Davies et al. 2010). FTI does not completely cure HGPS and requires further research to test new candidate drugs in combination with lonafarnib to further ameliorate HGPS conditions.

1.4.2 Inhibition of Inflammation Pathways

A common hypothesis on aging is that the balance between stressors and stress-buffering mechanisms is shifting towards a state of chronic damages resulting in an inflammatory response (Bektas et al. 2018). The development of chronic, low-grade

inflammation during aging has been termed as ‘inflammaging’ (Franceschi und Campisi 2014). It is now becoming evident that the expression of this pro-inflammatory phenotype is a major risk factor for many age-related diseases, including multimorbidity, physical and cognitive disability, frailty and death. At the cellular level, inflammation protects against infections; however, as inflammation becomes chronic, it usually leads to senescence or even apoptosis (Coppé et al. 2010). The prevention and therapy of diseases such as arteriosclerosis, Alzheimer’s disease, type 2 diabetes or HGPS with anti-inflammatory drugs are gaining more and more popularity (Tabas und Glass 2013; Piekarowicz et al. 2019). Although the results of many studies are very positive, targeting the exact pathway is difficult due to the variety of inflammatory regulation possibilities. In this work and other studies, NF- κB and JAK-STAT signaling have been identified as substantial inflammatory pathways implicated in HGPS (Liu et al. 2019; Griveau et al. 2020; Lai und Wong 2020; Osorio et al. 2012; Squarzoni et al. 2021).

The Janus kinase/signal transducers and activators of transcription (JAK-STAT) pathway is one of the pleiotropic cascades to maintain cellular homeostasis, implicated in processes such as cellular immunity, cell proliferation, differentiation, cell migration and apoptosis (Rawlings et al. 2004). The pathway serves as a principal mechanism for a wide range of cytokine-mediated signals and growth factors. Activation of the janus tyrosine kinases occur upon ligand-mediated receptor multimerization because two JAKs are brought into close proximity, allowing trans-phosphorylation. Subsequently, activated JAKs can phosphorylate seven different STAT proteins at their tyrosine residue near the C-terminus, permitting dimerization and the following translocation into the nucleus where they act as transcription factors (Rawlings et al. 2004). Many different JAK-STAT inhibitors are currently in preclinical development, in

various phases of clinical trials or already FDA approved to treat autoimmunity (Banerjee et al. 2017). In accordance with this concept, inhibition of JAK-STAT signaling was attributed to a decrease in senescence and SASP factors (Farr et al. 2017; Xu et al. 2016; Xu et al. 2015).

Just as JAK-STAT signaling, the nuclear factor kappa B (NF- κB) pathway is a central regulator that plays an essential role in the development of innate and adaptive immunity with hundreds of target genes of which many are pro-inflammatory, but others also promote cell survival and rebalance cellular homeostasis (Kumar et al. 2004). The NF- κB complex is a heterodimer of p50 and RelA held in the cytoplasm by the inhibitor-κBα (IkBα). Canonical activation involves phosphorylation of IkBα and subsequent proteasomal degradation, resulting in translocation of NF- κB into the nucleus where it binds to response elements as a transcriptional activator (Hayden und Ghosh 2008). Increased expression and the overactivation of NF- κB was described for normal aging and HGPS, leading to the induction of senescence and production of SASP factors (Kauppinen et al. 2013; Osorio et al. 2012; Wang et al. 2017b). To date, several HGPS studies demonstrated that both genetic and pharmacological inhibition of this pathway prevents age-associated features and extends lifespan *in vivo* (Osorio et al. 2012; Squarzoni et al. 2021). Due to the interconnectivity of these and other signaling pathways (e.g., Nrf2, UPR), inflammatory reactions will continue to receive much attention in diagnosis and therapy.

1.5 Aims of This Work

Studies in HGPS cell and mouse models have allowed a better understanding of the molecular and cellular mechanisms underlying progerin damage, identify therapeutic targets and test the efficacy of different treatments (Gordon et al. 2014b; Dorado und

Andrés 2017; Osorio et al. 2011). Although many therapeutic strategies have been developed, there is no complete cure as described in chapter 1.4. Therefore, the overall aim is to discover more efficient therapies to treat and eventually cure HGPS. This project started with a data mining approach, identifying dysregulated genes and underlying pathways in the four diseases commonly recognized as the main traits of HGPS (vascular disease, arthritis, alopecia, lipodystrophy). Furthermore, after identifying one or more possible implicated pathways, the aim was to characterize in detail its/their status during physiological aging and in HGPS fibroblasts. Cellular health aspects were analyzed after activation and inhibition of the pathway, especially those that are important for HGPS and progerin clearance.

Another research objective was to investigate whether drug combinations could possibly lead to further amelioration of the clinical phenotype of HGPS. In this context, the combination with farnesyltransferase inhibitors was of particular interest, as they have already been approved for the treatment of HGPS and show several improvements (Dhillon 2021). A focus was on already known side effects of FTI, such as donut-shaped nuclei and growth arrest that are contraindicative to the actual goal of lifespan extension. Efforts were made to analyze cellular mechanisms, eliminate side effects and enhance positive synergistic benefits of the drugs.

2 MATERIALS AND METHODS

2.1 Materials

A detailed list of the used equipment, chemicals, consumables and kits can be found in the appendix.

2.1.1 Real-Time Quantitative PCR Primers

Table 1: Primers used for real-time quantitative PCR analysis

Primer sequence	Target Gene	Product size (bp)	Melting Temp
FW:5'-AATGGCGAGATCCCCTTGA-3' REV:5'-GCACCGGCTTTCATAGAATCTCT-3'	JAK1	66	62.9°C 63.0°C
FW:5'-TGATTTTGTGCACGGATGGA-3' REV:5'-ACTGCCATCCCAAGACATTCTT-3'	JAK2	72	63.4°C 62.1°C
FW:5'-GCCTGGAGTGGCATGAGAA-3' REV:5'-CCCCGGTAAATCTTGGTGAA-3'	JAK3	55	62.4°C 62.0°C
FW:5'-GGGACCGTGGGCAGGAGCTA-3' REV:5'-GTGCGTGTGGGAGACCTGGC-3'	TYK2	116	69.0°C 68.7°C
FW:5'-TTCAGAGCTCGTTTGTGGTG-3' REV:5'-AGAGGTCGTCTCGAGGTCAA-3'	STAT1	419	60.0°C 60.0°C
FW:5'-CCAAGGCTACCATGCTATTC-3' REV:5'-GCTGGTCTTTCAGTTGGCTG-3'	STAT2	336	57.3°C 61.0°C
FW:5'-CAGGAGGGCAGTTTGAGTCC-3' REV:5'-CAAAGATAGCAGAAGTAGGAGA-3'	STAT3	218	62.1°C 53.4°C
FW:5'-CCTGACATTCCCAAAGACAAAGC-3' REV:5'-TCTCTCAACACCGCATACACAC-3'	STAT4	203	64.2°C 61.2°C
FW:5'-TTACTGAAGATCAAGCTGGGG-3' REV:5'-TCATTGTACAGAATGTGCCGG-3'	STAT5A	104	59.3°C 61.9°C
FW:5'-CATTTTCCCATTGAGGTGCG-3' REV:5'-GGGTGGCCTTAATGTTCTCC-3'	STAT5B	103	63.6°C 60.7°C
FW:5'-CCTTGGAGAACAGCATTCCTGG-3' REV:5'-GCACTTCTCCTCTGTGACAGAC-3'	STAT6	116	65.3°C 59.1°C
FW:5'-GAGCCAGGAGTGGACTATGTGTA-3' REV:5'-CAATGGCCATGATGTACTCG-3'	C3	85	60.6°C 59.9°C
FW:5'-AGCATGAAAGTCTCTGCCGC-3' REV:5'-GGCATTGATTGCATCTGGCTG-3'	CCL2	93	62.9°C 66.0°C
FW:5'-CTTTTGGCCAGACAGACATG-3' REV:5'-GTGTAGAAGTGGAGGCACA-3'	CRP	130	59.3°C 54.5°C
FW:5'-CTGGCCGTGGCTCTCTTG-3' REV:5'-CCTTGGCAAAACTGCACCTT-3'	CXCL8	69	63.2°C 62.5°C

FW:5'-TGAAGGACATGGCTTAGAAGTG-3' REV:5'-GGTGCAAGGGTCACAGTGTT-3'	FAS	118	59.4°C 61.0°C
FW:5'-ACTGCGTTCCTGCTCAACATC-3' REV:5'-GCTCTGGTCCTTGGTGTCATG-3'	HMOX1	75	62.7°C 63.0°C
FW:5'-ATGCCCAGACATCTGTGTCC-3' REV:5'-GGGGTCTCTATGCCCAACAA-3'	ICAM1	112	61.0°C 62.2°C
FW:5'-GTCCAACGCAAAGCAATACATG-3' REV:5'-CCTTTTTCGCTTCCCTGTTTTAG-3'	IFN-G	81	62.6°C 62.4°C
FW:5'-GGCACAATTACTGCTCCAAAGAC-3' REV:5'-CAAGGCCCTTTCTCCCCAC-3'	IGF1	121	62.2°C 64.1°C
FW:5'-CGCCAATGACTCAGAGGAAGA-3' REV:5'-AGGGCGTCATTCAGGATGAA-3'	IL-1α	120	59.7°C 59.0°C
FW:5'-ATCGCTTCCTCTCGCAACAA-3' REV:5'-CTTCTACTGGTTCAGCAGCCATCT-3'	IL18	64	63.3°C 63.3°C
FW:5'-AACAGCCTCACAGAGCAGAAGAC-3' REV:5'-GTGTTCTTGGAGGCAGCAAAG-3'	IL4	74	62.4°C 62.2°C
FW:5'-GGTACATCCTCGACGGCATCT-3' REV:5'-GTGCCTCTTTGCTGCTTTCAC-3'	IL6	81	63.6°C 62.4°C
FW:5'-TCCCCTCTTGACCCATCTC-3' REV:5'-GGGAACCTTGTTCTGGTCAT-3'	LEP	110	60.0°C 58.8°C
FW:5'-TGATTTTGTGCACGGATGGA-3' REV:5'-ACTGCCATCCCAAGACATTCTT-3'	PPARG	105	55.4°C 54.6°C
FW:5'-CCCAGCATCTGCAAAGCTC-3' REV:5'-GTCAATGTACAGCTGCCGCA-3'	TGFB1	101	62.1°C 63.4°C
FW:5'-TCAGATCATCTTCTCGAACCCC-3' REV:5'-ATCTCTCAGCTCCACGCCAT-3'	TNFa	134	62.7°C 62.3°C
FW:5'-CATGAGAGGGGAGTATGATG-3' REV:5'-GAAGAAGAGTGGGCATCCAC-3'	TRAF1	181	55.4°C 59.7°C
FW:5'-GCTTGGATTCCTACAAAGAAGCA-3' REV:5'-ATAGATGGTCAATGCGGCGTC-3'	IFN-β	166	59.2°C 60.8°C
FW:5'-CTCTGCTCCTCCTGTTCGAC-3' REV:5'-TTAAAAGCAGCCCTGGTGAC-3'	GAPDH	144	60.1°C 60.2°C

2.1.2 Primary Antibodies

Table 2: Primary antibodies used for western blot or immunofluorescence

Antibody	Isotype	Company	Dilution		Cat No
			WB (in 5% milk)	IF (in 1x PBS-T with 10% FBS)	
ß-Actin	Mouse mAb	Sigma-Aldrich	1:10000		#A1978
cGAS	Rabbit mAb	Cell Signaling		1:100	#15102

Lamin A	Rabbit pAb	Sigma-Aldrich		1:2000	#L1293
Lamin A/C	Rabbit pAb	Santa Cruz	1:10000		Sc-20681
Lamin A/C	Mouse mAb	Invitrogen	1:100		MA3-1000
Lamin A/C	Mouse mAb	Santa Cruz		1:2500	E-1 sc-376248
JAK1	Rabbit pAb	Cell Signaling	1:1000		#3332
JAK2	Rabbit mAb	Cell Signaling	1:1000		#3230
p21	Rabbit mAb	Invitrogen	1:1000	1:250	MA5-14949
P-H2A.X		Sigma-Aldrich		1:2000	#05-636
P-STAT1	Rabbit mAb	Cell Signaling	1:1000		#9167
P-STAT3	Rabbit mAb	Cell Signaling	1:1000		#9145
Prelamin A	Mouse mAb	Sigma-Aldrich	1:2000	1:250	MABT858
Progerin	Rabbit pAb	Self made	0.1 µg/mL	0.1 µg/mL	
STAT1	Rabbit mAb	Cell Signaling	1:1000		#14994
STAT3	Mouse mAb	Cell Signaling	1:1000		#9139
SUN1	Rabbit pAb	Sigma-Aldrich	1:500		HPA008346

2.1.3 Secondary Antibodies

Table 3: Secondary antibodies used for western blot

Antibody	Company	Dilution	Cat No
Goat anti mouse HRP conjugated	Jackson ImmunoResearch	1:3000	115-035-003
Goat anti rabbit HRP conjugated	Jackson ImmunoResearch	1:3000	111-035-003

Table 4: Secondary antibodies used for immunofluorescence

Antibody	Company	Dilution	Cat No
α-mouse-Alexa Fluor 488	Invitrogen	1:1000	A21202
α-rabbit-Alexa Fluor 488	Invitrogen	1:1000	A21206
α-mouse-Alexa Fluor 555	Invitrogen	1:1000	A31570
α-rabbit-Alexa Fluor 555	Invitrogen	1:1000	A31572

2.1.4 Solutions

All solutions and buffers were prepared under sterile conditions and with Milli-Q® ultrapure water.

Table 5: cDNA synthesis master mix

Component	Volume
10x RT Buffer	2 µl
25x dNTP Mix (100mM)	0.8 µl
10x RT Random Primers	2.0 µl
MultiScripe™ Reverse Transcriptase	1.0 µl
Nuclease-free H_2O	4.2 µl
Total per reaction	10 µl

Table 6: SA-ß-gal staining solution

Potassium Ferricyanide (III)	5 mM
Potassium Ferrocyanide (II)	5 mM
$MgCl_2$	200 mM
NaCl	3 M
X-gal	0.5mg/ml
Citrate/sodium phosphate buffer, pH 6.0	

Table 7: Lysis buffer

NaCl	150 mM
Triton	1%
Tris	50 mM
SDS	1%
EDTA	1 mM
Adjust to pH=8.0	

Table 8: Laemmli buffer (1ml)

2x Laemmli Sample Buffer	910 µl
2-Mercaptoethanol	60 µl
Protease-Inhibitor	10 µl
Phosphatase-Inhibitor	10 µl
200 mM PMSF	10 µl

Table 9: Running gel (depending on molecular weight of the protein, volume for one 1.5 mm mini gel)

	<50 kDa	20-50 kDa
Percentage	**8%**	**12%**
H2O	3.4 ml	2.1 ml
30% acrylamid	2.7 ml	4 ml
1 M TrisHCl pH 8.8	3.7 ml	3.7 ml

10% SDS	100 µl	100 µl
Ammoniumpersulfate	80 µl	80 µl
TEMED	10 µl	10 µl

Table 10: Stacking gel (volume for one 1.5 mini gel)

Percentage	**6%**
H2O	2.1 ml
30% acrylamid	600 µl
1 M TrisHCl pH 6.8	375 µl
10% SDS	30 µl
Phenol red	10 µl
Ammoniumpersulfate	15 µl
TEMED	3 µl

Table 11: Running Buffer, 10x, 1L

Tris	30 g
Glycine	144 g
SDS	10g

Table 12: Bjerrum transfer buffer (semi-dry), 1x, 1L

Tris	5.82 g
Glycine	2.93 g
Methanol	200 ml
10% SDS	3.75 ml

Table 13: Transfer buffer (wet), 1x, 1L

Tris	3 g
Glycine	14.25 g
Methanol	200 ml
Check the pH and adjust to 8.3	

Blocking buffer

-5% milk in TBS-T buffer

2.2 Methods

2.2.1 PubMed Text Mining

A PubMed text mining approach was used to find genes associated with one of the four diseases typically recognized as the main phenotypes of HGPS

(http://www.pubmed.gov). A semiautomated method screening all crucial paper abstracts was developed using the programming language R. It was searched for connections between two keywords; one of the associated diseases and all gene names in the human genome from HGNC (version of 01.01.2019 listed 19,194 protein-coding genes) (Yates et al. 2017). As a result, the number and names of the research articles were obtained. The algorithm construction was made with two R packages. The 'RISmed' package (https://cran.r-project.org/web/packages/RISmed/index.html) allowed us to extract bibliographic content from the National Center for Biotechnology Information (NCBI) database. Furthermore, the 'pubmed.mineR' package (https://cran.r-project.org/web/packages/pubmed.mineR/) was used to text mine PubMed abstracts (Pasolli et al. 2017; Rani et al. 2015). Next, all abstracts were manually checked for the regulatory link and the extent and direction it influenced the gene.

2.2.2 Identification of Signaling Networks

The text mining approach resulted in four different lists for each disease with associated genes. As HGPS resembles all of these traits, we created a Venn diagram to look for altered genes and genes that belong to more than one list. In this analysis, 17 genes were identified to be associated with all diseases. A protein-protein network was generated using STRING analysis to assess if there is a shared signaling pathway (https://string-db.org). The STRING (Search Tool for the Retrieval of Interacting Genes/Proteins) database helps predict protein-protein interactions and contains information from experimental data, computational prediction methods and public text collections (Szklarczyk et al. 2019). Because the STRING analysis showed close interconnection, identification of a general pathway was the next step. For this purpose,

regulators and targets were searched for in the following databases: 1. TRRUST Version 2 (http://grnpedia.org/trrst) (Han et al. 2018), 2. TfactS (http://www.tfacts.org) (Essaghir et al. 2010), and 3. Regulatory Circuits (http://regulatorycircuits.org) (Marbach et al. 2016). The list of targets and regulators was manually curated and aliases and repetitions were removed. NF- κB and JAK-STAT signaling pathways were identified to be connected to most of the 17 genes and a separate list containing relevant transcriptions factors for those signaling axes was created.

2.2.3 Cell Culture

All human cells used in experiments were fibroblasts either from patients with HGPS supplied by the Progeria Research Foundation Cell and Tissue Bank or from healthy control individuals provided by the Coriell Institute for Medical Research. Fibroblasts were maintained in an incubator at 37 °C under the humidified atmosphere of 5% CO_2. Cells grew in 10cm cell culture dishes and were passaged 1-2 times a week by trypsinization and subcultured in a ratio of 1:4. The following cell lines were used (Table 14):

Table 14: Characteristics of all cell lines used

Cell line	Disease	Sex	Age at Sampling	Category
GM01651	Healthy	Female	13Y	Finite cell line
GM01652	Healthy	Female	11Y	Finite cell line
GM01582	Healthy	Female	11Y	Finite cell line
GM00323	Healthy	Male	11Y	Finite cell line

GM03349	Healthy	Male	10Y	Finite cell line
HGADFN127	HGPS	Female	3Y9M	Finite cell line
HGADFN003	HGPS	Male	2Y	Finite cell line
HGADFN164	HGPS	Female	4Y8M	Finite cell line
HGADFN188	HGPS	Female	2Y3M	Finite cell line

Cells were grown in Dulbecco's modified Eagle's medium + GlutaMAX™, supplemented with 15% fetal bovine serum, 1% L-glutamine, 1% penicillin-streptomycin (10,000 U/ml) and 0.5% gentamicin.

In addition, several treatments were added every 2-3 days to the media as indicated. baricitinib (Bar) was used at a concentration of 1 µM, farnesyltransferase inhibitor lonafarnib was used at a concentration of 0.025 µM, etoposide was used at a concentration of 1 µM. Mock-treated cells were treated with the vehicle (DMSO).

As cells were used according to their senescence, the following table 15 shows the corresponding passages:

Table 15: Passage numbers for each cell line corresponding to the indicated senescence index (SNS)

Cell Line	**≤5% SNS (0–5%)**	**~15% SNS (13 – 17%)**	**~30% SNS (28 – 32%)**
1651	Passage ≤ 20	Passage 26-28	Passage 36-38
1652	Passage ≤ 19	Passage 26-27	Passage 34-36
P003	Passage ≤ 18	Passage 21-22	Passage 26-27
P127	Passage ≤ 18	Passage 22-23	Passage 27-28

2.2.4 Cell Number Determination

An equal number of cells were seeded before drug treatments. After trypsinizing, these cells were counted with a Muse™ Cell Analyzer using miniaturized fluorescence and microcapillary cytometry. For cumulative population doublings (CPDs), the following formula was used:

$$n = 3.32\ (\log cells\ harvested - \log cells\ seeded) + x,$$

where n = the final CPD number at the end of a given subculture, and x = the former CPD as described previously (Gabriel et al. 2015).

2.2.5 Senescence ß-Galactosidase Staining

Expression of pH-dependent ß-galactosidase activity, among many others, is a biomarker of cellular senescence (Itahana et al. 2007). The senescence-associated ß-galactosidase assay was performed according to Dimri et al. (Dimri et al. 1995). Before staining, cells were fixed with 2% formaldehyde for 5 min. This assay uses SA-ß-gal to catalyze the hydrolysis of X-gal, resulting in the accumulation of a characteristic blue color in senescent cells. For that purpose, cells were incubated with 5-bromo-4-chloro-3-indolyl-D-galactopyranoside (X-gal) solution overnight at 37 °C (without CO_2). The next day, the staining solution was changed with PBS and the blue cells were counted directly under a microscope. At least 1000 cells were counted in three independent experiments.

2.2.6 Cell Cytotoxicity

Cell death within a culture was assessed using the CellTox™ Green Cytotoxicity Assay. An asymmetric cyanine dye binds to exposed DNA of dead or damaged cells but is excluded from viable cells with an intact membrane. As soon as the stain recognizes and binds to DNA, a fluorescent signal is transmitted. In brief, an equal number of cells are plated in a 96-well plate and incubated overnight. Next, CellTox™ Green Dye and Assay buffer were combined to make a 2x solution. This solution can then be diluted 1:2 with medium containing the indicated treatments and switched with the standard growth media. The exceptional photo stability of the dye allows time course data for a period of up to 72 h. The signal was quantified using a plate reader (Excitation = 485 nm, Emission = 520 nm).

2.2.7 Cell Cycle Assay

The cell cycle and its regulation is one of the most essential mechanisms of the cell. The different phases of the process with their checkpoints and the final division of the cell play a unique role in cell survival, including repair of genetic damage or prevention of uncontrolled cell division through apoptosis or senescence. The proportion of cells in each phase (G0/G1, S, and G2/M) can be visualized using the Muse Cell Cycle Assay Kit. Using the nuclear DNA intercalating stain propidium iodide (PI) and RNAse A, the exact DNA content can be detected and assigned to a phase. Non-replicating cells have two copies of each chromosome during the G0/G1 phase while dividing cells start to synthesize new DNA (S phase) until finally, the duplicated set of chromosomes is present (G2/M phase). The signal was measured using the Muse Cell Cycle Analyzer.

2.2.8 Respirometric Assay

Measurement of the energy metabolism was conducted with the Seahorse XF Analyzer. Oxygen consumption rate (OCR) and extracellular acidification rate (ECAR) of live control and HGPS cells were assessed, interrogating key cellular functions such as mitochondrial respiration and glycolysis. The Mito Stress Test Kit obtained multiple parameters, including basal respiration, ATP-linked respiration, maximal and reserve capacities and non-mitochondrial respiration. 1.5×10^4 control and HGPS fibroblasts were seeded into each well of a 96-well plate. The Seahorse XF DMEM assay medium, including 10 mM glucose, 1 mM pyruvate and 2 mM L-Glutamine, was used for the experimental design. Further analysis of mitochondria was carried out adding drugs into the media to achieve a final working concentration of 2.5 µM oligomycin, 2 µM Carbonyl cyanide-4 (trifluoromethoxy) phenylhydrazone (FCCP) and 1 µM rotenone/antimycin A. Injection ports were loaded with the defined volumes of the respective compound. Oligomycin (20 µl) was applied to ports A, 22 µl FCCP was pipetted into ports B, and 25 µl rotenone/antimycin A was added to ports C.

2.2.9 Autophagy Assay

Autophagy is a fundamental cellular process to maintain cell homeostasis. It involves degradation and digestion of damaged organelles, misfolded proteins and invading microorganisms by the lysosome (Jin und White 2008). By recycling cellular constituents, autophagy enables the cells to prevent apoptosis, although it can also promote cell death if cells are too damaged. To measure autophagy levels, we used Cayman's Autophagy/Cytotoxicity Dual Staining Kit. The principle of the kit is based on the incorporation of a fluorescent compound (monodansylcadaverine), which can be found in multilamellar bodies of autophagic vacuoles. 3.2×10^4 cells were seeded

in quintets in transparent 96-well plates and were allowed to attach overnight. After aspirating the growth media, staining solution (MDC ratio 1: 1,000) was added and cells were incubated for ten minutes at 37 °C. Following two washing steps with assay buffer, measurements of the autophagic vacuoles intensities were performed using a Microplate Reader (Excitation = 355 nm, Emission = 512 nm).

2.2.10 Proteasomal Activity

The proteasome is a multicatalytic proteinase responsible for selective protein degradation that does not occur in the lysosomes. Many essential proteins are selectively degraded, including cell-cycle control factors, signal transduction factors, transcription factors, oncogene and anti-oncogene products and thus influence apoptosis, DNA repair endocytosis and cell cycle control (Adams 2003). To measure proteasomal activity levels, we used Cayman's 20S Proteasome Assay Kit. The kit employs a specific 20S substrate (SUC-LLVY-AMC), which generates a highly fluorescent product upon cleavage. 3.2×10^4 cells were seeded in quintets in 96-well plates and were allowed to attach overnight. The next day, the cells are washed once with assay buffer before incubation with the 20S proteasome lysis buffer for 30 min at room temperature. Followed by a centrifugation step at 1,000 × g for 10 min, 90 µl of the supernatant from each well was transferred to a new transparent 96-well plate and filled with 10 µl assay buffer or 10 µl of the 20S inhibitor solution. After that, 10 µl of the substrate solution was added to each well and the plate was incubated at 37 °C for 1 h. Fluorescence was measured with a Microplate Reader (Excitation = 485 nm, Emission = 520 nm).

2.2.11 Measurement of Reactive Oxygen Species

Reactive oxygen species (ROS) are a group of reactive molecules and free radicals derived from molecular oxygen. To measure these molecules, we used abcam's ROS Detection Assay Kit. 3.2×10^4 cells were seeded in quintets in 96-well plates and were allowed to attach overnight. Incubation with 25 µM 2',7'-dichlorofluorescein diacetate (DCFDA) at 37 °C for 45 min allowed the dye to diffuse into the cells passively. There, DCFDA is deacetylated by cellular esterases, giving a more polar compound that stays trapped. Oxidation of DCF by ROS forms a highly fluorescent dye that monitors real-time ROS. Fluorescence was measured with a Microplate Reader (Excitation = 485 nm, Emission = 520 nm).

2.2.12 Measurement of Intracellular ATP

The CellTiter-Glo® Luminescent Cell Viability Assay quantifies the ATP present in cell cultures. After cell lysis, cellular ATP is part of a luciferase reaction so that the luminescence produced is proportional to the total ATP within the cell. After seeding 3.2×10^4 cells in quintets in 96-well plates and letting them attach for 12 h, cells were directly incubated with the CellTiter-Glo reagent for 10 min. Luminescence was measured with a Microplate Reader. As a control, an ATP standard was performed.

2.2.13 Western Blot

Cultured cells in 10 cm petri dishes with indicated treatment were washed once with ice-cold 1x PBS, lysed in 150 µl of a 1:2 lysis buffer/laemmli buffer mix and harvested by scraping. Cell lysates were vortexed thoroughly for ~20 sec before storing at -20 °C. Alternatively, cells were washed once with 1x PBS, trypsinized and collected in a

15 ml tube. After centrifugation at 400 g for 5 min and another washing step with 1x PBS, cells were lysed with a 1:2 lysis buffer/laemmli buffer mix. Lysates were stored at -20 °C.

Before performing western blot, all samples were heated to 95 °C for 5 min while shaking at 600 rpm. Protein concentrations were calculated by Bradford assay (Bio-Rad) and subsequent analysis on a microplate reader. BSA protein standard was used (0.125 – 2.0 mg/ml). All protein lysates were diluted 1:50 and absorbance of the proteins was measured with a total of 80 µl. Finally, protein concentrations were calculated using a standard curve from the standard and linear regression analysis. Usually, 25 µg of protein were loaded into each well of the denaturing polyacrylamide gels.

To detect protein levels by western blot, they were separated by 8-12% SDS polyacrylamide gel electrophoresis (PAGE) according to size. Then proteins were blotted onto a nitrocellulose membrane. Following the transfer step, the membranes were incubated in Ponceau S solution for 3 min. Washing with Millipore water reduced the background of the membranes and allowed documentation and loading control. After washing in TBS-Tween to reverse the Ponceau S staining, the membrane was blocked for 1 h in 5% non-fat milk. Subsequently, the membrane was hybridized with an antibody specific for the protein of interest (1st antibody, Table 2) overnight at 4 °C and then incubated with another secondary antibody (Table 3) that binds the primary and is conjugated with an horseradish phosphatase for 1 h. Protein bands were visualized by performing luminol-enhanced chemiluminescence measured by a Chemi-Doc™ MP Imaging System. Blots were analyzed using ImageJ software and quantified by normalizing them to ß-actin.

2.2.14 Immunofluorescence

Cellular localization of proteins can be analyzed using specific antibodies against the protein of interest. Secondary antibodies conjugated with fluorescent labels helped visualize with a fluorescent microscope. Cells were grown on glass coverslips inside 6 cm cell culture plates. After indicated therapies, cells were fixed with either 2% paraformaldehyde solution in PBS (PFA) for 15 min at RT or in cold MeOH for 10 min at -20 °C. Next, coverslips were washed before and after permeabilization with 0.2% Triton-X-100 in PBS for 10 min at RT. Samples were then blocked with blocking solution (10% FBS in PBS) for 1 h at RT in a humidity chamber. Primary antibodies (Table 2) were diluted in blocking buffer and 80 µl were pipetted onto the coverslips for overnight incubation at 4 °C. Subsequently, samples were washed 3x with PBS before 80 µl of the secondary antibody diluted in blocking buffer was added (Table 4). Incubation of the secondary antibody was carried out for 1 h at RT. For negative control, one coverslip was only incubated with pure blocking solution. Lastly, coverslips were again washed 4x with PBS before counterstaining and mounting with DAPI in Vectashield mounting medium. Images were acquired using an Axio Imager D2 fluorescence microscope. When cells have been evaluated for statistics, at least 800 to 1000 cells were screened in 3 independent experiments.

2.2.15 Gene Expression Analysis

RNA was extracted using the GeneJET RNA Purification Kit. The kit utilizes silica-based membrane technology in the form of a spin column. In total, ~1 × 10^6 cells were collected to yield sufficient starting material for cDNA synthesis. To validate RNA

quantity and quality of RNA a spectrophotometric analysis was carried out on a NanoDrop ND-1000. Following extraction, cDNA synthesis is needed for gene expression analysis. The reverse transcriptase reaction involves using an RNA-dependent DNA polymerase to obtain a library of cDNA originating from the cells' mRNA. At first, the RNA is denatured and then hybridized to short non-specific DNA sequences (random hexamers). Subsequently, the cDNA obtained can be used for qPCR. 1 µg of RNA was reverse-transcribed using the High-Capacity cDNA Reverse Transcription Kit. The following thermal cycling conditions were used (Table 16):

Table 16: Temperature profile for cDNA synthesis

Settings	**Step 1**	**Step 2**	**Step 3**	**Step 4**
Temp.	25 °C	37 °C	85 °C	4 °C
Time	10 min	120 min	5 min	∞

As a negative control, the reverse transcription reaction was performed without adding reverse transcriptase.

Next, real-time qPCR was used to measure and monitor the amplification of the PCR products over time. By adding SYBR green, a fluorescent nucleic acid stain, to the master mix, double-stranded DNA becomes quantifiable. The SYBR green signal becomes stronger the more PCR products are produced. Primers were designed using NCBI/Primer-BLAST (Ye et al. 2012). All primers are evaluated and listed in the primer list (Table 1). For optimal results, PowerUp™ SYBR™ Green Master Mix was used in a StepOnePlus™ with 300 nM of each primer and 50 ng of the template cDNA in a 20 µl reaction volume. The following thermal cycling conditions were used (Table 17):

Table 17: Temperature profile for real-time quantitative PCR

Stage	Temperature	Time	Cycles
Initial denaturation	95 °C	20 s	1 cycle
Amplification	95 °C	3 s	45 cycles
	60 °C	30 s	
Final Hold	4 °C	∞	1 cycle

Three independent experiments and at least three replicates were carried out for every sample and gene. GAPDH was used as an endogenous control.

2.2.16 Statistics

Comparative analysis of different characteristics of HGPS and healthy control cells was conducted using the Student's t-test, repeated measures one-way or two-way ANOVA followed by Post-Tukey test, depending on the type of comparison. mRNA content was calculated by using a pairwise fixed reallocation randomization test (Pfaffl 2001). $p < 0.05$ was considered to be statistically significant ($n \geq 3$, * $p < 0.05$, ** $p < 0.01$, *** $p < 0.001$). Values are presented as mean ± standard deviation (mean ± SD). All statistical analyses were performed using the GraphPad Prism software version 6.01.

3 RESULTS

3.1 Identification and Inhibition of JAK-STAT Signaling

3.1.1 Identification of dysregulated genes in vascular disease, arthritis, alopecia and lipodystrophy and the finding of the underlying signaling pathway

Since therapeutic approaches for the Hutchinson-Gilford progeria syndrome have not yet led to a breakthrough, a new data mining approach was performed to identify dysregulated genes in the four diseases that are also considered as the main traits of HGPS, namely arthritis, lipodystrophy, alopecia and vascular disease. Using an algorithm within the software environment R, associations between one of the four diseases and all genes from the human gene list (HGNC, www.genenames.org) were searched in Pubmed Abstracts (https://pubmed.ncbi.nlm.nih.gov/). The resulting genes were then manually screened for a regulatory link and only significant expression changes were included. A total of 2843 genes were associated with at least one of the diseases, including 1049 dysregulated genes for arthritis, 67 dysregulated genes for lipodystrophy, 157 dysregulated genes for alopecia and 1560 genes for vascular diseases (Figure 3).

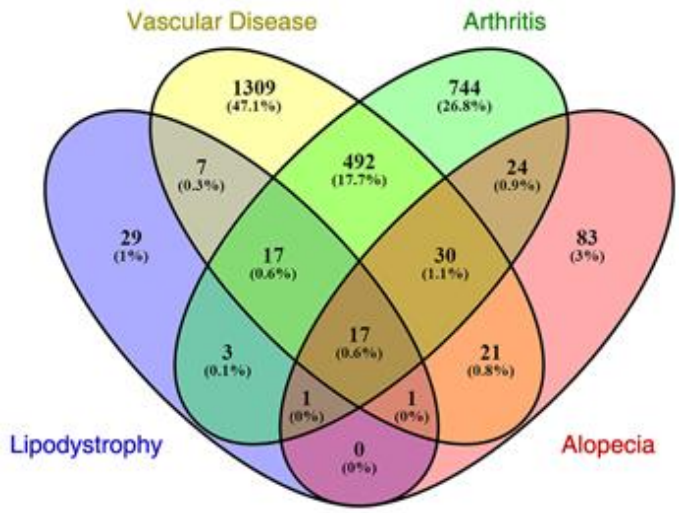

Figure 3: Text mining analysis to identify genes associated with vascular disease, arthritis, alopecia and lipodystrophy. Venn diagram of the 2778 genes linked to the four diseases as determined by text mining. (Liu et al. 2019)

A Venn diagram showing all dysregulated genes of the four diseases is shown. The overlapping areas indicate those dysregulated genes in more than one disease and 17 genes were dysregulated in all disorders. For further analyses, the genes associated with all four conditions were of particular interest, suggesting deregulation in HGPS. The following 17 genes were included: complement 3 (C3), chemokine (C-C motif) ligand 2 (CCL2/MPC1), C-reactive protein (CRP), C-X-C motif chemokine ligand 8 (CXCL8/IL8), cell surface death receptor (FAS), heme oxygenase 1 (HMOX1), intercellular adhesion molecule 1 (ICAM1), insulin-like growth factor 1 (IGF1), interleukin 18 (IL18), interleukin 4 (IL4), interleukin 6 (IL6), interferon gamma (IFNG), peroxisome proliferator activated receptor gamma (PPARG), transforming growth factor beta 1 (TGFB1), tumor necrosis factor alpha (TNFα), leptin (LEP) and TNF receptor-associated factor 1 (TRAF1).

Of these genes, the four diseases' expression patterns were assessed and the function was summarized (Table 18).

Table 18: Expression profile of the 17 genes identified by keyword searches in association to vascular disease (VD), arthritis (AR), lipodystrophy (LD) and alopecia (AL). Indicated expression (↑ = overexpressed; ↓ = downregulated) is shown according to the curated literature. (Liu et al. 2019)

Gene (swiss-prot gene ID)		**Expression**	**Function**
PPARγ (receptor) ID: 5468	**VD**	↓(Wei et al. 2016)	Protects endothelia, regulates the differentiation of adipocytes and lipid metabolism, inhibits proliferation and the migration of smooth muscle cells, and reduces inflammatory chemokines (Wei et al. 2016).
	AR	↓(Butt et al. 2006)	Inhibits major signaling pathways of inflammation and reduces the synthesis of cartilage catabolic factors responsible for articular cartilage degradation (Giaginis et al. 2009).
	LD	↓(Victoria et al. 2010)	Essential in the differentiation of adipocytes (Jiang et al. 1998).
	AL	↓(Gaspar 2016)	Required for the maintenance of a functional epithelial stem cell compartment in murine hair follicles (Harries und Paus 2009).
CCL2 (chemokine) ID: 6347	**VD**	↑(Dinh et al. 2017)	Recruits macrophages and monocytes to the vessel wall (Harrington 2000).
	AR	↑(Haringman et al. 2006)	Mediator of the migration of monocytes, macrophages and T cells. These are directly involved in the induction and perpetuation of synovitis and subsequent joint destruction (Haringman et al. 2006).
	LD	↑(Villarroya et al. 2010)	Recruits macrophages to adipose tissue and induces an inflammatory response (Wee et al. 2014).

	AL	↑(Hong et al. 2006)	Recruits monocytes and lymphocytes T in the acute inflammatory condition and it may also be an important mediator in chronic inflammation (Alzolibani et al. 2012).
TGFβ1 (growth factor) ID: 7040	**VD**	↑(Misiakos et al. 2001)	There is a link between increased levels of circulating TGFβ and hypertension, a cardiovascular risk factor which contributes to the development of organ damage such as renal sclerosis, stroke, and coronary heart disease (Laviades et al. 2000).
	AR	↑(Niu et al. 2012)	Transforming growth factor beta1 (TGFbeta1) has been reported to have important roles in unresolved inflammation, immune suppression, fibrosing processes, and angiogenesis (Sugiura et al. 2002).
	LD	↑(Clouthier et al. 1997)	Potent inhibitor of adipocyte differentiation (Clouthier et al. 1997).
	AL	↑(Lu et al. 2016)	Influences the epithelial cell growth, and modulates androgen receptor transactivation and androgen sensitivity in dermal papilla cells(Lu et al. 2016).
CXCL8 (Chemokine) ID: 3576	**VD**	↑(Kizilay Mancini et al. 2017)	Stimulates the adhesion of monocytes to endothelial cells, and has a role in plaque destabilization (Abke et al. 2006; Koenen und Weber 2010).
	AR	↑(Manivel et al. 2016)	Induces synovial inflammation, regulates leukocyte adhesion molecule expression, and it is a mediator of angiogenesis (Szekanecz et al. 2003).
	LD	↑(He et al. 2005)	Major regulator of adipose tissue metabolism. Its overexpression in subcutaneous adipose tissue may be associated with wasting processes that lead to atrophy (He et al. 2005; Gallego-Escuredo et al. 2013).
	AL	↑(Zhang et al. 2015)	Plays a role in perturbing keratinocyte differentiation in the AA follicle (Barahmani et al. 2010).
ICAM1 (adhesion molecule) ID: 3383	**VD**	↑(Marzolla et al. 2017)	Key molecule in atherogenesis, when circulating monocytes adhere to the endothelium and subsequently transmigrate into the intima (Kitagawa et al. 2002).
	AR	↑(Garg et al. 2016)	Promotes leukocyte adhesion to endothelial cells and synovial fibroblasts, and promotes leukocyte migration (Yang et al. 2010).
	LD	↑(Melendez et al. 2008)	UNKNOWN
	AL	↑(Gilhar et al. 2003)	Together with gamma interferon mediates T cell trafficking in the skin (Gupta et al. 1990).
CRP (pentraxin) ID: 1401	**VD**	↑(Pleskovič et al. 2017)	Directly influences complement activation, apoptosis, vascular cell activation, monocyte recruitment, lipid accumulation and thrombosis. Associated with the formation and progression of atherosclerotic lesions (Paffen und DeMaat 2006; Yu et al. 2012).
	AR	↑(Sarkar et al. 2017)	Plays a role in the bony destructive process through the induction of RANKL expression and direct differentiation of osteoclasts precursors into mature osteoclasts (Kim et al. 2015b).
	LD	↑(Miehle et al. 2016)	Its levels are strongly associated with adipose tissue mass (Samaras et al. 2009).
	AL	↑(Mahamid et al. 2014)	UNKNOWN
C3 (Chemokine) ID: 718	**VD**	↑(Howard und Thurnham 2017)	Essential in the maturation of atherosclerotic lesions beyond the foam cell stage (Buono et al. 2002).
	AR	↑(Ballanti et al. 2011)	Contributes to inflammation and tissue injury. Has a role in the induction and progression of the disease (Ballanti et al. 2011).

	LD	↓(Jansen et al. 2013)	Excessive consumption of C3 in the alternative complement pathway leads to an increased expression of Factor D. Lipodystrophy and tissue destruction are more significant in tissues where Factor D expression is increased (Savage et al. 2009; Yavuz und Acartürk 2010).
	AL	↑(Kulkarni et al. 2014)	C3 deposition reflects the morphological state of hair follicles in each stage of the hair cycle, suggesting a relationship between the hair cycle and C3 deposition (Fairhurst et al. 2009).
TRAF1 (tumor necrose factor associated) ID: 7185	**VD**	↑(Zirlik et al. 2007)	Involved in monocyte recruitment to the vessel wall (Missiou et al. 2010).
	AR	↑(Cheng et al. 2016)	Plays a crucial role in the pathogenesis of autoantibodies and may serve as a serologic inflammatory marker of disease activity (Cheng et al. 2016).
	LD	↑(Souza Dantas Oliveira et al. 2014; Oliveira Pinto et al. 2002)	UNKNOWN
	AL	↑(Redler et al. 2010)	UNKNOWN
IL18 (Interleukin) ID: 7185	**VD**	↑(Paramel Varghese et al. 2016)	Has a proatherogenic effect through stimulation of IFN-γ secretion. It polarizes T helper 1 cells and induces the production of inflammatory cytokines, chemokines, and vascular adhesion molecules (Tenger et al. 2005; Meiler et al. 2016).
	AR	↑(Kanameishi et al. 2017)	Promotes articular Th1 responses, acts directly on macrophages to induce proinflammatory cytokine production, and contributes to cartilage degradation (Gracie et al. 1999).
	LD	↑(Iannello et al. 2010)	Induces apoptosis of subcutaneous adipocytes in lipoatrophic areas, and it contributes towards HALS by downregulating the production of adiponectin (Iannello et al. 2010; Lindegaard et al. 2004).
	AL	↑(Lee et al. 2010)	Induces the production of IFN-γ, a factor that induces alopecia (Lee et al. 2015).
IGF1 (growth factor) ID: 3479	**VD**	↓(Higashi et al. 2012)	Reduces atherosclerosis burden and improves features of atherosclerotic plaque stability through induction of the reduction of oxidative stress, cell apoptosis, proinflammatory signaling, and endothelial dysfunction (Higashi et al. 2012).
	AR	↓(Soler Palacios et al. 2015)	Enhances the synthesis of components such as proteoglycan and collagen in normal cartilage, and blocks cytokine-stimulated cartilage degradation. It is an important regulator of the repair processes during joint diseases (van den Berg 1999; Hui et al. 2001).
	LD	↓(Boucher et al. 2016)	IGF1 signaling is essential for the development and function of adipose tissue. The IGF1 receptors play a role in gene expression in white adipose tissue and in the maintenance of normal serum leptin and adiponectin levels (Boucher et al. 2016).
	AL	↓(Bergfeld 2013)	Stimulates follicular epithelial cell growth (Tang et al. 2003).
IL6 (Interleukin) ID: 3569	**VD**	↑(Leung et al. 2016)	Plays a central role in propagating the downstream inflammatory response responsible for atherosclerosis. Contributes to both atherosclerotic plaque development and plaque destabilization (Okazaki et al. 2014; Hartman und Frishman 2014).
	AR	↑(Dong et al. 2016)	Contributes to the induction and maintenance of the autoimmune process through B cell modulation and Th17 cell differentiation, and it plays a role in angiogenesis by inducing intracellular

			adhesion molecules (Kim et al. 2015a).
	LD	↑(Loonam et al. 2016)	Leads to increased apoptosis and thus contributes to the loss of subcutaneous fat (Kannisto et al. 2003).
	AL	↑(Rossi et al. 2012)	Induces a rise in immunoglobulin G which can have a key role in long-standing disease due to humoral autoimmune pathology, and plays a partial role in hair growth inhibition (Rossi et al. 2012; Yu et al. 2008).
TNFα (tumor necrosis factor) ID: 7124	**VD**	↑(Bruunsgaard et al. 2000)	Promotes cholesterol uptake into monocytes and macrophages and cholesteryl ester-laden cell formation from differentiating monocytes, resulting in foam cell accumulation; it is involved in the production of chemokines and in the recruitment of leucocytes during inflammatory reactions; induces VSMCs proliferation; increases adherence of leucocytes to endothelial cells by inducing the expression of cell adhesion molecules; stimulates apoptosis of VSMCs; and it can induce autophagy in plaque VSMCs (Bruunsgaard et al. 2000; Kleinbongard et al. 2010; Jia et al. 2006).
	AR	↑(Mewar und Wilson 2011)	Stimulates the production of cytokines, chemokines and prostaglandins in RA synovium; stimulates the production of matrix-degrading enzymes like MMPs; leads to an increase of the destructive potential of RASF; induces the expression of RANKL and synergizes with RANKL to directly promote osteoclast differentiation; and stimulates bone loss by mobilizing $CD11b^+$ osteoclast precursors from the bone marrow and by reducing bone formation by inhibiting osteoblast differentiation and function (Müller-Ladner et al. 2005; Brennan et al. 1989; Moelants et al. 2013).
	LD	↑(Mahajan et al. 2015)	Stimulates lipolysis; induces insulin resistance, leptin production, suppression of lipogenesis, adipocyte dedifferentiation, and apoptosis in preadipocytes and adipocytes; and impairs preadipocyte differentiation (Prins et al. 1997; Lichtenstein 2005).
	AL	↑(Kasumagic-Halilovic et al. 2011)	Causes the condensation and distortion of the dermal papilla, marked vacuolation of the hair follicle matrix, abnormal keratinization of the follicle bulb and inner root sheath, disruption of follicular melanocytes and the presence of melanin granules within the dermal papilla, resulting in the formation of dystrophic anagen hair follicles (Gregoriou et al. 2010; Philpott et al. 1996).
HMOX1 (oxygenase) ID: 3162	**VD**	↓(Brydun et al. 2007)	Its expression in macrophages increases antioxidant protection and decreases inflammatory components of atherosclerotic lesions, having a role in the protection against atherogenesis (Wu et al. 2011).
	AR	↓(Zwerina et al. 2005)	Inhibits cartilage erosion, decreases proinflammatory cytokine secretion, and suppresses osteoclastogenesis and bone destruction (Rueda et al. 2007).
	LD	↓(Manente et al. 2012)	UNKNOWN
	AL	↓(Yun et al. 2009)	Its decreased expression causes the impairment of the protective mechanism from oxidative stress in the scalp (Yun et al. 2009).
LEP (adipokine) ID: 3952	**VD**	↑(Payne et al. 2014)	leptin as an important mediator in endothelial dysfunction and neointimal hyperplasia, both key steps in the evolution of atherosclerotic vascular changes. Additionally, aracrine leptin release from perivascular adipose tissue (PVAT) has deleterious effects on the underlying endothelium and vascular smooth muscle cells (SMC), including the coronary circulation (Payne et al. 2014).
	AR	↑(Abella et al. 2017)	Adipocyte-derived leptin induces proinflammatory cytokine release from innate and adaptive immune cells, producing an inflammatory milieu that encourages cartilage damage and rheumatoid arthritis (Abella et al. 2017).

	LD	↓(Paz-Filho et al. 2015)	Leptin has key roles in the regulation of energy balance, body weight, metabolism, and endocrine function. Leptin levels are undetectable or very low in patients with lipodystrophy, hypothalamic amenorrhea, and congenital leptin deficiency (CLD) due to mutations in the leptin gene (Paz-Filho et al. 2015).
	AL	↑(Yang et al. 2017)	The plasma leptin level was significantly higher in AGA subjects, compared to non-AGA subjects (4.45 vs 2.76 ng/mL, P<.05). Leptin from the circulation might impact the development of AGA (Yang et al. 2017).
IL4 (Interleukin) ID: 3565	**VD**	↑(Lee und Hirani 2006)	IL-4 can induce apoptosis of human vascular endothelial cells through the caspase-3-dependent pathway, suggesting that IL-4 can increase endothelial cell turnover by accelerated apoptosis, the event which may cause the dysfunction of the vascular endothelium (Lee und Hirani 2006).
	AR	↑(Wojdasiewicz et al. 2014)	IL4 improves anti-inflammatory effect and suppresses several pro-inflammatory cytokines and systemic IL4 treatment protects the cartilage and bone destruction in established murine type II collagen-induced arthritis. IL-4 has an inhibiting effect on the degradation of proteoglycans in the articular cartilage, by inhibiting the secretion of MMPs metalloproteinases, as well as reducing the variation in the production of proteoglycans that are visible in the course of OA (Wojdasiewicz et al. 2014).
	LD	↓(Dragović et al. 2017)	IL-4 has important role in lipid metabolism and regulation of glucose by promoting insulin sensitivity and glucose tolerance.Lower insulin sensitivity reduced uptake of fatty acids, reduced glucose transport, and increased free fatty acids (FFA) in the general circulation and that can lead to lipodystrophy (Dragović et al. 2017).
	AL	↑(Alli et al. 2012)	Alopecia development is associated with CD8(+) T cell activation, migration into the intrafollicular region, and hair follicle destruction. The disease may be adoptively transferred with T lymphocytes and is class I and not class II MHC-dependent. Pathologic T cells primarily express IFNG and IL-17 early in disease, with dramatic increases in cytokine production and recruitment of IL-4 and IL-10 production with disease progression (Alli et al. 2012).
IFNG (Interferon) ID: 3458	**VD**	↑(McLaren und Ramji 2009)	IFN-g, known to be a pro-inflammatory cytokine, can also display anti-inflammatory properties. it is likely that it acts in both ways in atherosclerosis. it is possible that its proatherogenic actions out-weigh its anti-atherogenic ones or vice versa. IFN-g promotes foam cell formation, plaque development and a Th1-driven adaptive immune response. These effects can be attributed to an array of key genes, involved in atherosclerosis, that are regulated by IFN-g (McLaren und Ramji 2009).
	AR	↓(Lee et al. 2017)	IFN-γ activity associated with necroptosis suggests that IFN-γ may modulate necroptosis and improve RA progression by preventing or reducing inflammatory cell death (Lee et al. 2017).
	LD	↑(Liu et al. 2012)	Cytokines play important roles in the pathogenesis of lipodystrophy syndrome. Single nucleotide polymorphisms (SNPs) at position +874 (T/A) of the interferon-gamma gene are related to the expression of these cytokines (Castelar et al. 2010).
	AL	↑(Arca et al. 2004)	IFN-γ rapidly inhibited hair elongation in cultured human anagen hair follicles and induced morphological signs of catagen transformation. IFN-γ can also inhibit proliferation, increase apoptosis and follicular melanogenesis (Arca et al. 2004).

Three of the genes' expressions (PPARG, IGF1 and HMOX1) were downregulated in all diseases. On the contrary, CCL2, CXCL8, ICAM1, CRP, TRAF1, IL18, IL6, TNFα,

TGFB1 and FAS showed a significant upregulation in the four conditions. The rest of the genes did not show a consistent pattern. Although C3, LEP and IL4 decreased in lipodystrophy, all of them were upregulated in the other three conditions. IFNG was the only downregulated gene in lipodystrophy, alopecia and vascular disease, whereas it was elevated in arthritis. In addition, the function of the 17 entities in general and especially in the four conditions suggested an interconnection as many of them were involved in pro-inflammatory signaling cascades, especially those which drive the senescence-associated secretory phenotype (SASP). SASP cytokines, including CRP, IL6, IL8, CCL2 and TNFα, are permanently secreted in senescent cells, leading to chronic inflammation, and increase most age-related diseases (Chovatiya und Medzhitov 2014; Frasca und Blomberg 2016). To support the assumption of a common regulatory link, a STRING analysis (https://string-db.org) showed that all 17 entities showed protein-protein interactions (Figure 4).

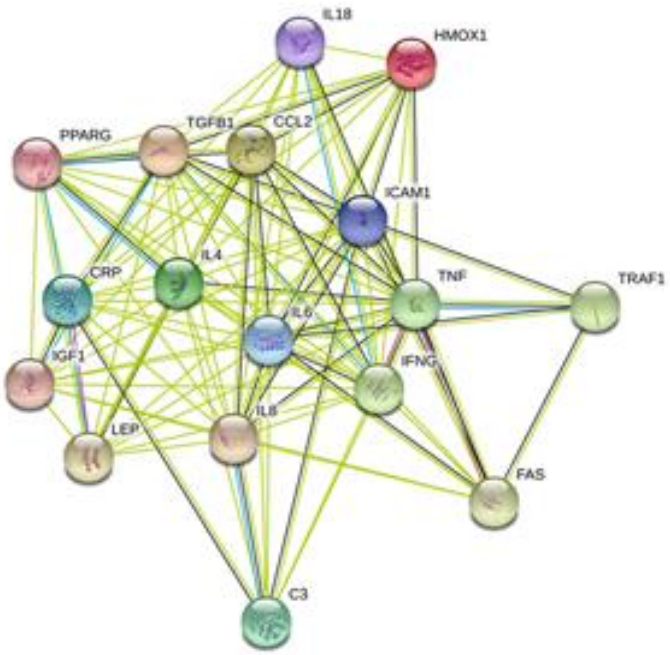

Figure 4: Protein interaction network of the 17 genes found by data mining. Interaction network of the 17 gene products visualized by STRING. Nodes are proteins and lines represent functional associations between proteins. A green line indicates neighborhood evidence; a blue line indicates cooccurrence evidence; a purple line indicates experimental evidence; a light blue line indicates database evidence; a black line indicates coexpression evidence. (Liu et al. 2019)

Even if not all proteins were directly linked to each other, they were at least connected via intermediate pathways. Of interest are the proteins with the most interactions; TNF, TGFB1, CCL2, CRP, IL4, IL6, IL8, ICAM1 and IFNG. This finding again demonstrated the critical role of inflammatory components in aging and age-related diseases.

To identify an underlying signaling pathway, further analysis of regulators and targets was performed using three public databases: TRRUST Version 2 (Han et al. 2018), TfactS (Essaghir et al. 2010) and Regulatory Circuits (Marbach et al. 2016). In total, 140 different transcription factors were found (Table 19).

Table 19: All targets and regulators of the 17 genes identified by text mining. (Liu et al. 2019)

Transcription factors			
AHR	FOXO1	MYCN	SFPQ
APEX1	GATA1	NCOR1	SIRT1
AR	GATA2	NCOR2	SMAD3
ASH1L	GATA3	NEAT1	SMAD4
ATF2	GBX2	NFAT5	SMAD7
ATF3	GLI1	NFATC1	SP1
ATF4	GLI2	NFATC2	SPI1
ATM	HDAC1	NFE2L2	SPIC
BACH1	HDAC11	NFIC	SREBF1
BRCA1	HDAC2	NFIL3	SREBF2
CDX1	HDAC3	NFKB1	STAT1
CEBPA	HDAC9	NFKBIA	STAT2
CEBPB	HDGF	NFYA	STAT3
CEBPD	HIF1A	NFYB	STAT4
CIITA	HMGB2	NFYC	STAT5A
CREB1	HNF1A	NR1I2	STAT5B
BREBBP	HSF1	NR4A1	STAT6
DDIT3	IFI16	NR4A2	TBP
DEK	IKBKB	NR4A3	TBX21
E2F1	ING4	OTX2	TFAP2A
E2F4	IRF1	PARP1	TFAP4
EGR1	IRF2	POU2F1	TP53
EGR2	IRF3	PPARA	TWIST1
ELF4	IRF5	PPARG	TWIST2
EOMES	JUN	PREB	UHRF1
EP300	JUNB	PROX1	USF1
ERG	JUND	PURA	USF2
ETS1	KHDRBS1	RARA	VDR
ETS2	KLF2	RARG	WT1
ETV4	KLF4	RB1	XBP1
ETV5	LRRFIP1	RBPJ	YBX1
FLI1	MAF	REL	YY1
FOS	MSC	RELA	ZFP36
FOSB	MYB	RFX5	ZMYND11
FOSL2	MYC	SATB1	ZNF300

We identified a small number of transcription factors that could modulate several of our genes, including nuclear factor kappa B subunit 1 (NF-kB1, regulated 14 genes), Rela proto-oncogene (Rela, regulated 12 genes), STAT1 (regulated 8 genes), STAT3 (regulated 12 genes), STAT5a (regulated 4 genes), STAT5b (regulated 4 genes) and STAT6 (regulated 2 genes) (Table 20).

Table 20: Transcription factors that regulate most of the 17 genes identified by text mining. (Liu et al. 2019)

Gene	NF-κB1	Rela	STAT3	STAT1	STAT5A	STAT5B	STAT6
C3							
CCL2	√	√	√	√			
CRP	√	√	√				
CXCL8	√	√	√	√			√
FAS	√	√	√	√			
HMOX1	√	√	√	√			
ICAM1	√	√	√	√			
IGF1			√		√	√	
IL6	√	√	√	√	√		
IL18	√	√					
PPARG	√			√		√	
TGFB1	√		√				
TNF	√	√	√		√	√	
TRAF1	√	√					
LEP			√				
IL4	√	√					√
IFN-G	√	√	√	√	√	√	

The NF-κB pathway is already well described as a primary driver of aging (Osorio et al. 2016). Activation of this signaling pathway has also been identified in HGPS and interventions have been applied to improve the HGPS phenotype (Osorio et al. 2012; Mozzini 2020). However, discovering different STAT proteins and an association to the JAK-STAT signaling pathway was novel and suggested a possible new therapeutic approach for HGPS patients. In summary, we found 17 mostly pro-inflammatory genes

dysregulated in vascular diseases, arthritis, lipodystrophy, alopecia and possibly also in HGPS. Based on these, we identified the signaling pathway JAK-STAT that may offer a therapeutic approach if adequately regulated.

3.1.2 Establishment of a novel cell-based aging model

In previous studies of HGPS cells, we noticed that comparisons with 'normal' healthy cells were always based on their passage number. However, as HGPS cells display premature aging, including decreased growth rate and early senescence entry (Figure 5), analyses were not reliable. Cell cultures can exhibit distinct characteristica at different time points and are influenced by intrinsic and external factors that might not be represented by passage numbers (Hayflick und Moorhead 1961). We proposed and established a new cell-based aging model because we wanted to know if differences between HGPS and control fibroblasts were disease-specific or resemble the physiological normal aging process (Figure 5).

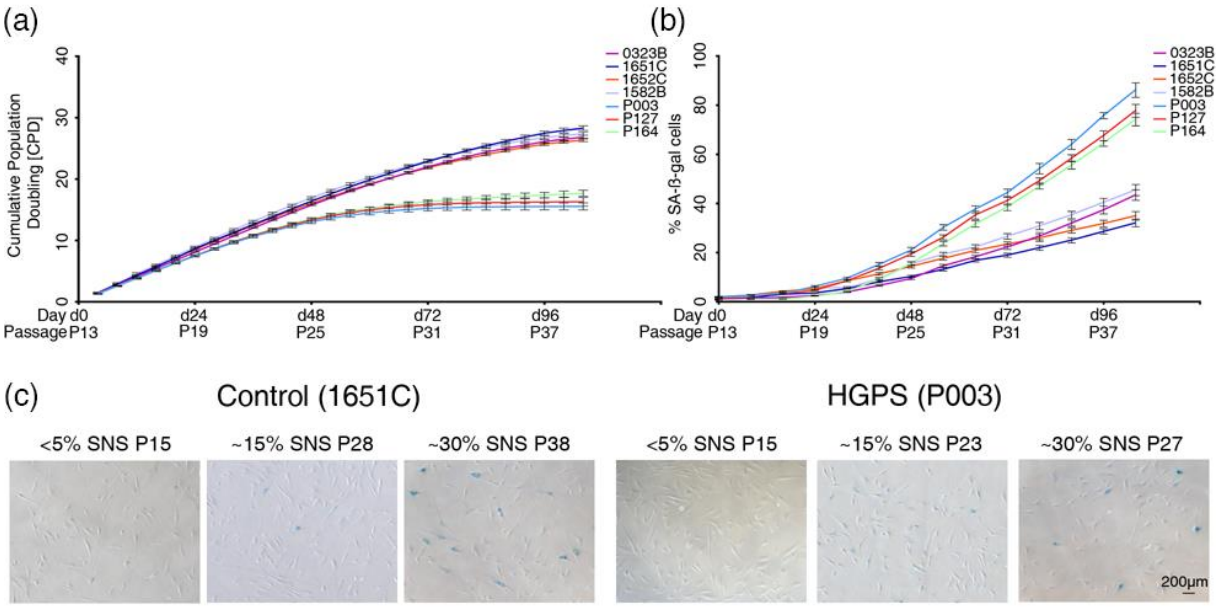

Figure 5: Characterization of the cell-based aging model. (a) Growth curves of four independent control cell strains (purple, blue, orange, gray) and three Hutchinson-Gilford progeria syndrome (HGPS) cell strains (light blue, red, and turquoise). All cultures started at passage 13, and at this passage, the percentage of SA-ß-gal-positive cells was less than 5% in all cell strains. Proliferation rates were determined over 26 passages over 104 days. (b) The percentage of SA-ß-gal-positive cells was scored every other passage in cultures from panel a. (c) Representative images of SA-ß-gal-positive cells in cultures exhibiting <5% SNS, 15% SNS and 30% SNS.

GMO1651c corresponds to normal fibroblasts and P003 corresponds to HGADFN003, an HGPS cell strain. All experiments were performed at least three times (n = 3). (Liu et al. 2019)

First, we characterized the cells of this study in terms of their growth and senescence index in every other passage (Figure 5). All cultures started at passage 13 with a senescence index of <5%. Initially, both cell types displayed similar growth rates before the HGPS cells showed premature growth arrest after six to seven passages. Ultimately, control cells also lost their proliferative capacity, but about five to ten passages later. Performing senescence-associated beta-galactosidase (SA-ß-Gal) assays in parallel confirmed that in long-term cultures at matching passage numbers, the percentage of senescence was higher in HGPS cells than in control cultures. To avoid this discrepancy, we compared cells with matching senescence levels. More specifically, we rigorously scored all cultures and started assays when <5%, 15% or 30% senescence was reached.

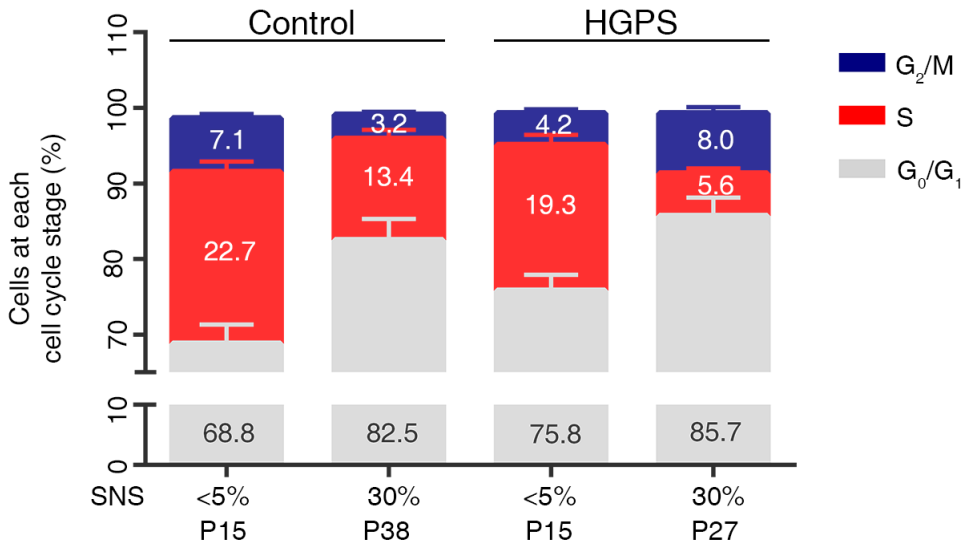

Figure 6: Cell cycle analysis of the cell-based aging model. Relative percentage of cells in the G0/G1, S and G2/M phases of the cell cycle are shown for control (1651c) and HGPS (P003) cultures with a senescence index of <5% and 30%. PI was used for DNA staining. All experiments were performed at least three times (n = 3). (Liu et al. 2019)

To further support our cell-based aging model, we performed a cell cycle assay and compared control and HGPS cells at <5% and 30% senescence (Figure 6). In brief, during S phase, cells synthesize or replicate their DNA. This is done in preparation for M phase when the cell divides. During G_1 and G_2 phases, the cell conducts a series of checks before entering S or M phase, respectively. In G_0 phase, cells have left the cell cycle and stopped dividing. As expected, the percentage of cells growing decreased during replicative senescence in both cell types, as indicated by the reduced number of cells in S phase. In accordance with this loss of proliferative capacity, the percentage of cells in G_0/G_1 phase increased in control and HGPS cultures. Interestingly, despite normalizing to senescence, we noticed a slightly decreased portion of S phase cells in HGPS cells, indicating a lower reproduction ability. For the G_2/M phase, we noticed a decrease in control cultures as cells age, meaning fewer cells are dividing as previously reported (Neurohr et al. 2019). However, in HGPS cultures, the portion of cells increased in that phase. One explanation could be found in the checkpoints of G_2 phase, which might lead to arrest more frequently in HGPS cells due to increased DNA damage.

Moreover, we analyzed p21 levels as a senescence marker to confirm ß-gal scored senescence levels (Figure 7) (Campisi 2013).

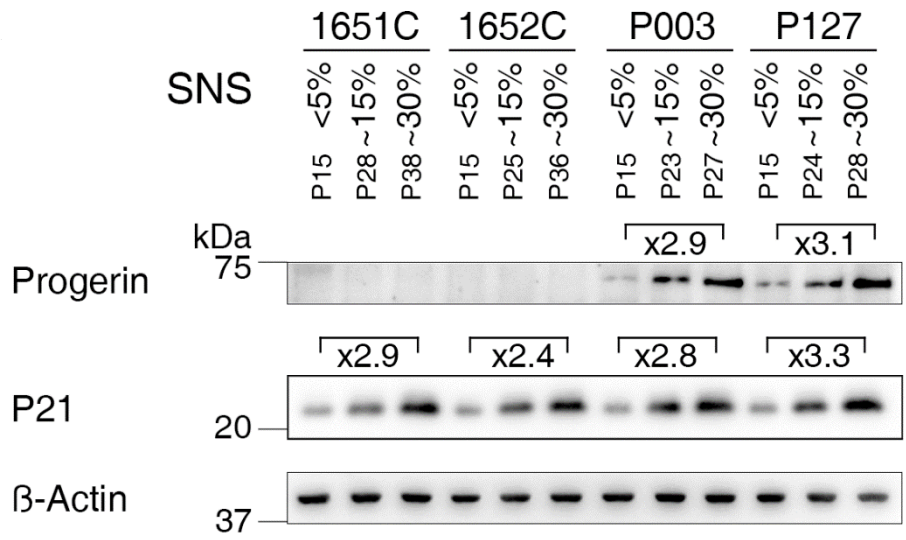

Figure 7: Progerin and p21 levels of the cell-based aging model. Representative western blot of control (1651c, 1652c) and HGPS (P003, P127) fibroblasts from cultures at the indicated percentages of senescence. Antibodies directed against the indicated proteins were used. All experiments were performed at least three times (n = 3). (Liu et al. 2019)

p21 levels were similar throughout different control and HGPS cell lines, indicating a close association to ß-gal senescence levels. Because the disease-associated protein progerin accumulates during replication cycles, we also probed progerin. Following previous results, progerin levels increased in old cultures, while it was not detectable in control fibroblasts (Goldman et al. 2004).

3.1.3 Expression profile of genes identified by data mining

Having established our cell-based aging model, we analyzed the expression profile of the 17 genes altered in vascular disease, arthritis, lipodystrophy and alopecia during replicative senescence (Figure 8). By comparing control and HGPS cells, we determined whether and to what extent these genes are dysregulated in HGPS and physiological aging.

(a)

Cell line	≤ 5% SNS (0 - 5%)	~15% SNS (13 - 17%)	~30% SNS (28 - 32%)
1651C	Passage ≤ 20	Passage 26-28	Passage 36-38
1652C	Passage ≤ 19	Passage 26-27	Passage 34-36
P003	Passage ≤ 18	Passage 21-22	Passage 26-27
P127	Passage ≤ 18	Passage 22-23	Passage 27-28

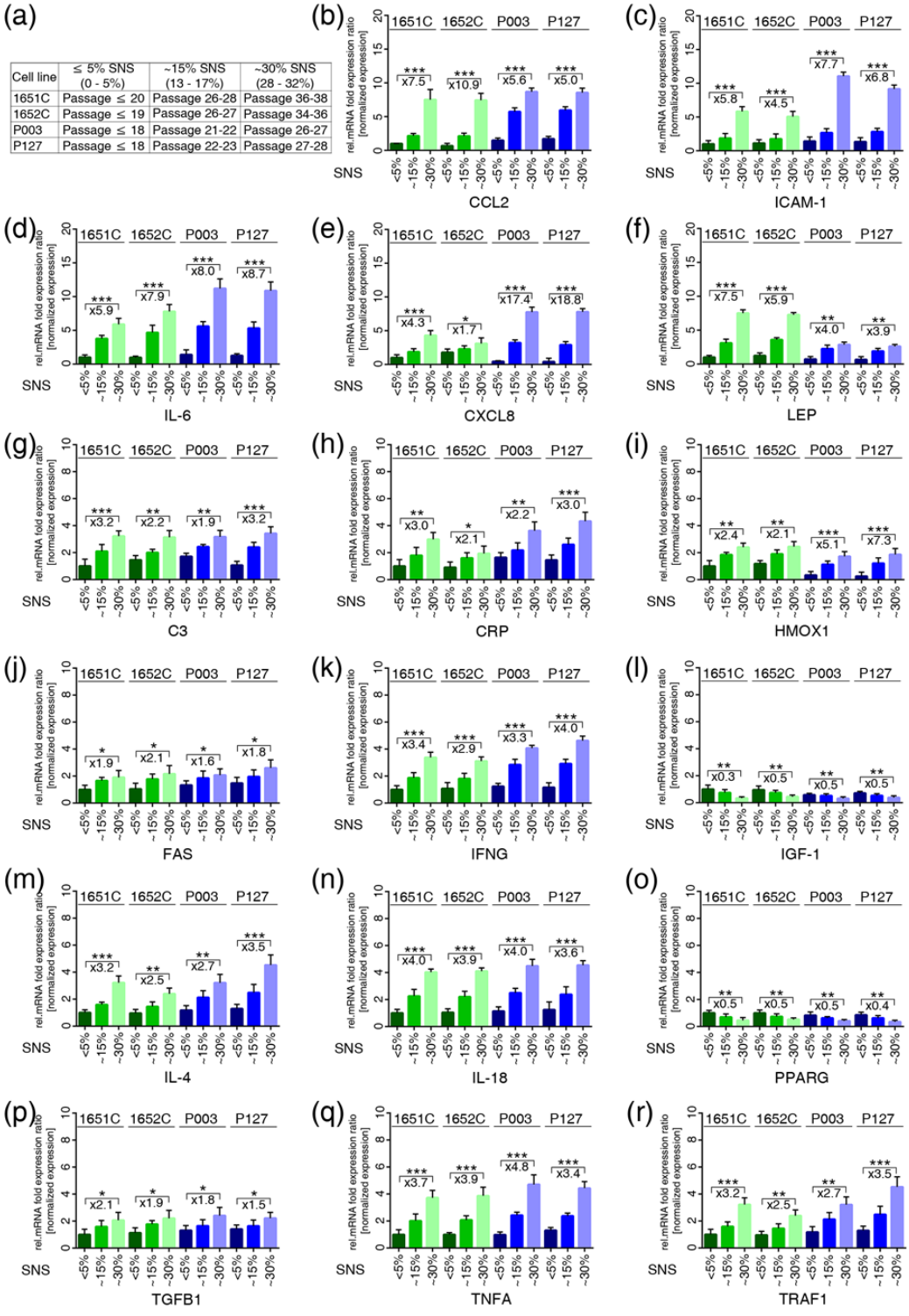

Figure 8: Quantitative real-time PCR analysis of the 17 genes identified by text mining in normal and HGPS cells during replicative senescence. (a) Table showing the cell strains and the passages corresponding percentage of senescence (SNS). (b–r) mRNA levels of the indicated genes were determined in controls (GMO1651c, and GMO1652c) and HGPS (HGADFN003 and HGADFN127) cell strains at the indicated percentage of senescence (SNS). Relative expression was normalized to the expression of GAPDH. Graphs show the mean ± SD (* $p < 0.05$, ** $p < 0.01$, *** $p < 0.001$, n = 3). The mean fold changes between 5% and 30% SNS for control and HGPS are indicated. (Liu et al. 2019)

All of the genes showed significant changes during replicative aging. Notably, there were no major differences between the expression profiles of control and HGPS cells for many of the analyzed genes, including C3, CRP, FAS, IFNG, IGF1, IL4, IL6, IL18, PPARG, TGFB1, TNFA and TRAF1. CCL2 expression in HGPS cells showed a strong upregulation at 15% senescence compared to control cells but showed comparable levels again at 30% senescence. In contrast, ICAM-1 and CXCL8 mRNA levels of progeria cells at 30% senescence were significantly elevated compared to control cultures at 30% senescence. Eventually, LEP and HMOX1 mRNA levels of progeria cells showed markedly less expression than control cultures in all levels of senescence. As described in the literature, PPARG and IGF-1 decreased in both cell types when challenged with replicative aging. In conclusion, we showed that the regulation of all 17 genes identified by literature search were consistent with the expected result. Furthermore, a very similar pro-inflammatory signaling pattern was observed between control and progeria cells.

3.1.4 JAK-STAT signaling during cellular aging

After identifying the JAK-STAT signaling to be implicated in vascular disease, arthritis, alopecia, lipodystrophy and presumably also in HGPS, we analyzed the levels of various proteins involved in the pathway. The status of the JAK-STAT pathway was of great relevance due to its regulatory properties to activate the inflammatory cellular response found in the expression profile of the 17 genes (Meyer und Levine 2014). We evaluated JAK1/2 as well as total and phosphorylated levels of STAT1/3 by western blot (Figure 9).

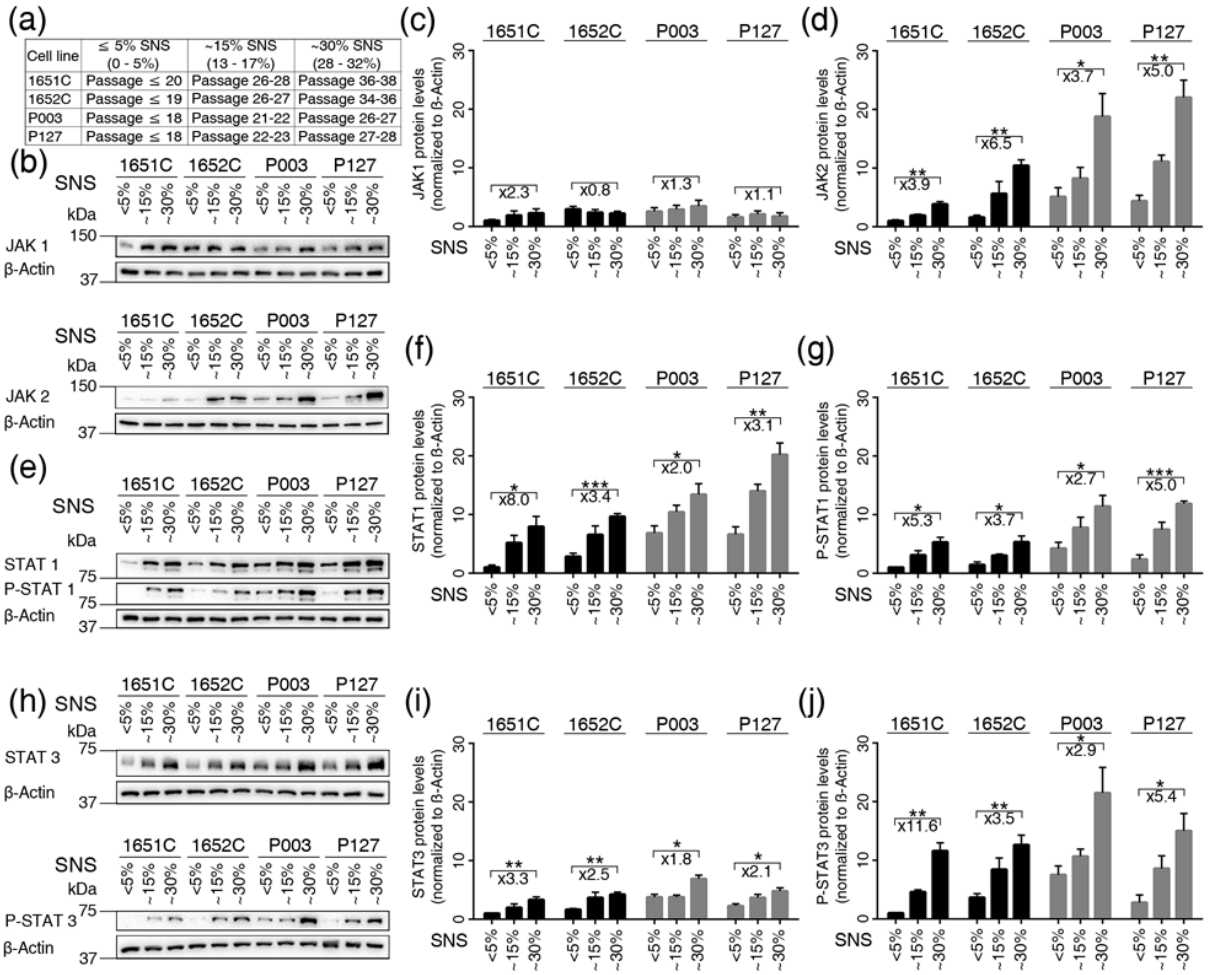

Figure 9: Status of the JAK-STAT signaling pathway in control and HGPS cells during replicative senescence. (a) Table showing the cell strains and the passages corresponding percentages of senescence (SNS). (b,e,h) Representative western blot images for JAK1/2, STAT1/3, p-STAT1 (tyr701), p-STAT3 (tyr705) and β-actin in control (GMO1651c, and GMO1652c) and HGPS (HGADFN003, and HGADFN127) cell strains at the indicated percentages of senescence. (c) Quantification of JAK1, (d) JAK2, (f) STAT1, (g) p-STAT1, (i) STAT3, and (j) p-STAT3. Graphs show the mean ± SD. (* $p < 0.05$, ** $p < 0.01$, *** $p < 0.001$, n = 3). Fold changes between the samples with 5% and 30% senescence are indicated. (Liu et al. 2019)

While JAK1 did not show a regulation upon replicative aging in any of the cells, JAK2 protein levels multiplied in a cellular-age-dependent manner in both cell types. Downstream of the JAK proteins, STAT1 and STAT3 were analyzed and showed similar cellular-age-dependent expression signatures. Both total and phosphorylated forms of STAT1 and STAT3 increased significantly in both cell types during replicative aging, indicating a clear JAK-STAT activation. Although the increase in both cell types was apparent, it was even more prominent in HGPS and started at <5% senescence.

Taken together, these data indicate an overactivation of the JAK-STAT signaling pathway during replicative aging in control and HGPS cells.

3.1.5 Baricitinib treatment inhibited JAK-STAT signaling

Overactivation of the JAK-STAT signaling in cultures with high senescence prompted us to rebalance this pathway in order to restore cell homeostasis. To block excessive signaling, we used baricitinib (Bar, LY3009104), a drug that selectively and reversibly inhibits two of the JAK protein family members (JAK1/2) and already received FDA approval (Fridman et al. 2010). First, we assessed the cellular toxicity of Bar using different concentrations (Figure 10).

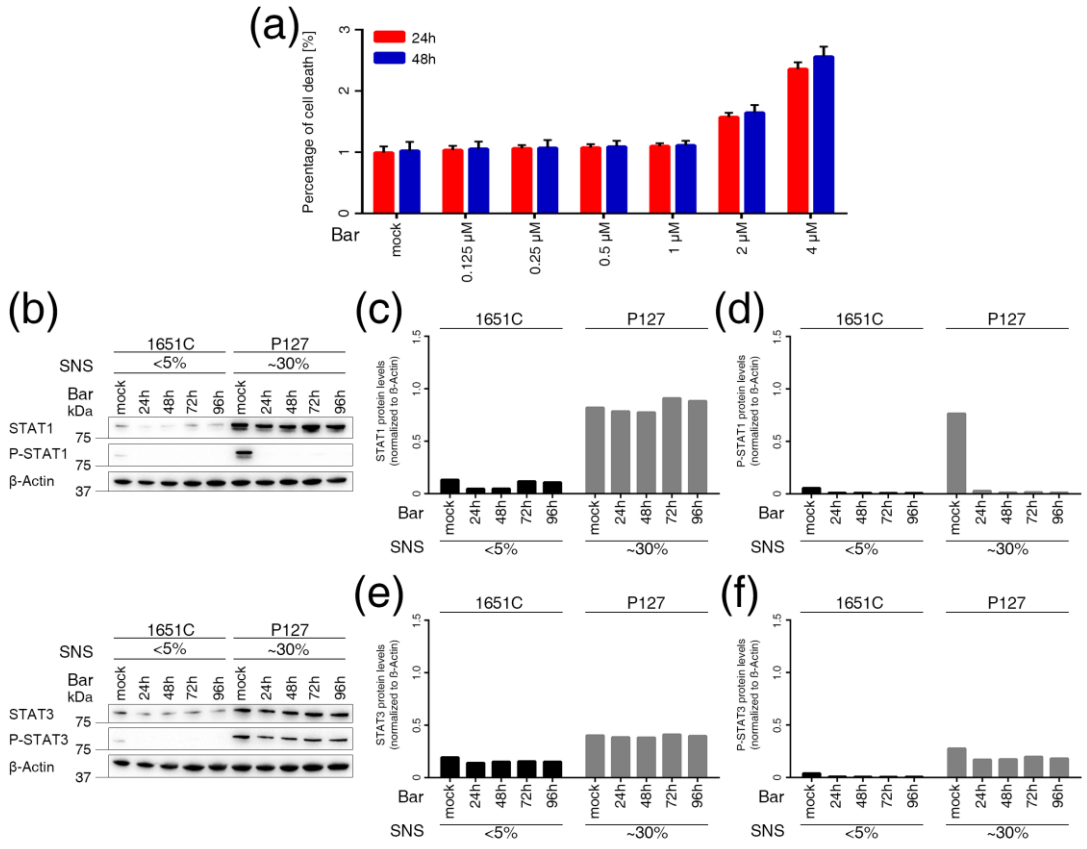

Figure 10: Cytotoxicity and stability of Bar in a cell-based aging model. (a) Cell cytotoxicity was determined by CellTox™ Green Cytotoxicity Assay kit on control fibroblasts GMO1651C. Cells were treated with Bar at different concentrations (0.125 µM, 0.25 µM, 0.5 µM, 1 µM, 2 µM, 4 µM) for 24 and 48 hours. (b) Representative western blots images for STAT1/3 and p-STAT1/3 and ß-actin of control (GMO1651) and HGPS (HGDFN127) at the indicated senescence index were treated with Bar or DMSO for the indicated period without changing the medium. (C-f) Quantification of STAT1, p-STAT1, STAT3, and p-STAT3, respectively. Graphs show mean (n = 3). (Liu et al. 2019)

No cellular toxicity was detected up to a concentration of 1 µM, regardless if cultures were treated for 24 h or 48 h. From 2 µM, an increase in toxicity was observed. Next, we selected 1 µM of Bar, which showed similar basal toxicity as mock-treated cells and analyzed the potency and stability of inhibition. Phosphorylated forms of STAT1 and STAT3 were effectively inhibited and lasted for up to 96 h.

After that, because many cellular processes are relatively slow (e.g. senescence entry), we used Bar for a long-term treatment (van Deursen 2014). The treated medium was changed every two to three days according to our stability experiments. After one month, we again assessed JAK-STAT signaling by western blot (Figure 11).

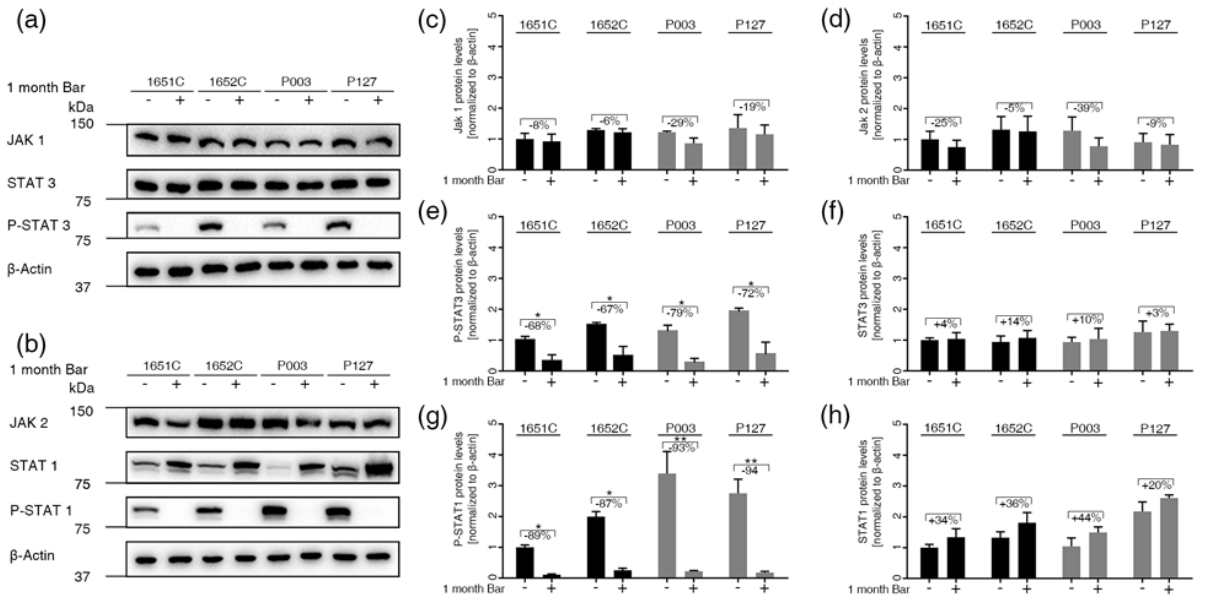

Figure 11: Status of the JAK-STAT signaling pathway in normal and HGPS cells. (a,b) Representative images of western blots for JAK1/2, STAT1/3, P-STAT1/3 and β-actin in normal (GMO1651c, and GMO1652c) and HGPS (HGADFN003, and HGADFN127) cells treated as indicated. Cultures exhibiting <5% senescence were treated with Bar or DMSO for a period of one month. (c) Quantification of JAK1, (d) JAK2, (e) P-STAT3, (f) STAT3, (g) P-STAT1, and (h) STAT1. Graphs show the mean ± SD. (* $p < 0.05$, ** $p < 0.01$, *** $p < 0.001$, $n = 3$). (Liu et al. 2019)

JAK1 and JAK2 proteins remained at the same level under all conditions. As expected, phosphorylated STAT1 and STAT3 levels were significantly reduced in both cell types when treated with Bar. At total STAT1 levels, there was an upregulating trend in Bar-treated cultures that might be an adaptation. However, total STAT3 levels remained

constant. In summary, these results showed that Bar effectively inhibits activation of STAT1 and STAT3 and thereby blunts the JAK1/2-STAT1/3 signaling pathway in control and HGPS cells.

3.1.6 Assessing cellular health aspects in cultures treated with baricitinib

Our analysis of the JAK-STAT signaling pathway revealed stable inhibition with Bar for up to one month. To understand how this affects cellular homeostasis, we investigated some of the critical health aspects in HGPS, including growth, senescence, autophagy, proteasomal activity, ROS and ATP levels (Figures 12-14). Replicative senescence in healthy cultures and during HGPS development is characterized by a functional decline of various tissues and a proinflammatory secretory phenotype (Coppé et al. 2010). We first assessed growth rates and senescence (Figure 12).

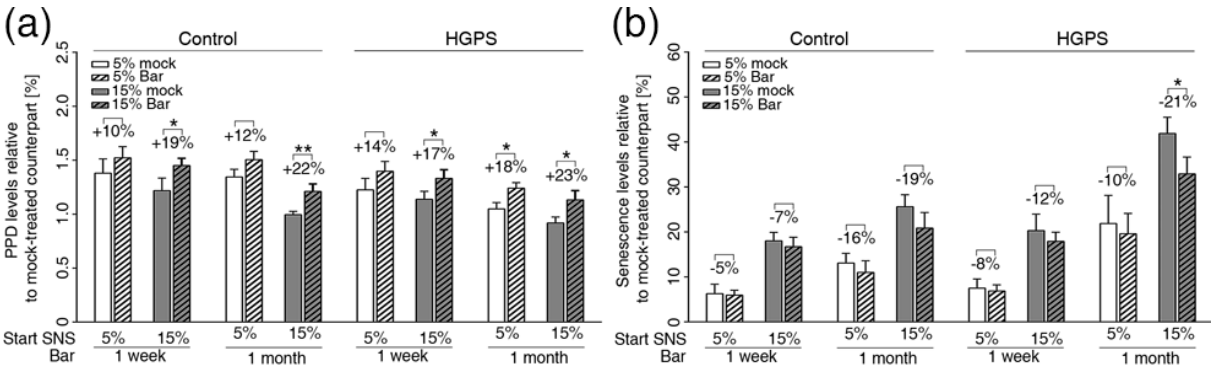

Figure 12: Bar treatment ameliorates cell growth and senescence during long-term treatment. (a) Graph shows the population doublings of control (GMO1651c, and GMO1652c) and HGPS (HGADFN003, and HGADFN127) cells. Bar (1 µM) or DMSO treatment was administrated for one week or one month as indicated. The percentage of senescence (SNS) in cultures prior to treatment is indicated. (b) Graph shows the percentage of SA-ß-gal-positive cells measured after treatment. Graphs show the mean ± SD. (* $p < 0.05$, ** $p < 0.01$, *** $p < 0.01$, ($n = 3$)). (Liu et al. 2019)

Population doublings and senescence indices were determined either with a starting senescence of ~5% or ~15% and then treated for one week and one month. In contrast to HGPS cells, control cells showed a higher PPD and correspondingly lower senescence under the same conditions. This effect increased over time and was

particularly evident in cultures that were treated for one month. Bar treatment increased cellular growth rates of both control and HGPS cells after one week and one month. However, the best improvement was particularly seen in HGPS cells with ~15% senescence, i.e., those with active JAK-STAT signaling (Figure 12). In line with growth rates, senescence levels decreased under all conditions, but this effect was also most pronounced in ~15% senescence HGPS cells treated for one month.

Of particular interest in aging research in general, and in HGPS because of the accumulation of progerin is the cellular degradation system consisting of two mechanisms; autophagy and proteasomal activity (Aman et al. 2021). These processes eliminate and recycle unnecessary and dysfunctional molecules and subcellular elements (e.g. progerin) and therefore promote homeostasis, development and survival (Figure 13).

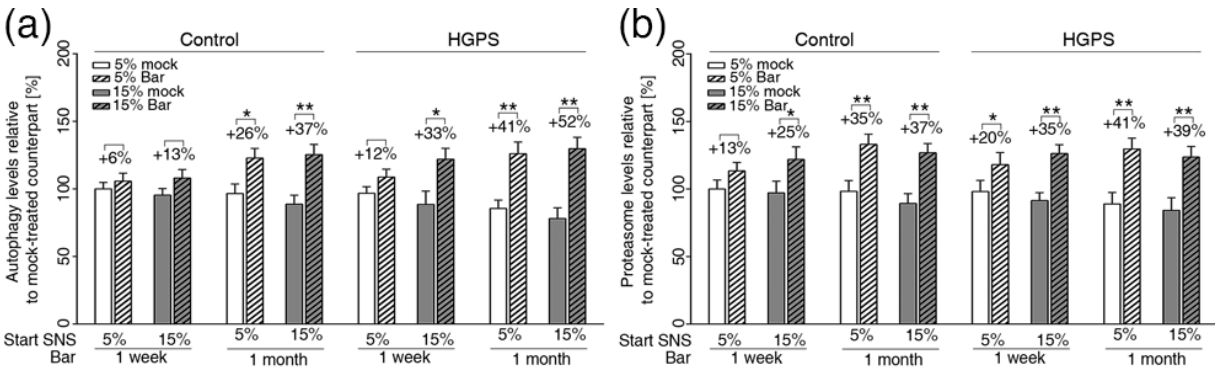

Figure 13: Bar treatment ameliorates normal and HGPS autophagy and proteasomal levels during long-term treatment. (a) Autophagy activity was determined by measuring MDC levels using fluorescence photometry. (b) Proteasome activity was determined by measuring chymotrypsin-like proteasome activity using Suc-LLVY-AMC as a substrate. Graphs show the mean ± SD. (* $p < 0.05$, ** $p < 0.01$, *** $p < 0.01$, ($n = 3$)). (Liu et al. 2019)

For both parameters, autophagy and proteasomal activity, the basal levels of HGPS cultures were slightly reduced in all conditions compared to control cells. Furthermore, an increase in senescence inhibited the degradation system, as previously described (López-Otín et al. 2013). The greatest improvement was shown after one month treatment in HGPS cells with a starting senescence of ~15%. Nevertheless, Bar

enhanced all autophagy levels independently of their senescence or treatment duration. Similarly, proteasomal degradation showed an increase in both cell types when treated with Bar. The treatment eventually showed normalization of both parameters comparable with mock-treated cells exhibiting ~5% senescence or even a further increase.

Next, we assessed mitochondrial function by analyzing total ATP and ROS levels (Figure 14). Mitochondrial dysfunction is heavily implicated in the aging process and is one of the hallmarks of aging (Trifunovic und Larsson 2008). In addition, further mitochondrial alterations were detected in HGPS cells, which are attributed to the progerin protein (Rivera-Torres et al. 2013).

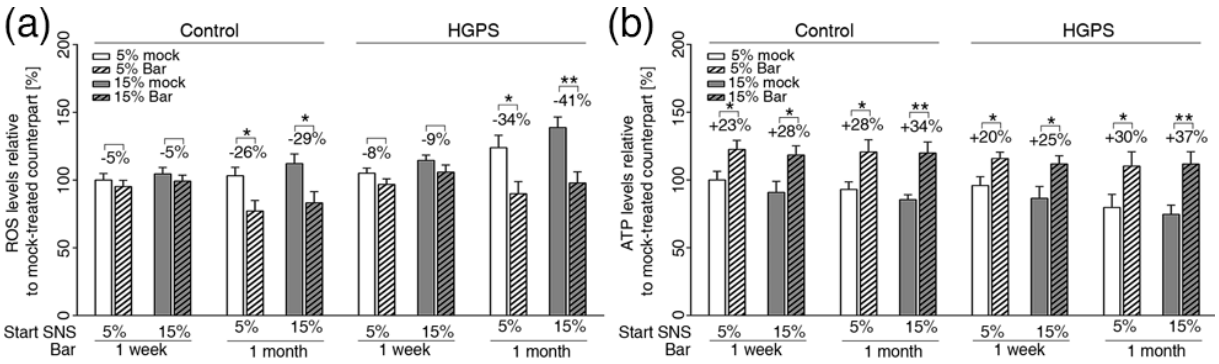

Figure 14: Bar treatment ameliorates mitochondrial function during long-term treatment. (a) Intracellular ROS levels were determined by measuring oxidized dichlorofluorescein (DCF) levels using a DCFDA cellular ROS detection assay. (b) Cellular ATP levels were measured using a CellTiter-Glo luminescence ATP assay. Graphs show the mean ± SD. (* $p < 0.05$, ** $p < 0.01$, *** $p < 0.01$, (n = 3)). (Liu et al. 2019)

First of all, an aging effect was seen in ATP and ROS levels. While ATP levels decreased with senescence, the quantity of ROS increased. Cultures of both cell types continued to show similar ROS levels after one week of Bar treatment compared to mock counterparts. In contrast, ROS levels were significantly reduced after one month of Bar treatment in both cell types, starting from ~5% or ~15% senescence. ATP levels seemed to respond more quickly to Bar treatment, showing a significant change after only one week and remained similarly elevated after one month.

Western blot was performed to assess if the protein degradation system affects progerin levels (Figure 15). Moreover, the amount of progerin also has an impact on almost all cellular health aspects.

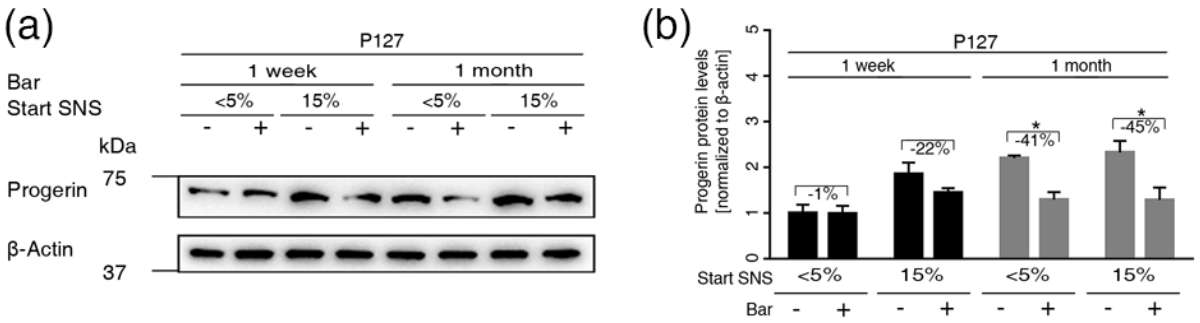

Figure 15: Bar treatment reduces HGPS progerin levels during long-term treatment. (a) Representative images of a western blot for progerin in HGPS (HGADFN127) cells from cultures at 5% and 15% senescence that were administrated the mock or Bar treatment for one week or one month as indicated. (b) Quantification of the progerin signal. Graphs show the mean ± SD. (* $p < 0.05$, ** $p < 0.01$, *** $p < 0.01$, ($n = 3$)). (Liu et al. 2019)

Since progerin accumulates during replicative senescence, we observed a reduction especially in cultures with a high senescence index. Progerin was decreased by 45% after one month Bar treatment, starting with ~15% senescence. In conclusion, Bar treatment reduced progerin levels by enhancing autophagy and proteasomal activity. In addition, JAK-STAT inhibition restored proliferation, proteostasis and mitochondrial function, thus ameliorating cellular homeostasis and reversing key hallmarks of aging.

3.1.7 Bar treatment reduces proinflammatory cytokine expression

Having identified the 17 mainly proinflammatory genes through text mining and their association to the JAK-STAT pathway, we aimed to investigate the downstream effects when inhibited. Assuming the overactivation shown in Fig. 8 and 9 are linked to each other, we specifically tested if inhibition of the JAK1/2-STAT1/3 signaling axis can rebalance the expression of the identified genes and therefore ameliorate progression of HGPS and other age-related diseases (Figure 16).

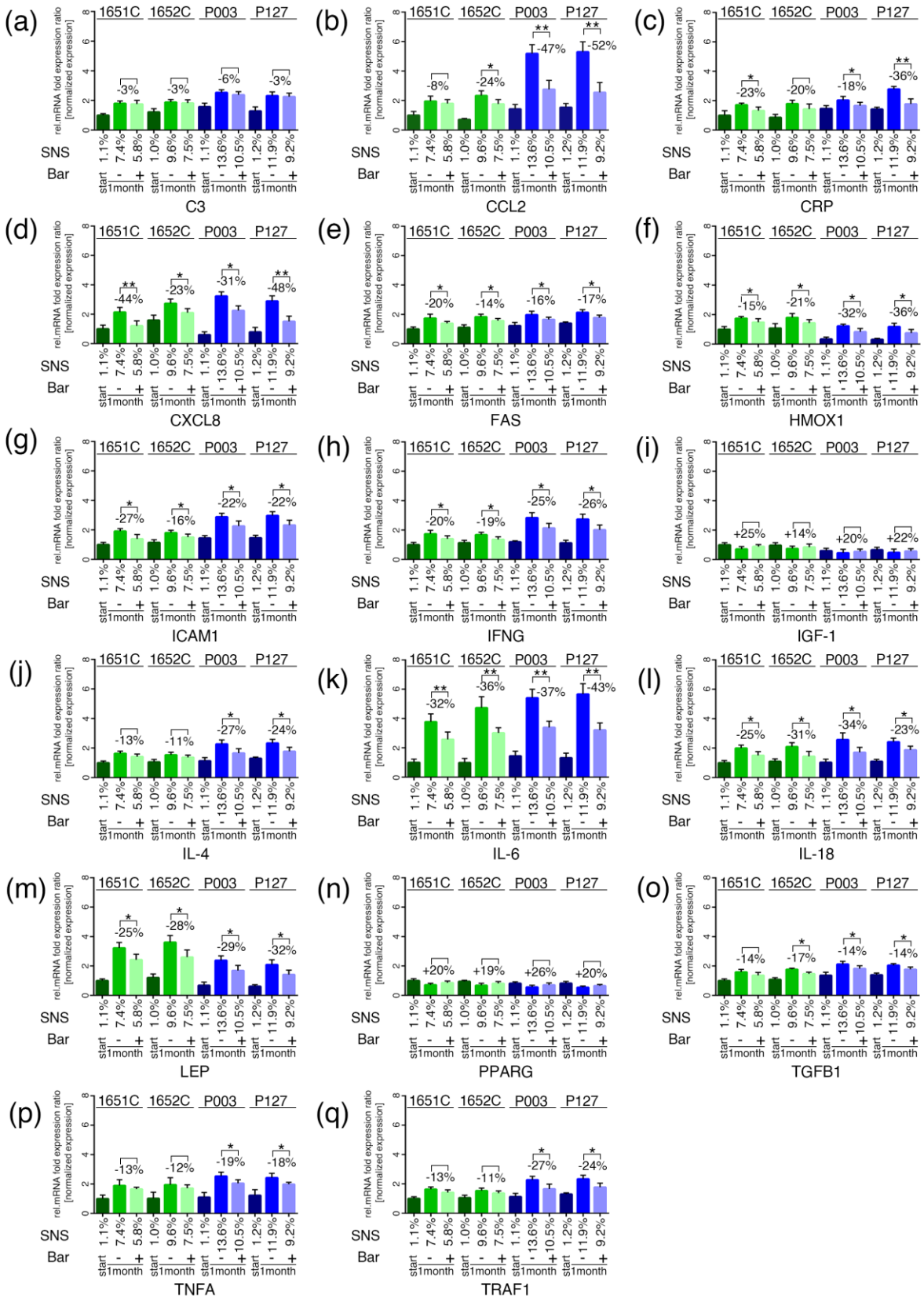

Figure 16: Real-time PCR analysis of the 17 genes identified by text mining in normal and HGPS cells treated with Bar for a period of 1 month. (a-q) mRNA of indicated genes were determined in controls (GMO1651c, GMO1652c) and HGPS (HGADFN003 and HGADFN127) cell lines. The starting senescence index of the culture is indicated (Start SNS). The senescence index of the cultures at the end of the treatment is indicated. Relative expression was normalized to the expression of GAPDH. Graphs show the mean ± SD. (* $p < 0.05$, ** $p < 0.01$, *** $p < 0.01$, ($n = 3$)). (Liu et al. 2019)

Gene expression profiles of the 17 identified genes are shown. Senescence indices before the start of therapies as well as after one month mock or Bar treatment are indicated. All cultures had low senescence indices (<5% SNS) in the beginning and after one month Bar treatment the senescence in treated cultures were lower than the senescence of one month mock treatment in both cell types. Furthermore, Bar lowered most of the cytokine levels; CCL2, CRP, CXCL8, FAS, HMOX1, ICAM1, IFNG, IL4, IL6, IL18, LEP, TGFB1, TNFA and TRAF. C3, IGF-1 and PPARG showed no significant change. Bar thus inhibited and rebalanced many of the cytokine/chemokine levels belonging to the SASP, leading to a delay in senescence in these cells.

3.1.8 Bar inhibits etoposide induced JAK-STAT overactivation

To further validate the therapy strategy, we exposed control and HGPS cells to etoposide, a topoisomerase inhibitor that leads to DNA damage and subsequent DNA damage-induced senescence (te Poele et al. 2002). Etoposide is commonly used as an anti-cancer drug in form of a chemotherapy. In brief, etoposide forms a ternary complex with DNA and the topoisomerase II, which leads to double-stranded breaks and hindrance to repair that site. This in turn results in a sustained damage response, eventually triggering cell cycle arrest and senescence (Montecucco et al. 2015). Nevertheless, etoposide-induced senescence shows a similar signaling signature compared to replicative senescence, including elevated p21 levels, activated P53, ATM and ATR proteins and increased secretion of cytokines, chemokines, growth factors and proteases (Novakova et al. 2010; Rodier et al. 2011).

To see how Bar could prevent etoposide-induced senescence, we performed qPCRs for key cytokines, SA-ß-Gal assays and western blots for p21, progerin and STAT1/3 (Figure 17). Both cell types were pre-treated for two days with either mock or Bar

treatment and then exposed to 5 µM of etoposide for six days. Following these steps, standard media was used for another four days.

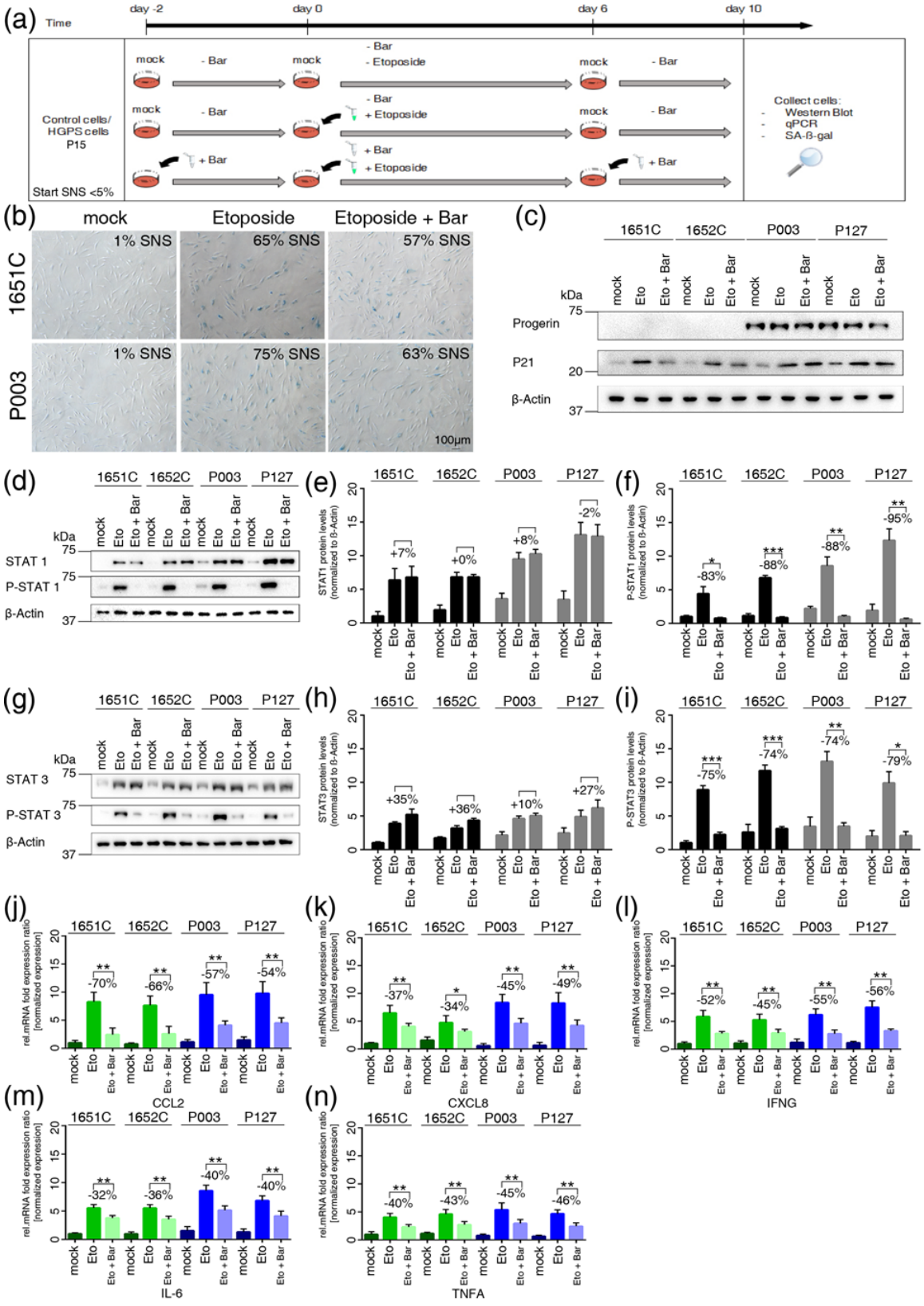

Figure 17: Etoposide treatment activates the JAK-STAT signaling pathway in HGPS and normal cells. (a) Schematic representation of the etoposide treatment protocol. All treatments started with cultures exhibiting <5%

senescence (SNS). Cells were either pretreated with or without 1 µM Bar for two days and then expose to medium with or without etoposide in the presence or absence of Bar for a period of six days. Next, cells were grown for four days with or without Bar as indicated. (b) Representative images of SA-ß-gal-positive cells in mock-, etoposide- and etoposide + Bar-treated cultures (GMO1651c and HGADFN003) are shown. The percentages of senescence (SNS) after treatment are indicated. (c) Representative images of western blots for progerin, p21 and ß-actin in normal (GMO1651c, and GMO1652c) and HGPS (HGADFN003, and HGADFN127) cells treated as indicated. (d) and (g) Representative images of western blots for JAK1/2, STAT1/3, P-STAT1/3 and ß-actin in normal (GMO1651c, and GMO1652c) and HGPS (HGADFN003, and HGADFN127) cells treated as indicated. (e) Quantification of STAT1, (f) p-STAT1, (h) STAT3, and (i) p-STAT3. The percent change between etoposide- and etoposide+Bar-treated cells is indicated. (j–n) Quantitative real-time PCR analysis of CCL2, CXCL8, IFNG, IL6, and TNFα in cells treated as indicated. Relative expression was normalized to the expression of GAPDH. Graphs show the mean ± SD. (* $p < 0.05$, ** $p < 0.01$, *** $p < 0.01$, ($n = 3$)). (Liu et al. 2019)

At first, we tested if and how much etoposide could induce senescence by performing a SA-ß-Gal assay. In control cells, we could induce senescence to 65% and in HGPS cells even up to 75%. Co-treatment with Bar led to a ~10% reduction, but most cells seemed to have accumulated too much DNA-damage. In line with this result, p21 levels increased sharply when cells were exposed to etoposide. Progerin levels were not affected and remained almost identical. Similar to replicative senescence, DNA damage-induced senescence showed an overactivation of STAT1 and STAT3, both in the total and phosphorylated forms. Using Bar blocked phosphorylation of both proteins even if the total levels did not change. In addition, qPCR analysis for six of the key proinflammatory cytokines CCL2, CXCL8, IFNG, IL6 and TNFA showed that all of them were upregulated in etoposide-treated cultures. As assumed, Bar-co-treatment significantly reduced those levels to almost normal under 5% mock-treated cultures. Collectively, etoposide-induced senescence resembled replicative senescence very much, including its overactivation of the JAK-STAT signaling and consecutive cytokines/chemokines expression. Inhibition of the JAK1/2-STAT1/3 signaling axis reduced this expression and delayed senescence.

3.2. Combination Treatment of Baricitinib and Lonafarnib

3.2.1 Bar normalizes FTI induced senescence and improves proliferative rate of control and HGPS fibroblasts

Combined therapy of Bar and FTI (lonafarnib) is a promising approach to further improve the clinical picture of HGPS. These drugs target different sites and can thus act synergistically and complementary. Bar, as already shown, inhibited the JAK-STAT signaling and dampened inflammation resulting in delayed senescence and ameliorated cellular homeostasis. FTI, on the other hand, prevents farnesylation of cysteine residues in proteins harboring a carboxyl-terminal CAAX motif, e.g., blocking the farnesylation of progerin (Toth et al. 2005). It was shown that this reverses nuclear envelope abnormalities in HGPS cells and most importantly extends the lifespan of HGPS animal models and patients (Capell et al. 2005; Glynn und Glover 2005; Dhillon 2021).

Previously, we showed that 0.025 µM FTI was sufficient to reduce progerin levels while still remaining cell growth (Gabriel et al. 2017). All treatments in the following experiments were carried out for nine days and started with an initial senescence index of ~15%. Since Bar and FTI have different effects on the proliferative capacity of cells, we first analyzed cell growth and expression of senescence markers (Figure 18).

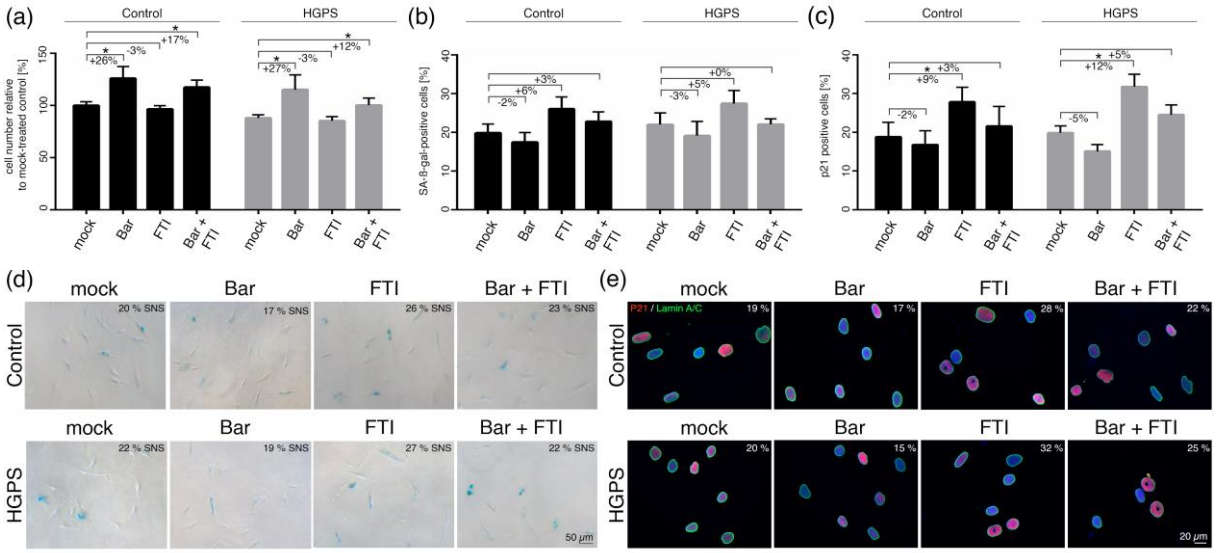

Figure 18: Replicative senescence of control and HGPS fibroblasts after treatment with baricitinib and FTI. (a) Cell numbers relative to mock-treated control cells. All cultures were started with ~15% senescence. Cells were either treated with vehicle (DMSO), Bar (1 µM), FTI (0.025 µM), or combined drugs for a period of nine days. (b) Graph shows the percentage of SA-ß-gal-positive cells measured after indicated treatments. (c) Percentage of cells positive for p21 after indicated treatment. (d) Representative images of SA-ß-gal-positive cells in treated cultures. Scale bar: 50 µm. (e) Representative immunofluorescence images of control GM01651C and HGPS HGADFN127 fibroblasts after the indicated treatment. Antibodies against p21 (red) and lamin A/C (green) were used, and DNA was stained with DAPI. Fluorescence images were taken at 40× magnification. Scale bar: 20 µm. Graphs show mean ± SD. Representative images are shown (n = 3; * p < 0.05, ** p < 0.01). (Arnold et al. 2021)

Cell numbers of control and HGPS fibroblasts revealed a significant upregulation when treated with Bar or in combination. FTI-treated cells remained on the same level as mock-treated counterparts, confirming that noticeable growth inhibition only occurs with higher concentrations (Gabriel et al. 2017). SA-ß-gal positive cells remained constant after nine days therapy regimen. In addition, we checked p21 levels as this senescence marker is considered an early indicator and might visualize effects that normally take more time to manifest. In fact, FTI-treated cultures showed a significant increase in p21 positive cells, while Bar-treated cells exhibited a slight decrease in both cell types. Combination therapy had similar p21 levels compared to mock-treated counterparts. This suggests that after nine days of treatment, Bar could in part prevent cellular senescence caused by FTI.

Furthermore, the JAK-STAT signaling status was important. We investigated the effect of FTI on that pathway and wanted to confirm successful inhibition in combination

therapy. We assessed phosphorylated and total forms of STAT1 and STAT3 (Figure 19).

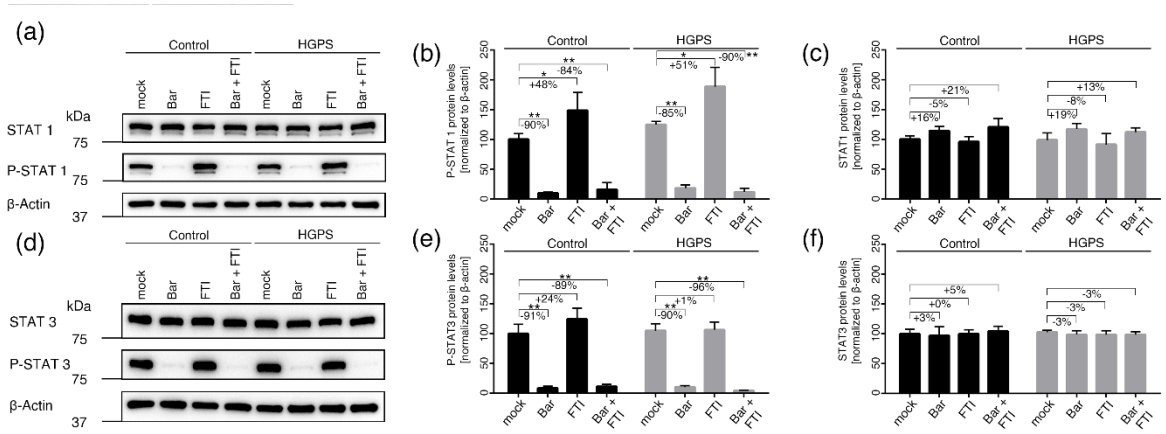

Figure 19: JAK-STAT signaling status of control and HGPS fibroblasts after treatment with baricitinib and FTI. (a, d) Representative images of western blots for STAT1, P-STAT1, STAT3 and P-STAT3. Quantification of P-STAT1 (b), STAT1 (c), P-STAT3 (e), and STAT3 (f). Graphs show mean ± SD. Representative images are shown (n = 3; * p < 0.05, ** p < 0.01). (Arnold et al. 2021)

Total levels of STAT1 and STAT3 remained constant in all treatment regimens and in both cell types, although STAT1 tended to increase in Bar-treated cells. As expected, cultures containing Bar or combined drugs demonstrated effective inhibition of phosphorylated STAT1 and phosphorylated STAT3. In contrast, FTI-treated control and HGPS cells showed increased levels of phosphorylated STAT1. However, phosphorylated STAT3 was not increased, indicating a STAT1-dependant overactivation in FTI-treated cells.

3.2.2 Cellular separation defects are caused by FTI-treatment

To find the cause and cellular mechanism for the increased p-STAT1 levels upon FTI treatment, we first analyzed the commonly described side effect, namely donut-shaped cells (Verstraeten et al. 2011). In particular, separation defects of mitotic cells due to lack of farnesylation of cenp proteins seem to be deleterious (Verstraeten et al. 2011). In addition, an accumulation of toxic levels of prelamin A, mislocalization of lamin B2

to the nucleoplasm and decreased lamin B1 levels at the nuclear envelope are found (Adam et al. 2013). As these defects may also result in further phenotypic abnormalities, we assessed the number of micronuclei and cytoplasmic DNA fragments (Figure 20).

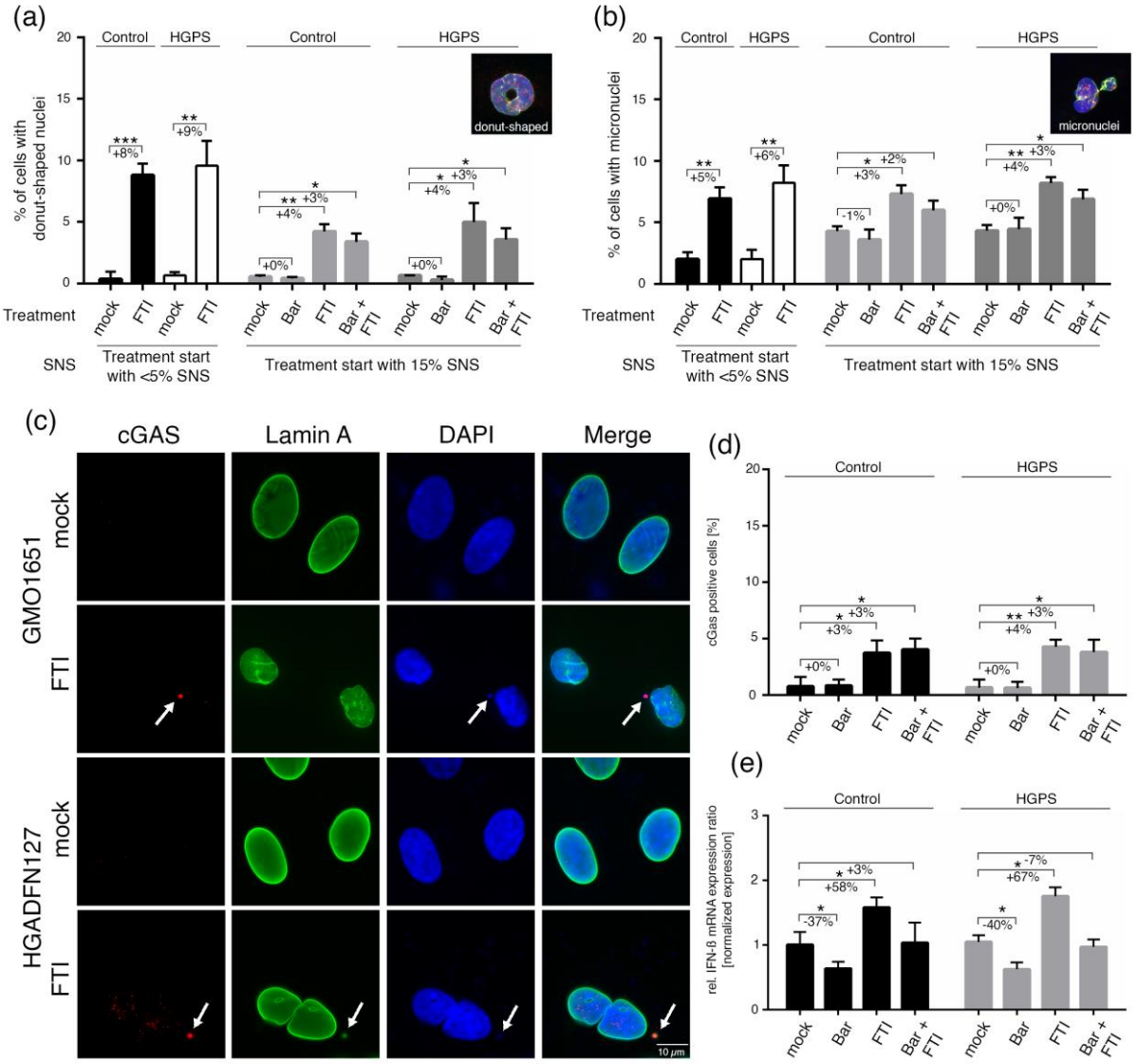

Figure 20: FTI treatment activates the cGAS-STING pathway. (a) Determination of the frequency of donut-shaped nuclei with indicated treatment and senescence (SNS). Cells were either treated with vehicle (DMSO), Bar (1 µM), FTI (0.025 µM), or combined drugs for a period of nine days. (b) Determination of the frequency of micronuclei at indicated treatment and senescence after a period of nine days. (c) Representative immunofluorescence images of an HGPS (HGADFN127) fibroblast cell strain treated for nine days as indicated. Antibodies against lamin A (green) and cGAS (red) were used, counterstained with DAPI. Fluorescence images were taken at a 60× magnification. Scale bar: 10 µm. (d) Percentage of cells positive for cGAS after indicated treatment. (e) Quantitative real-time PCR analysis of IFN-β in cells treated as indicated. Relative expression was normalized to expression of GAPDH. Graphs show mean ± SD. Representative images are shown (n = 3; * $p < 0.05$, ** $p < 0.01$, *** $p < 0.001$). (Arnold et al. 2021)

As expected, the number of donut-shaped cells was significantly increased in FTI-treated cultures in both control and HGPS cells. Furthermore, combination treatment did not improve the damage associated with FTI alone. An FTI-induced effect was also seen in the number of micronuclei, again in control and HGPS cultures. Similarly, Bar did not lead to a relevant improvement. Since these two phenomena are particularly prominent in dividing cells, we analyzed young mitotic cultures. Indeed, we showed that the FTI-induced effect was even more pronounced in the cells with a low senescence index.

Interestingly, we not only observed micronuclei in the immunofluorescence samples but also cytoplasmic DNA fragments, suggesting an active cytosolic DNA-sensing cGAS-STING pathway of the innate immune system (Sun et al. 2013; Wu et al. 2013). FTI and combined treatment resulted in an increased percentage of cGAS positive cells in control and HGPS cells. Bar-treated cells showed similar levels compared to mock-counterparts. cGAS activation upon FTI treatment revealed that the separation defects still extend beyond the donut-shaped cells already described. Following, it presumably also activated signaling pathways such as cGAS-STING signaling, which will further regulate the expression of inflammatory genes (e.g., SASP factors such as type I interferons (Sun et al. 2013)). At this point, the feedback loop closes since type I IFNs are known to activate different JAK proteins that in turn phosphorylate STAT1 and STAT2 (Capobianchi et al. 2015). Relative mRNA levels showed the anticipated upregulation in FTI-treated cultures of both cell types. However, Bar-treated cells reduced IFN-ß mRNA levels, while the combination treatment showed similar levels as the mock treatment. Taken together, we show a novel side effect of FTI, including the cellular mechanism which activated cGAS-STING signaling, leading to the induction of p-STAT1.

3.2.3 Bar and FTI reduce proinflammatory cytokine expression

Proinflammatory cytokine expression as part of the SASP is a major driver of aging and senescence (Coppé et al. 2010). Figure 8 showed that control and HGPS fibroblasts exhibited a strong upregulation of those cytokines during replicative senescence (Liu et al. 2019). As Bar and FTI interfere with signaling involved in inflammation, through inhibiting JAK-STAT and blocking farnesylation of Ras, we assessed the expression profiles of IL-1α, CCL2, IL-6 and CXCL8 upon treatment (Figure 21).

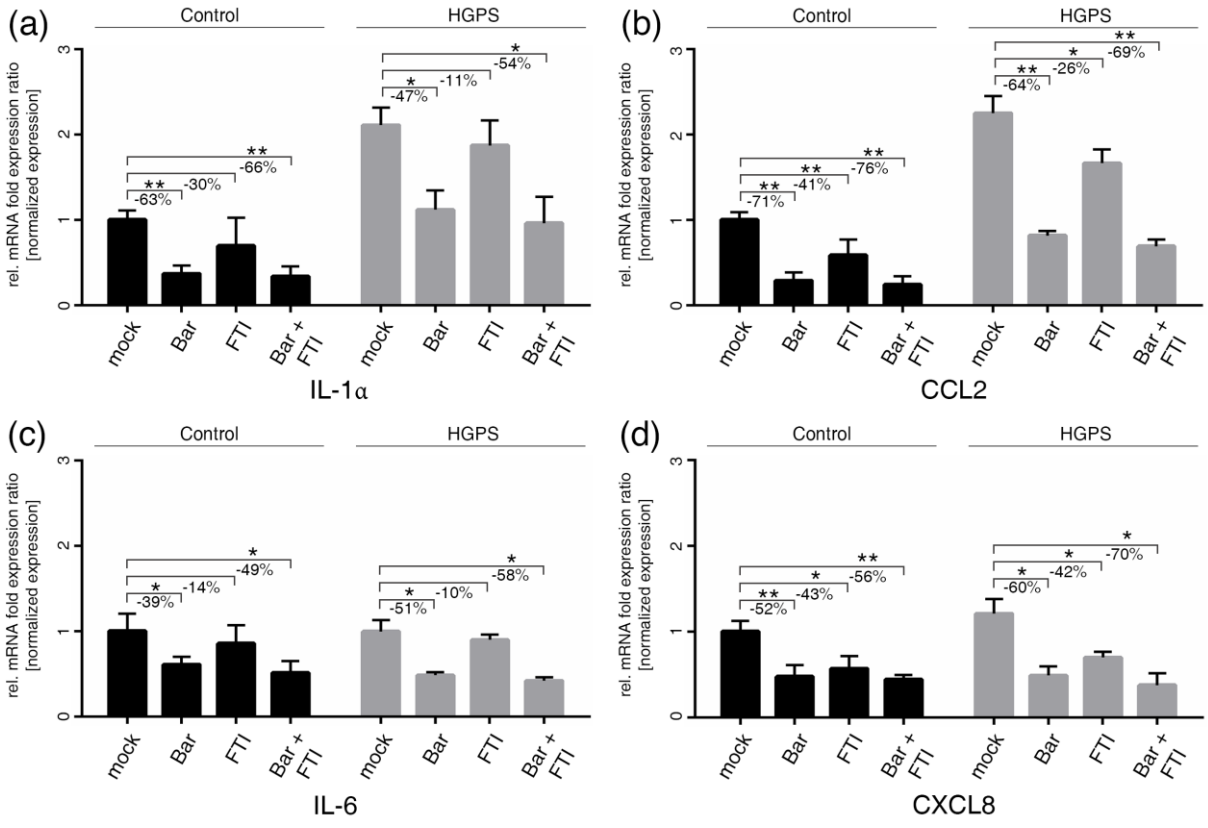

Figure 21: SASP factors are blunted by treatment with Bar and FTI. (a–d) Quantitative real-time PCR analysis of IL-1α, CCL2, IL-6, and CXCL8. Cultures at 15%SNS were either treated with vehicle (DMSO), Bar (1 µM), FTI (0.025 µM), or combined drugs for a period of nine days. Relative expression was normalized to expression of GAPDH. Graphs show mean ± SD (n = 3; * p < 0.05, ** p < 0.01). (Arnold et al. 2021)

Bar treatment in both cell types reduced the mRNA level of all cytokines significantly. FTI treatment reduced the expression of CCL2 and CXCL8 but did not reach

significance in IL-1α and IL-6. Interestingly, combining both drugs did not lead to an additional inhibition over that of Bar-treated cells alone. Nevertheless, Bar and FTI seem to reduce proinflammatory cytokine production, expressed by senescent cells and further increase inflammation in those cultures.

3.2.4 Combined treatment rescues nuclear shape abnormalities by reducing progerin levels

To maintain proteostasis, the cell utilizes two proteolytic mechanisms: lysosomal autophagy and the ubiquitin-proteasome system (Gamerdinger et al. 2009). In principle, both can reduce toxic progerin protein and thus prevent other harmful processes. Therefore, we started to investigate progerin and prelamin A levels (Figure 22).

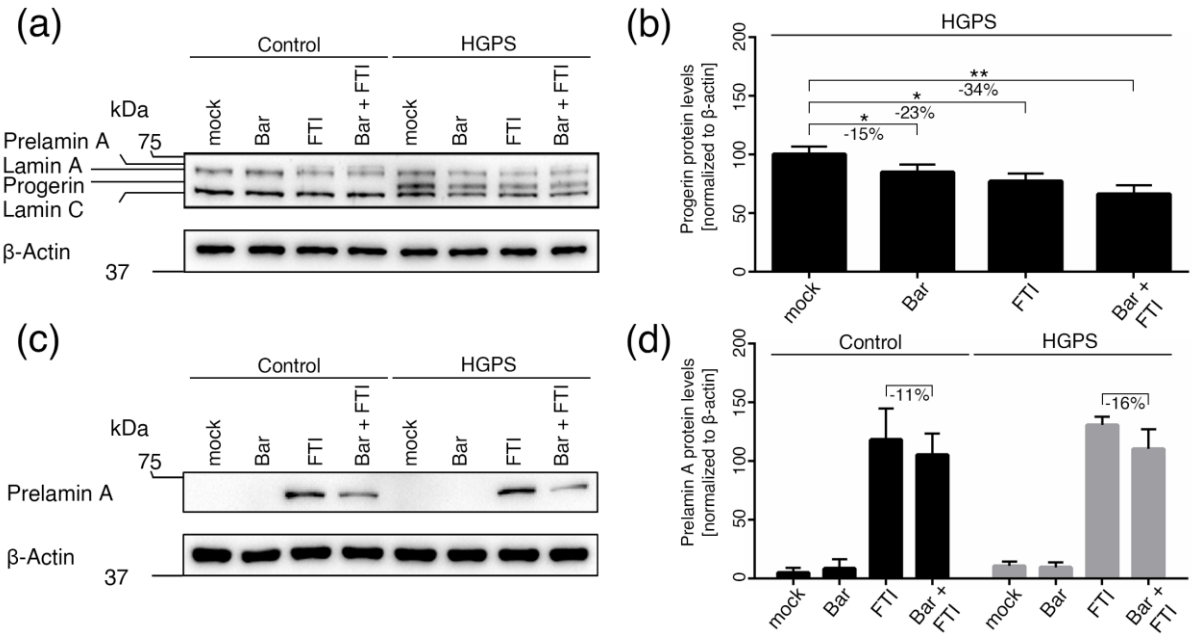

Figure 22: Bar, FTI and combined treatment prevent progerin nuclear accumulation. (a,c) Representative images of western blots for lamin A/C and prelamin A. Cultures at 15% SNS were either treated with vehicle (DMSO), Bar (1 µM), FTI (0.025 µM), or combined drugs for a period of nine days. Quantification of progerin (b) and prelamin A (d). Graphs show mean ± SD. Representative images are shown (n = 3; * p < 0.05, ** p < 0.01). (Arnold et al. 2021)

Progerin levels were visualized by performing a western blot using a lamin A/C antibody. As expected, control cells did not express progerin. In cultures treated with

FTI, an additional prelamin A band can be seen in both cell types. In HGPS cells, Bar and FTI reduced progerin levels and the combination enhances the effects even more, indicating that both compounds synergistically cleared progerin levels. With the use of a specific prelamin A antibody, the known accumulation in FTI-treated cultures was clearly presented. However, although prelamin A levels was visible in FTI and combined treatment, the addition of Bar decreased the accumulation to a certain degree.

Next, we assessed the proposed underlying mechanisms of protein clearance and analyzed autophagy and proteasomal activity (Figure 23).

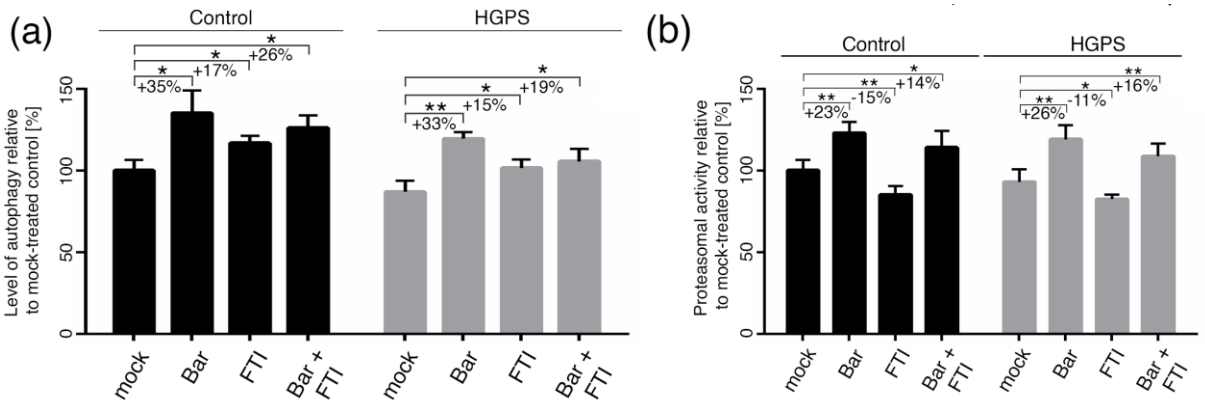

Figure 23: Autophagy and proteasomal activity are elevated in combined treatment. (a) Autophagy activity was determined by measuring MDC levels using fluorescence photometry. (b) Proteasome activity was determined by measuring chymotrypsin-like proteasome activity using Suc-LLVY-AMC as a substrate. Graphs show mean ± SD. Representative images are shown (n = 3; * $p < 0.05$, ** $p < 0.01$). (Arnold et al. 2021)

Autophagy levels in mock-treated HGPS fibroblasts were lower than in those of mock-treated control cells. Both drugs, alone and in combination, enhanced the activity in control and HGPS cultures. Nevertheless, Bar treatment alone showed the biggest amelioration. Similar to autophagy, proteasomal activity levels of mock-treated HGPS cells were again lower than those of mock-treated control cells and Bar also increased the activity levels the most. In contrast, FTI reduced those levels, but did not play a major role in the combined treatment as the proteasomal activity was increased to

nearly Bar-treated levels. Collectively, these results showed that combined treatment could induce both degradation systems of the cell and therefore help to clear progerin. Some of the first described hallmarks of HGPS cells were cellular invaginations and blebbings, which is a phenomenon that also occurs in healthy senescent cells (Goldman et al. 2004; Röhrl et al. 2021). To identify progerins' cellular implications, we evaluated the localization of progerin and prelamin A in control (Figure 24) and HGPS cells (Figure 25). In addition, we investigated the linker of the nucleoskeleton and cytoskeleton (LINC) complex SUN1 protein levels, because it accumulates concurrently with progerin levels at the nuclear envelope (Chen et al. 2012).

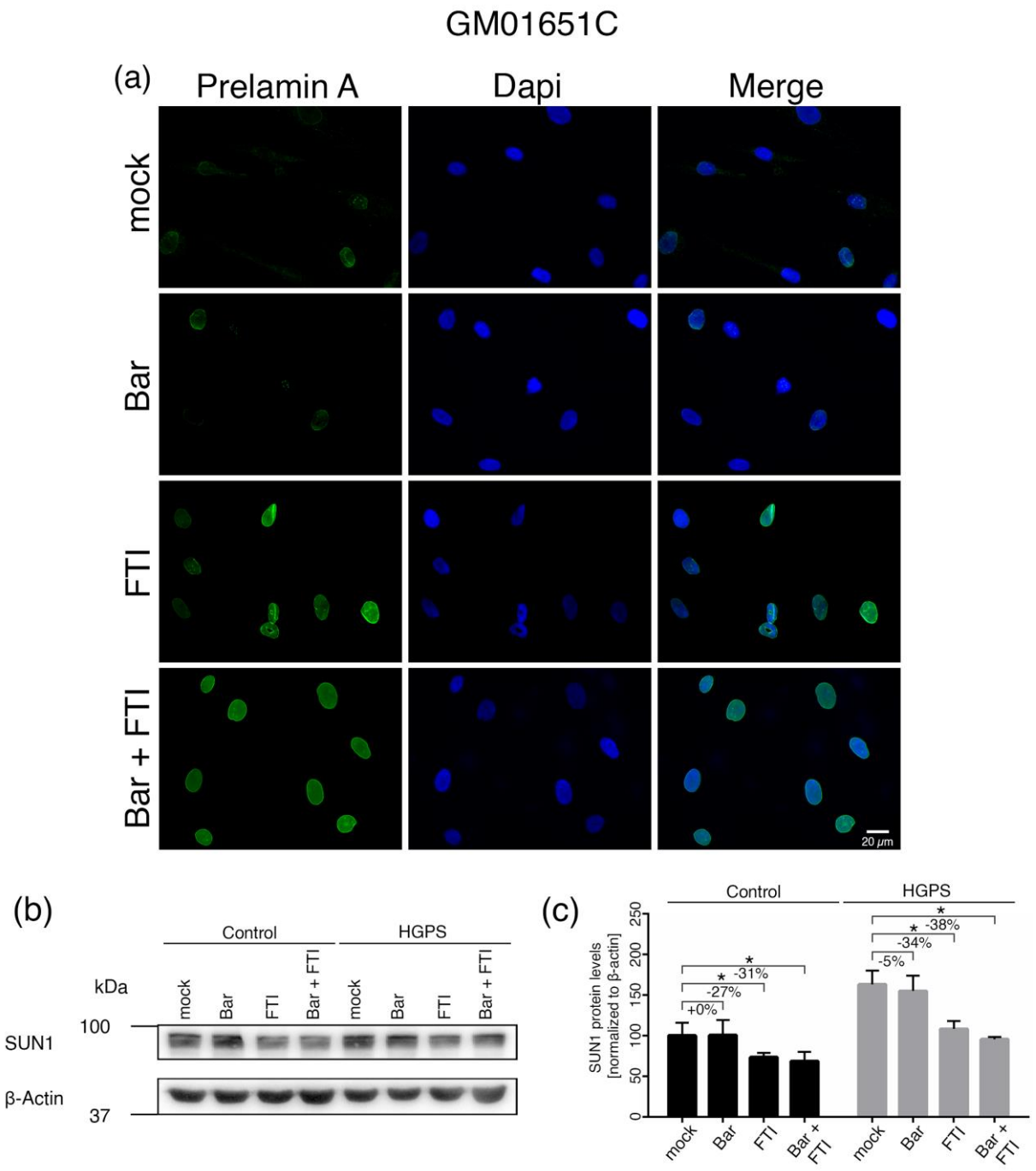

Figure 24: Bar and FTI combination treatment prevent nuclear blebbing in control cells and reduces SUN1 levels. (a) Representative immunofluorescence images of control (GM01651C) fibroblasts treated for nine days as indicated. Antibody against prelamin A (green) was used, and DNA was stained with DAPI. Fluorescence images were taken at 40x magnification. Scale bar 20 µm. (b) Representative images of western blots for SUN1 and (c) quantification of SUN1. Graphs show mean ± SD. Representative images are shown (n = 3; *p < 0.05, **p < 0.01, ***p < 0.001). (Arnold et al. 2021)

In control fibroblasts, prelamin A staining showed a bright signal in FTI and combined treatment cultures. However, low levels were also found in mock- and Bar-treated cells. SUN1 mock-treated HGPS protein levels were higher than those of control cells.

Treatment with Bar did not change the expression of SUN1, but FTI significantly decreased SUN1 levels alone and in combination in both cell types.

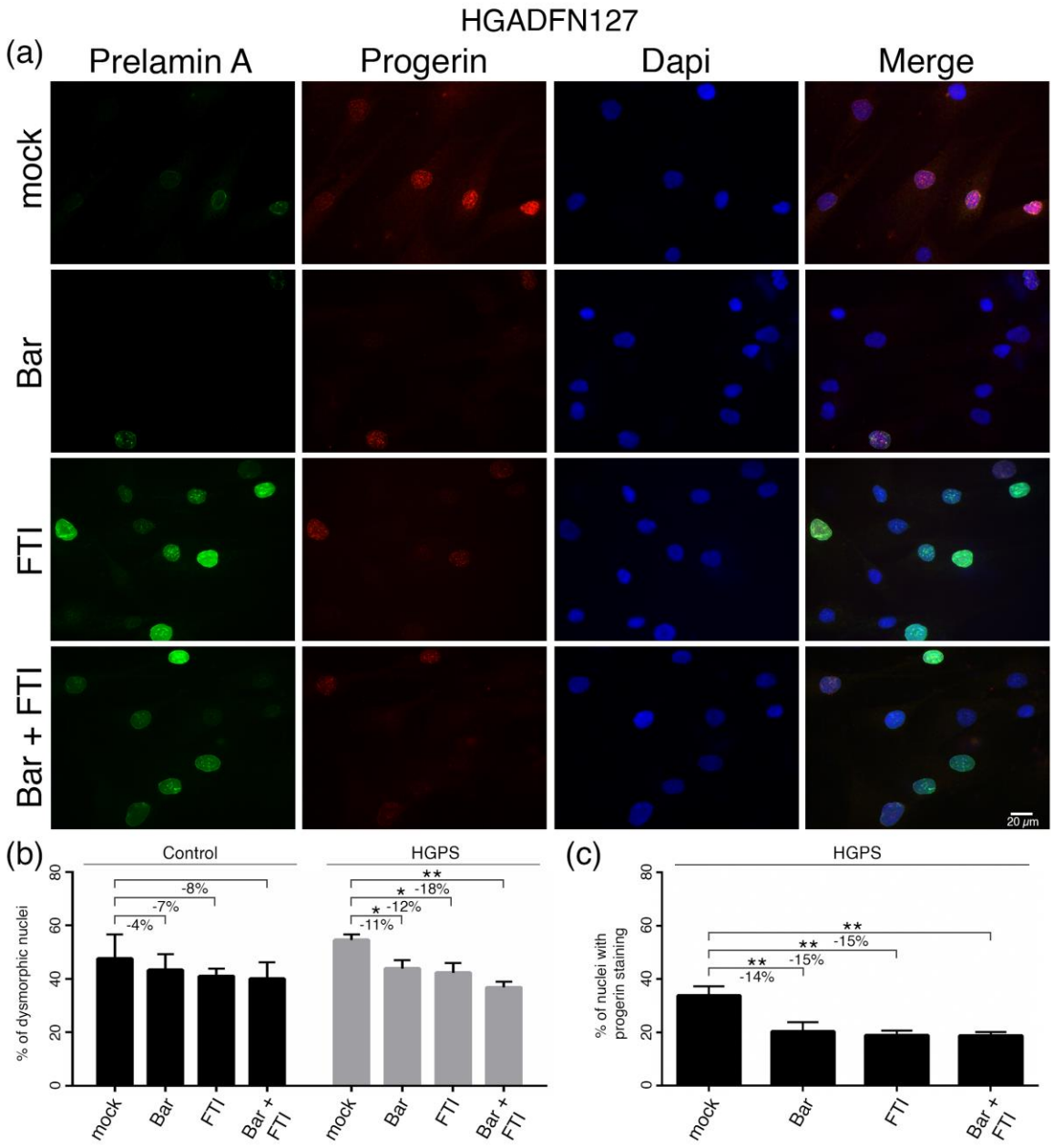

Figure 25: Bar, FTI and combination treatment prevent nuclear blebbing and progerin nuclear accumulation. (a) Representative immunofluorescence images of HGPS (HGADFN127) fibroblasts were treated for nine days as indicated. Antibodies against prelamin A (green) and progerin (red) were used, and DNA was stained with DAPI. Fluorescence images were taken at 40× magnification. Scale bar: 20 µm. (b,c) The same staining as in (a) and figure 24 was used to determine the frequency of misshapen nuclei (dysmorphic) and the number of nuclei with bright progerin signals. An average of at least 900 nuclei were counted. Graphs show mean ± SD. Representative images are shown (n = 3; * $p < 0.05$, ** $p < 0.01$). (Arnold et al. 2021)

Again, in FTI- and combined-treated HGPS fibroblasts high levels of prelamin A were detected. Only a weak signal could be observed for mock- and Bar-treated cells. In

contrast to control cells, progerin was found in all HGPS cultures, albeit to varying degrees. In general, more dysmorphic cells were detected in HGPS cultures. Interestingly, all treatments lowered the percentage of dysmorphic control cells, but none of the treatments reached significance. In HGPS cells, Bar, FTI and combined treatment led to a reduction, noticeably ameliorating the cells' shape. This can be explained by the number of bright positive nuclei with progerin staining, as all treatments reduced progerin. These results showed that autophagy and proteasomal activity were increased with combined therapy. Thus, progerin, prelamin A and SUN1 levels were cleared, thereby contributing to the normalization of the nuclear envelope morphology.

3.2.5 Combined treatment reduces DNA damage in HGPS fibroblasts

Genomic instability is another hallmark of aging and genetic damage is hypothesized to be the cause of many age-related diseases (López-Otín et al. 2013). Previously it was shown that HGPS cells accumulate endogenous DNA damage, particularly DSBs (Liu et al. 2005). To elucidate the cellular response of DSBs, we determined the basal and treated levels of p-H2A.X and counted the cells' foci (Figure 26).

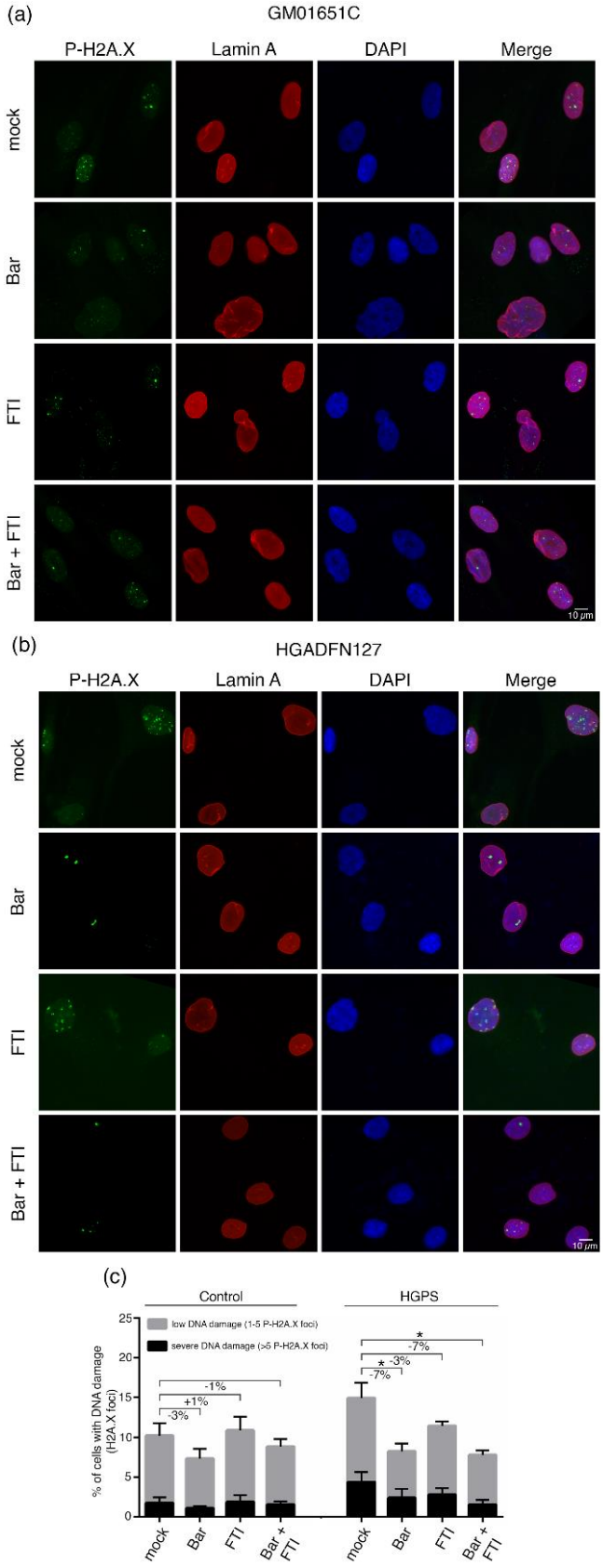

Figure 26: Bar and FTI combination treatment reduce P-H2A.X levels in control and HGPS cells. (a) Representative immunofluorescence images of control GM01651C and (b) HGPS HGADFN127 fibroblasts treated for nine days as indicated. Antibodies against P-H2A.X (green) and lamin A (red) were used, and DNA was stained with DAPI. Fluorescence images were taken at 60× magnification. Scale bar: 10 µm. (c) Number of nuclei with low DNA damage (1–5 P-H2A.X foci) and severe DNA damage (>5 P-H2A.X foci) in control and HGPS cultures treated as indicated. Graphs show mean ± SD. (n = 3; * p < 0.05). (Arnold et al. 2021)

The number of HGPS cells with low and severe DNA damage was higher than the number in control fibroblasts. In control cells, none of the treatments showed a significant effect. However, in HGPS fibroblasts Bar- and combined-treated cells reduced the number of cells with low and severe DNA damage. This result indicates that combined treatment can prevent accumulation of DNA damage to a certain degree.

3.2.6 Bar and FTI change cellular bioenergetics and thus improve ATP levels

Cellular metabolism and in particular ATP synthesis plays an essential role in the function of cells, tissues and whole organisms. Mitochondria detect changes in the cellular environment and can adapt accordingly. This process seems to deteriorate during normal aging and in HGPS patients (Rivera-Torres et al. 2013; Lopez-Mejia et al. 2014). Thus, upon ATP deficiency, toxic ROS are produced and premature cell senescence or apoptosis is induced (Wiley et al. 2016). Using the mitochondrial stress test on an XF96 seahorse analyzer, we were able to determine oxygen consumption rate (OCR) and extracellular acidification rate (ECAR) as indicators of the two major energy-producing pathways: glycolysis and oxidative phosphorylation (Figure 27). By adding different compounds that inhibit specific complexes of the oxidative phosphorylation chain, we identified basal respiration, ATP production, proton leak, maximal respiration, spare respiratory capacity, non-mitochondrial respiration and ECAR levels, as schematically indicated in Figure 27 and 28.

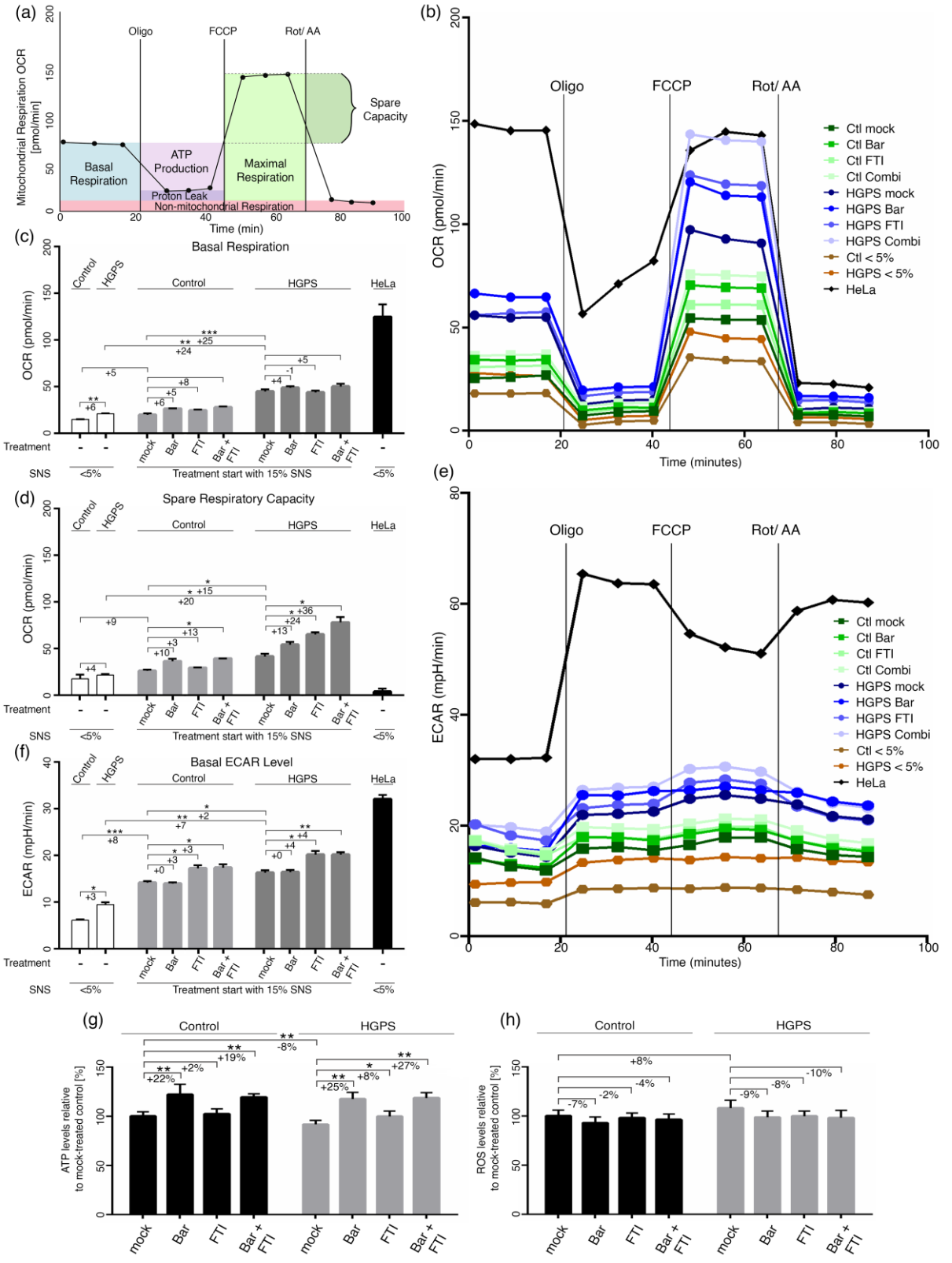

Figure 27: Mitochondrial function and glycolysis are impaired in HGPS fibroblasts. (a) Schematic representation of Seahorse XF Cell Mito stress test and calculated values are indicated. Oxygen consumption rates (OCR) (b) and extracellular acidification (ECAR) (e) were determined with a Seahorse XF96 Flux analyzer in basal and stimulated conditions (n = 3). Additional parameters like basal respiration (c), spare respiratory capacity (d), and basal ECAR levels (f) were calculated with Wave software v2.6.1.53 (Agilent Technologies, Santa Clara, CA, USA). (g) Cellular ATP levels were measured using a CellTiter-Glo luminescence ATP assay. (h) Intracellular ROS levels were determined by measuring oxidized dichlorofluorescein (DCF) levels using a DCFDA cellular ROS detection assay (n = 3). Graphs show mean ± SD. (* $p < 0.05$, ** $p < 0.01$, *** $p < 0.001$). (Arnold et al. 2021)

The OCR was first measured under basal conditions following sequential addition of oligomycin (inhibitor of the ATP synthase), carbonyl cyanide-p-(tri-flluromethoxy) phenyl-hydrazone (FCCP) (uncoupling agent) and rotenone/antimycin A (inhibitors of electron transport chain complexes I and III). We included the HeLa cancer cell line in our bioenergetics profile because it is known that cancer cell lines are dependent on glycolysis and already operate at maximum capacity under basal respiration conditions (Liberti und Locasale 2016). Furthermore, we included control and HGPS cells with a senescence index of <5% and ~15%.

Under basal conditions, young control and HGPS cells (<5%) showed a significantly lower OCR than their older counterparts. Interestingly, HGPS fibroblasts (<5% and ~15% SNS) exhibited a higher OCR compared to control cultures, indicating a shift in energy production already in young HGPS cells. Basal respiration remained similar upon treatment regimens. As expected, the HeLa cell line ran at its maximal capacity under basal conditions and OCR was significantly higher than all other cell types. This occurrence can also be observed by the low spare respiratory capacity of HeLa cells. Looking at the therapies, a difference in spare respiratory capacity was detected predominantly in combined-treated cells compared to mock-treated cultures. This result showed that these cells became more oxidative and developed an adaptation to meet their energy demands. A higher respiratory capacity was also observed during replicative senescence in older (~15% SNS) vs. younger (<5% SNS) cells. As expected, basal ECAR levels were highest in HeLa cells and were used as positive control. Increased dependence of ECAR was found in cells with higher senescence. Of particular note is the consequent increase of ECAR levels in HGPS cultures compared to control during replicative aging, which can already be seen in young cells. This shift towards a more glycolytic state during replicative senescence was described in several previous papers (Bittles und Harper 1984; Zwerschke et al. 2003). However,

FTI and combined treatment cultures further increased ECAR levels in both cell types, while Bar did not change.

To investigate the benefit of changed OCR and ECAR, we assessed total ATP and ROS levels. In control cells, Bar and combined treatment increased the amount of ATP significantly. However, FTI-treated cultures showed no effect compared to the control mock-treated cells. Similarly, in HGPS cultures, Bar and combined treatment led to a sharp increase. FTI did show an amelioration, albeit much smaller than the other treatments. ROS levels remained similar under all treatment conditions. Collectively, our results show that Bar is efficient in restoring ATP levels in aged and HGPS cells. ECAR revealed a shift towards more glycolysis in HGPS and normal cells during replicative senescence.

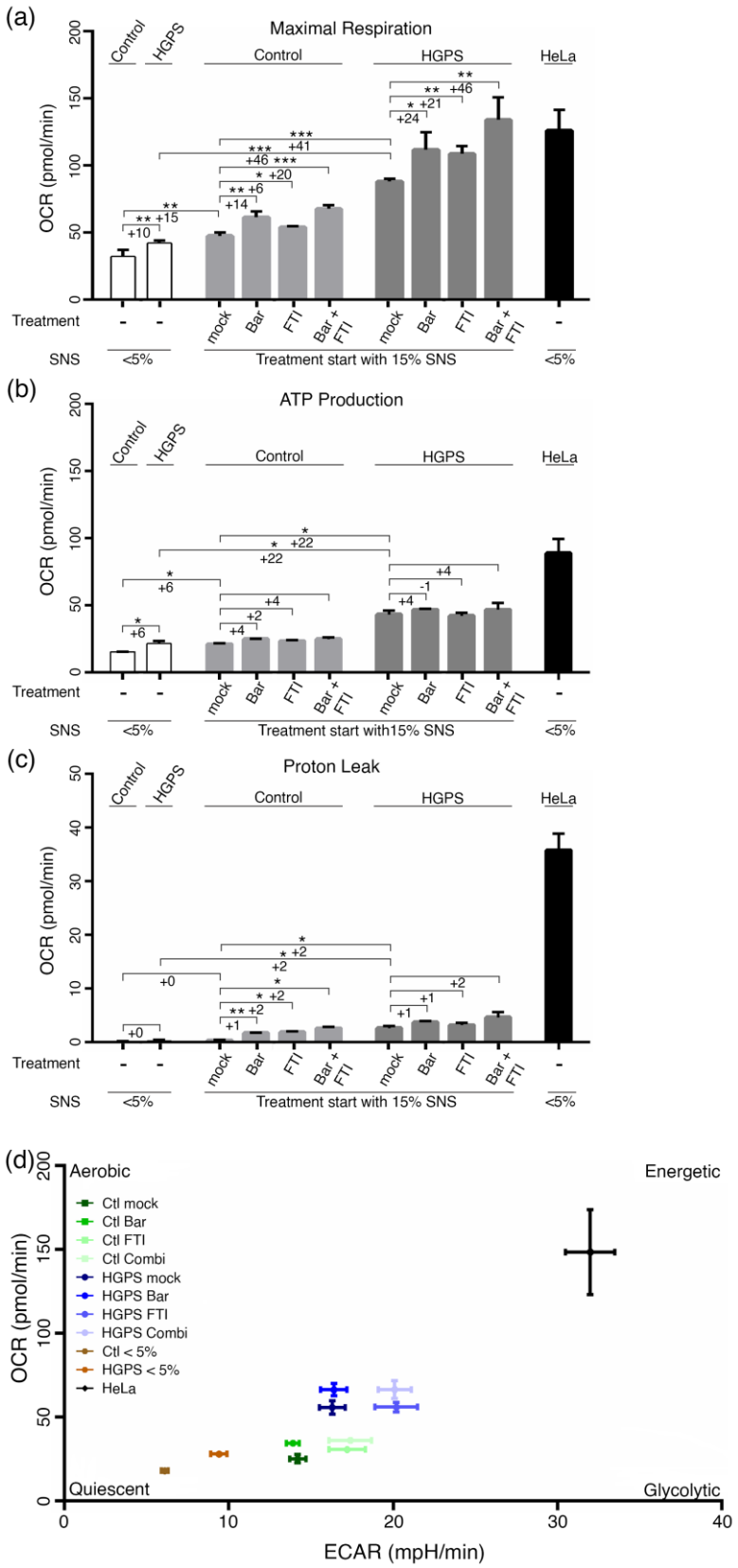

Figure 28: Mitochondrial function and glycolysis are altered in HGPS fibroblasts. Oxygen consumption rates (OCR) and extracellular acidification (ECAR) were determined with a Seahorse XF Flux Analyzer in basal and stimulated conditions (n=3). Maximal respiration (a), ATP production (b), and proton leak (c) were calculated with Wave software v2.6.1.53 (Agilent Technologies). (d) Plotting basal ECAR and OCR levels provides a snap-shot of the bioenergetics profiles. Graphs show mean ± SD. (*p < 0.05, **p < 0.01, ***p < 0.001). (Arnold et al. 2021)

Maximal respiration showed the same pattern as basal respiration; OCR in young HGPS cells (<5% SNS) were higher than in young controls. Furthermore, the rates increased during replicative SNS in both cell types. All treatments resulted in higher OCR, but combined treatment was most effective. Again, calculated ATP production showed higher levels in HGPS cells compared to young controls and in both cases the level rose with replicative aging. Proton leakage remained low in all cells, except the HeLa cell line.

To visualize differences in oxidative phosphorylation and glycolysis, we combined basal OCR and ECAR in a bioenergetics profile. As already described, cells shifted towards a more energetic state during replicative aging and this tendency was greater in HGPS cells. FTI additionally increased glycolysis, while Bar elevated oxidative phosphorylation. Taken together, combined treatment of control and HGPS cells showed a metabolic shift towards glycolysis and oxidative phosphorylation, which resulted in improved mitochondrial spare respiratory capacity and basal ECAR levels. Ultimately, both drugs together lead to increased total ATP levels and can better adapt to energy-demanding challenges.

4 DISCUSSION

4.1 Discussion

Research focusing on the molecular mechanisms of HGPS and the associated insights of normal aging is of significant interest to our society. This study unravels basic aging pathways in a time-dependent manner and proposes a novel treatment strategy for HGPS patients. Specifically, we could demonstrate that:

a) The four diseases (alopecia, arthritis, lipodystrophy, vascular disease) that are typically recognized as the main traits of HGPS share 17 dysregulated genes. 14 of those are implicated in the same pathways, namely NF-κB and JAK-STAT.
b) All 17 genes could serve as biomarkers for scoring the stage and severity of these four conditions and HGPS.
c) Overactivation of the JAK-STAT pathway is dependent on cellular senescence rather than HGPS specific.
d) The SASP is critical for the development of HGPS.
e) Inhibition of JAK-STAT delayed senescence and rebalanced cellular health aspects, thereby correcting several hallmarks of aging.
f) Combination treatment of Bar and FTI act synergistically on many key mechanisms in HGPS, i.e., reduction of progerin levels through autophagy and blockage of farnesylation.
g) Separation defects in FTI-treated cells lead to activation of the cGAS-STING pathway, contributing to inflammation and senescence.
h) FTI-induced cellular side effects can be mitigated by Bar.

Previous attempts to treat HGPS have primarily focused on degrading or blocking progerin production, the causative toxic protein causing this disease (Saxena und

Kumar 2020). Since this has not led to a breakthrough, we investigated altered gene expression using a novel data mining approach. By searching for dysregulated genes in the four diseases (alopecia, arthritis, lipodystrophy, vascular disease) considered as main traits of HGPS, we identified 17 genes that appear to be altered in all conditions, and thus possibly also impact HGPS. Interestingly, 14 of the 17 genes were part of two pro-inflammatory signaling pathways, namely, NF-κB and JAK-STAT. Analysis of all genes in a time-dependent manner during replicative aging revealed that these are significantly altered in control and HGPS cultures with high senescence. Furthermore, we showed increased JAK-STAT signaling in senescent cells, a possible therapeutic target for HGPS.

In this study, we used primary fibroblasts from patients and healthy controls because all four diseases affect mesenchymal tissues, including the heart, vessels, skin, bone and joints. All of these contain resident immune cells, tissue-specific cell types and fibroblast subtypes. Importantly, it was shown that although fibroblasts are heterogeneous, they are all involved in functions such as wound healing, remodeling fibrosis and stem cell maintenance and upon senescence, express many SASP factors (Campisi 2013). Therefore, cellular senescence developing in fibroblasts may play a essential role in the four pathologies.

JAK-STAT overactivation leads to a pro-inflammatory milieu that contributes to the SASP and vice versa and is following emerging evidence that many age-related diseases share fundamental mechanistic pillars and largely converge on inflammation (Fulop et al. 2018). The chronic and low-grade inflammation during aging leads to loss of function in many tissues and is referred to as ‘inflammaging’ (Franceschi und Campisi 2014). In this process, senescent cells accumulate and their location and number determine which age-related pathology will develop. By using Bar, an already FDA-approved JAK1/2 inhibitor for rheumatoid arthritis (Al-Salama und Scott 2018),

we were able to inhibit JAK-STAT overactivation and lowered many pro-inflammatory cytokines that are part of the SASP, including CCL-2, IL6, IL8 and TNFa. Dysregulated JAK-STAT signaling is involved in many essential cellular processes such as cellular immunity, cell death and tumor formation (Rawlings et al. 2004). By now, there are also other studies with an anti-inflammatory approach underlying the importance of inflammation in HGPS. Ruxolitinib, an alternative JAK1/2 inhibitor, was used to treat an HGPS mouse model (Griveau et al. 2020). This study showed that inhibition of the JAK-STAT pathway in ZMPSTE24-/- mice led to a decrease in the incidence of bone fractures, elevated mineral bone density, improved grip strength and most importantly, increased lifespan (Griveau et al. 2020). ATM-dependent activation of NF-κB has also been described (Osorio et al. 2012). This pathway's pharmacological and genetic inhibition resulted in extended longevity of the $LMNA^{G609/G609}$ HGPS mouse model and reduced inflammatory cytokines such as IL-6, CXCL1 or TNFa (Osorio et al. 2012). This also led to another study presenting a successful antibody therapy directed against IL6 (Squarzoni et al. 2021). Intriguingly, in our experiments, not only Bar showed a reduction of pro-inflammatory cytokines, but also FTI led to a unique inflammation signature with many of the critical cytokines reduced. This reduction presumably results from the inhibition of the oncogene Ras by FTI as described by Degeorge et al. 2008. Reduction of inflammation appears to be promising for the treatment of HGPS. Nevertheless, characterization of different targets within inflammation pathways are still needed to determine the most effective treatment and downstream effects. Research also needs to address how normal inflammation induced during infections or tissue injury can be maintained. In this context, the treatment period and concentration gain importance. Strategies that start in early life and permanently prevent subliminal inflammation are just as conceivable as later inhibitions, when chronic inflammation is already present so that long term side effects

can be avoided. Although Bar is usually well tolerated in humans, there is evidence of opportunistic infections and laboratory parameters such as small dose-related decreases in neutrophil count and hemoglobin levels, as well as small increases in creatinine and lipoprotein levels (T Virtanen et al. 2019).

To be noted is the establishment of our new cell-based aging model to compare control and HGPS fibroblasts. In contrast with previous studies that used the cellular passage number to indicate age, we rigorously scored the senescence index of all cultures. The problem of comparing cells by their passage number arises because HGPS cells age prematurely due to the presence of progerin. Therefore, comparisons can often detect differences but cannot determine whether this effect is HGPS specific and may also be seen in control cells at a later time point. Moreover, we noticed inconsistent p-STAT1 and p-STAT3 levels when comparing different control and HGPS cell strains with each other. Therefore, we chose three different SNS indexes (<5%, 15% and 30%) for our experiments and analyzed the development. Interestingly, we could indeed see that when both control and HGPS cells are young (<5% SNS), many cell properties like growth rates, autophagy levels, proteasomal activity, ROS or ATP are very similar. In aged control and HGPS cells, a functional decline was observed. Thus, these results indicate that increased senescence in both cell types lead to the alteration of the parameters mentioned above, rather than an exclusive effect due to progerin. The similarities between control and HGPS showed that the onset of senescence is a general process. The SASP and its associated alterations evolve in control and HGPS cells, as seen by our analysis of the pro-inflammatory factors, e.g., CCL2, CRP, IL8, TNFa. Because many stimuli can induce senescence, we also examined JAK-STAT signaling and SASP factors in the setting of DNA-induced senescence by treating cells with etoposide (Muñoz-Espín und Serrano 2014). Just as with replicative senescence, DNA-induced senescence showed an overactivation of JAK-STAT indicated by

elevated p-STAT1 and p-STAT3 levels in control and HGPS cells. Subsequently, the activation of JAK1/2-STAT1/3 led to the expression of several inflammatory cytokines (CCL2, CXCL8, IFNG, IL6 and TNFa). This demonstrated that the overactivation of JAK-STAT in senescent cells is a general mechanism occurring independently of the stress that induces senescence. Furthermore, to study the effect of normal aging and progerin-induced alterations, we started our combination treatment when cultures reached 15% senescence. In those cultures, increased JAK-STAT signaling and elevated progerin levels can be observed.

To test the consequences of targeting the pro-inflammatory phenotype by inhibiting JAK-STAT through Bar, we evaluated key cellular mechanisms implicated in the development of HGPS. Bar improved the growth rates, delayed senescence, ameliorated proteostasis and mitochondrial function, decreased pro-inflammatory marker levels and reduced progerin levels in HGPS cells. The data provides evidence that anti-inflammatory therapies offer benefits for children with HGPS. Recently, overactivation of this pathway has also been associated with other diseases in progeria patients, including lipodystrophy, alopecia, atopic dermatitis, eye diseases and different forms of arthritis (Fragoulis et al. 2019; Pandey et al. 2021). Research and treatment of these diseases with JAK inhibitors will thus hopefully improve the knowledge for HGPS, too.

In November 2020, an FTI sold under the name Zokinvy became the first treatment for progeria to be approved by the FDA (Dhillon 2021). The data collected from clinical trials since 2007 showed that FTI reduced the incidence of mortality by 60% (p=0.0064) and increased average survival time by 2.5 years (Gordon et al. 2018). However, the treatment is still not a cure and patients suffer from side effects including nausea, vomiting, diarrhea and fatigue (Kieran et al. 2007). On a molecular level, especially FTI-induced separation defects during mitosis are problematic as they lead to genomic

instability and donut-shaped nuclei (Verstraeten et al. 2011). In light of our positive results with Bar, we combined both drugs to enhance the positive effects and ameliorate cellular functions that are not restored by either medication alone while abrogating FTI-induced cellular side effects. The combination treatment was most effective in lowering inflammation and reducing toxic progerin levels, which subsequently ameliorated nuclear morphology, reduced DNA damage and improved mitochondrial function.

However, Bar could not rescue the separation defects caused by FTI. A more detailed analysis of this FTI-induced phenomenon revealed a high frequency of cytoplasmic chromatin foci (CCF) that is considered as a form of DNA damage and ultimately triggers inflammation and senescence (Dou et al. 2017; Lan et al. 2019).

In general, any DNA localized in the cytoplasm is a potent danger signal. It can have exogenous (e.g., viral or bacterial infections) or endogenous origins (e.g., faulty mitosis, loss of membrane integrity). The cause of cytoplasmic chromatin foci in FTI-induced cells can most likely be found in several mechanisms interacting with each other. Blockage of farnesylation affects many essential proteins, including some involved in cell cycle progression. A special focus should be attributed to two centromere-associated kinetochore proteins, namely CENP-E and CENP-F that need to be farnesylated to function (Ashar et al. 2000). During mitosis, CENP-E is proposed to be a kinesin-like motor protein that appears during prometaphase and is responsible for stable spindle microtubule capture at kinetochores, allowing the segregation of the sister chromatids (Zecevic et al. 1998). CENP-F is a nuclear matrix component and associates with the kinetochores during the G2 phase of interphase. Its localization at the spindle midzone and the intracellular bridge in late anaphase and telophase suggests a role in the orientation of microtubules and chromosome segregation (Hussein und Taylor 2002). In FTI-treated cultures, both proteins, due to their

unfarnesylated status, may have great influence on the formation of CCF. Moreover, membrane integrity is a crucial mechanism to maintain genomic stability and any disruption can lead to several forms of cytoplasmic DNA, including micronuclei or CCF (Ivanov et al. 2013). The correct protein composition of the nuclear lamina is crucial for its integrity and it consists of lamin A, B1, B2 and C intermediate filament proteins (Prokocimer et al. 2009). Loss of Lamin B1 is not only a well-known feature of cell senescence, but its processing is also affected by FTI, leading to depletion of lamin B1 from the nuclear envelope and delocalization of lamin B2 to the nucleoplasm (Freund et al. 2012; Shimi et al. 2011; Adam et al. 2013). Thus, both senescence and FTI-induced disruptions of lamin B1 lead to an altered nuclear lamina, loss of membrane integrity and subsequent formation of CCFs (Adam et al. 2013). In our experiments, an increase of micronuclei and CCFs were observed in control and HGPS cells, indicating that their presence is linked to FTI activity and not to progerin expression. However, the exact role of CENP-E, CENP-F and lamin B in the formation of cytoplasmic DNA remains unclear. It is also unknown whether therapeutic approaches can causally prevent the formation of CCFs in FTI-treated cells. For example, a recent study showed that histone deacetylase inhibitors (HDACis) prevent CCF formation and SASP indirectly through activation of mitochondrial function (Vizioli et al. 2020). Another option would be a symptomatic treatment downstream of CCF formation, which will be discussed further.

Nucleic acid of pathogens or endogenous damaged DNA in the cytoplasm is sensed by the cyclic GMP-AMP synthase (cGAS) receptor and its downstream signaling effector stimulator of interferon genes (STING) (Dou et al. 2017; Glück et al. 2017). Detection of cytosolic DNA and the subsequent activation of cGAS-STING triggers an innate immune response implicating two downstream pathways: type I interferon through interferon regulatory factor 3 (IRF3) and pro-inflammatory responses through

NF-κB (Barber 2015). In accordance with the cGAS-STING activation in FTI-treated cells, we observed an increase in IFN-ß mRNA expression. Interestingly, IFN-ß seems to activate STAT 1 further, as indicated by p-STAT1 protein levels. This implies that the JAK-STAT pathway is activated, too. Bar could prevent this overactivation by nearly completely inhibiting p-STAT1 even in the presence of FTI. Therefore, combined treatment revealed a downstream target to dampen the effects caused by cGAS-STING activation. In addition, recent studies showed that the cGAS-STING pathway is a crucial regulator of senescence and the SASP in normal cells exposed to various stresses (Lan et al. 2019). Consequently, senescence and dose-dependent growth inhibition observed in FTI-treated cancer cells could be explained by FTI-induced mitotic defects and cGAS-STING activation (Bolick et al. 2003; Mazzocca et al. 2003). Since this process also occurs during normal replicative senescence, inhibition of the effects downstream of cGAS-STING in combined treatment could thus even lead to further improvement of inflammation and senescence in normal and HGPS cells.

Mitochondrial dysfunction, another hallmark of aging, is considered to be a crucial contributor to cellular senescence and aging (Bratic und Larsson 2013). In this context, previous studies identified alterations of the mitochondrial function in HGPS and this may further accelerate the aging process and organ decline (Rivera-Torres et al. 2013). In general, the purpose of mitochondria is the production of ATP to meet cellular energy demand. It has been shown that senescent cells become more dependent on glycolysis and oxidative phosphorylation (Rivera-Torres et al. 2013; Sabbatinelli et al. 2019; Nacarelli et al. 2018). Controversially, senescent fibroblasts have an increase in mitochondrial mass but a decreased membrane potential resulting in a functional decline (Chapman et al. 2019). The abundance of mitochondria during aging may compensate for processes like protein degradation with high energy demands associated with age-related malfunctions such as misfolding of proteins (Peth et al.

2013). In our experiment, we measured the oxygen consumption rate to analyze oxidative phosphorylation and ECAR as an indicator of glycolysis. Both processes were increased during replicative senescence. However, HGPS cells constantly exhibited increased oxidative phosphorylation and glycolysis compared to control cells with the same senescence index. This data suggests a metabolic adaptation in response to the cellular stress induced by progerin expression. Previous metabolic studies already showed increased levels of glycolysis in HGPS compared to control cells, some even a metabolic switch from oxidative phosphorylation to glycolysis (Aliper et al. 2015; Rivera-Torres et al. 2013; Gabriel et al. 2016; Nacarelli et al. 2018). However, the correlation of these results within the aging process and HGPS is unclear as the studies did not score the senescence index, rate of oxygen consumption or other parameters of the respiratory chain. Metabolic analysis of treated cultures showed that Bar increased oxidative phosphorylation, while FTI increased glycolysis in both cell types. The combination treatment elevated both processes to the levels reached by single drugs. Interestingly, basal respiration was not significantly altered in any treatment. Instead, combined therapy showed an increase in maximum and spare respiratory capacity, indicating an adaptive advantage when high energy expenditure is required. Glycolysis levels were higher in FTI and combined treatment of both cell types. To better interpret these processes, we also evaluated the outcomes at ATP and ROS levels. Treatment of Bar increased ATP levels but had no significant effect on ROS. Combined treated cells exhibited the same increase in ATP levels as Bar-treated cultures alone. FTI did not show any significant ameliorations. In general, especially total ROS levels of all treatments in both cell types show a deficient result and indicate that mitochondrial dysfunction was not effectively rescued. The exact mechanisms of both drugs on mitochondria and whether other metabolic interventions were helpful in the treatment of HGPS remain to be examined. An explanation for the

changes in Bar-treated cells could at least in part be accounted to mitochondrial STAT3 (mitoSTAT3) (Rincon und Pereira 2018). Recent studies provide evidence that activated STAT3 can translocate into mitochondria, binds to GRIM-19, a component of complex I and act as a modulator of mitochondrial function (Lufei et al. 2003). Nevertheless, increased ATP levels after Bar treatment might have other positive outcomes for HGPS patients. In this context, previous research showed that children with HGPS and HGPS mouse models have decreased levels of extracellular pyrophosphate, a regulator of calcification that leads to characteristic vascular calcifications (Villa-Bellosta 2018, 2019; Lomashvili et al. 2014). Since the primary source of pyrophosphate is generated when ATP is consumed during hydrolysis, treating HGPS mice with ATP could prevent vascular calcification (Villa-Bellosta 2019). Further *in vivo* experiments must determine whether the increase of ATP by Bar is sufficient to elevate pyrophosphate levels and avoid calcification, which would reduce the vascular stiffness affecting patients with HGPS.

In summary, we identify Bar as a potential therapy in the development of HGPS and provide evidence that combined treatment with FTI significantly ameliorates the clinical picture of HGPS patients. Of great clinical interest will be our finding that FTI induces donut-shaped cells, micronuclei and extranuclear DNA fragments. These defects were associated with an activated cGAS-STING-STAT1 signaling axis, increased expression of SASPs and a metabolic shift towards glycolysis. However, combined treatment strategy could prevent some of these FTI-induced side effects. Administration of both drugs ameliorated cell growth, inhibited the cGAS-STING-STAT1 pathway, reduced levels of SASPs, increased OCR and ameliorated cellular ATP levels. Since all children suffering from HGPS already take FTI (Zokinvy®) permanently, Bar might further contribute to several health aspects, especially by delaying premature senescence. This would significantly impact the progression of

various symptoms developed in patients. In line with this idea is the fact that Bar (Olumiant®) is already prescribed for patients with rheumatoid arthritis, a common symptom in patients with HGPS (Jabbari et al. 2015). Furthermore, Bar has been investigated in numerous clinical trials, including alopecia areata, which also develops in HGPS patients. As a next step, *in vivo* studies are urgently needed to evaluate the efficacy and safety of this treatment. The functional ameliorations observed in HGPS cells are promising and lifespan extension experiments in HGPS mouse models will determine its potential value as a therapeutic strategy for children with HGPS and possibly other age-related conditions.

4.2 Outlook

This study presents a novel therapeutic strategy to treat patients with the Hutchinson-Gilford progeria syndrome. By identifying dysregulated genes and implicated signaling pathways such as JAK-STAT, we have improved the molecular understanding of this disease. In addition, we established a new cell-based intervention with Bar and tested its effect in combination with FTI, which has already been FDA-approved for HGPS. Each drug improves different aspects of the disease and this study shows how modulation of signaling can remedy the HGPS phenotype. Moreover, our data shows many benefits of using a combined approach to mitigate side effects and better counteract the complex signaling networks that evolve during pathogenesis. This knowledge should be considered in any *in vivo* experiments and future clinical trials. Nevertheless, even though our results are promising and will hopefully extend lifespan and give patients a new quality of life, our treatment is not a cure. Research will continue to be necessary to improve already known therapies and to develop new ones. With today's genetic engineering options such as CRISPR/Cas, a complete cure is in reach.

Therapeutically, the link of HGPS to other age-related diseases such as Alzheimer's disease or Parkinson's disease is compelling. Patients might benefit from the same drugs as these conditions share mechanistic links, e.g. loss of proteostasis. Future work needs to determine how effective the treatments are for each condition. In particular, the control of the immune system is becoming critical for more and more diseases. For example, Bar is even used as a covid-19 therapy to counteract the cytokine storm that occurs in late stages in some patients (Favalli et al. 2020). In the end, the question remains whether age-related diseases including HGPS initially lead to the hallmarks of aging, shown in this study, or whether aging itself creates a toxic environment that serves as a breeding ground for the development of these conditions in the first place. In this case, it would allow diagnosis and therapies to start at an early point in time, thus redefining aging and age-related diseases.

5 APPENDIX

5.1 Abbreviations

%	Percentage
°C	Celsius
*p	Significance value
µl	Micro liter
µM	Micro molar
AA	Antimycin A
ab	Antibody
ATP	Adenosine triphosphate
Bar	Baricitinib
bp	Base pair
BSA	Bovine serum albumin
CAAX	C = cysteine, A = aliphatic amino acid, X = variable
C3	Complement 3
CCF	Cytoplasmic chromatin fragment
CCL2	Chemokine (C-C motif) ligand 2
CRP	C-reactive protein
CXCL8/IL8	C-X-C motif chemokine ligand 8
cGAS	Cyclic GMP-AMP synthase
CPD	Cumulative population doubling
DNA	Deoxyribonucleic acid
DCF(DA)	2', 7' –dichlorofluorescin (diacetate)
DMSO	Dimethyl sulfoxide
DSB	Double-strand break
ECAR	Extracellular acidification rate
Eto	Etoposide
FAS	Cell surface death receptor
FBS	Fetal bovine serum
FCCP	Carbonyl cyanide-4 (trifluoromethoxy) phenylhydrazone
FDA	Food and Drug Administration
FTI	Farnesyltransferase inhibitor
h	Hour
HCl	Hydrochloric acid
HGNC	HUGO Gene Nomenclature Committee
HGPS	Hutchinson-Gilford progeria syndrome
HRP	Horseradish peroxidase
HMOX1	Heme oxygenase 1
ICAM1	Intercellular adhesion molecule 1
IF	Immunofluorescence
IFNG	Interferon gamma
IGF1	Insulin-like growth factor 1
IL4	Interleukin 4
IL6	Interleukin 6
IL18	Interleukin 18

IMPC	International Mouse Phenotyping Consortium
iPSC	Induced pluripotent stem cell
JAK	Janus kinase
LEP	Leptin
LMNA	Lamin A/C
M	Molar
mA	Milliampere
MAD	Mandibuloacral dysplasia
MDC	Monodansylcadaverine
Mg	Milligram
$MgCl_2$	Magnesium chloride
ml	Milliliter
mM	Milimolar
m-RNA	Messenger ribonucleic acid
mTOR	Mammalian target of rapamycin
MW	Molecular weight
NCBI	National Center for Biotechnology Information
NF-κB	Nuclear factor ‘kappa-light-chain-enhancer’ of activated B-cells
nm	nanometer
OCR	Oxygen consumption rate
Oligo	Oligomycin
PAGE	Polyacrylamide gel electrophoresis
PBS	Phosphate buffered saline
PCR	Polymerase chain reaction
PI	Propidium iodide
PPD	Population doubling
PPARG	Peroxisome proliferator activated receptor gamma
p-STAT	Phosphorylated-signal transducers and activators of transcription
Ras	Rat sarcoma protein
RB	Retinoblastoma protein
RD	Restrictive dermopathy
RNA	Ribonucleic acid
ROS	Reactive oxygen species
Rot	Rotenone
RT	Room temperature
SA-ß-gal	Senescence-associated beta-galactosidase
S.D.	Standard deviation
SASP	Senescence-associated secretory phenotype
SDS	Sodium dodecyl sulfate
SNS	Senescence
STAT	Signal transducers and activators of transcription
STING	Stimulator of interferon genes
STRING	Search Tool for the Retrieval of Interacting Genes
SUN	Sad1 and UNC84 Domain Containing
TBS	Tris buffered saline
TGFB1	Transforming growth factor beta 1
T_m	Melting temperature

TNFα	Tumor necrosis factor alpha
TRAF1	TNF receptor-associated factor 1
WB	Western Blot
X-gal	5-bromo-4-chloro-3-indolyl-D-galactopyranoside
ZMPSTE24	Zink-Metalloprotease 24

5.2 Equipment

Table 21: Equipment

Device	**Company**
Autoclave	KSG
Axio Image D2	Zeiss
Axiovert 40CFL	Zeiss
Balance Cp 4202 S	Sartorius
Benchtop pH meter	Carl Roth
Biofuge fresco	Themo Scientific
Chemi-Doc MP Imaging System	Bio-Rad
FLUOstar Omega	BMG Labtech
HeraSafe	Thermo Scientific
ICycler PCR System	Bio-Rad
Incubator	Binder
Laboratory Shaker RS-RS5	Phoenix Instrument
Magnetic stirrer MR3001	Heidolph
Mastercycler DNA Engine Thermal cycler PCR	Eppendorf
Millipore water supply	Millipore GmbH
Mini Gel cell/ Mini Trans-Blot cell	Bio-Rad
MS2 Minishaker	Ika
Multifuge 3S-R+	Thermo Scientific

Muse Cell Analyzer	Merck Millipore
Nano Drop Spectrometer ND-1000	PeqLab
Pwer Pac Universal/ HC	Bio-Rad
Rocking platform	VWR
Sonifier 250	Branson
StepOnePlus	Thermofisher
Thermomixer comfort	Eppendorf
Trans-Blot Turbo	Bio-Rad
Vortex Genie-2	VWR
XF96 Seahorse Analyzer	Agilent Technologies

5.3 Chemicals

Table 22: Chemicals

Name	**Company**
0.25% Trypsin EDTA	Invitrogen
2-Mercaptoethanol	Bio-Rad
2-Propanol	Carl Roth
Aceton	Carl Roth
Agarose ultrapure	Bio-Rad
Ammonium Persulfate	Bio-Rad
Antimycin A	Agilent Technologies
Baricitinib	Selleckchem
Citrate acide	Sigma Aldrich
Dapi Vectashield mounting medium	Vector Inc.

DEPC treated water	Invitrogen
Dimethylformamide	Merck
Dimethylsulfoxide (DMSO)	Carl Roth
DMEM (1x) GlutaMax 4.5 g/l D-glucose + pyruvate	Gibco
Dodecyl sulfate sodium salt (SDS)	Merck
Ethanol absolut ≥99,8%	VWR
Ethidium bromide	Sigma Aldrich
Etoposide	Sigma Aldrich
FCCP	Agilent Technologies
Farnesyltransferase Inhibitor (lonafarnib)	Eiger BioPharmaceuticals
Fetal bovine serum (FBS)	Invitrogen
Formaldehyde solution 37%	Merck
Gentamycin (10 mg/ml)	Invitrogen
Glutamine (200mM)	Invitrogen
Glutaraldehyde	Sigma Aldrich
Glycine	Sigma Aldrich
Hydrochloric Acid 37%	Sigma Aldrich
2x Laemmli Buffer	Bio-Rad
Magnesium chloride	Sigma Aldrich
Methanol	Roth
Modified porcine trypsin protease	Promega
Oligomycin	Agilent Technologies
Penicillin-Streptomycine (5,000 U/ml)	Invitrogen

Phenylmethylsulfonyl fluoride (PMSF)	Sigma Aldrich
Phosphate-buffered saline (PBS)	Invitrogen
Ponceau S	Sigma Aldrich
Potassium chloride	Fisher Scientific
Potassium Ferricyanide (III)	Merck
Potassium Ferrocyanide (II)	Sigma Aldrich
Precision Plus protein standards (dual color)	Bio-Rad
Rotenone	Agilent Technologies
Sodium chloride	Merck
Sodium dodecyl sulfate	Sigma Aldrich
Sodium hydroxide	Merck
Sodium phosphate	Sigma Aldrich
SYBR™ Master Mix	Applied Biosystems
SYBR™ Safe DNA Gel Stain	Invitrogen
Sucrose	Sigma Aldrich
Triton® X-100	Sigma Aldrich
Trizma base	Sigma Aldrich
Tween® 20	Sigma Aldrich
X-gal	Sigma Aldrich

5.4 Consumables

Table 23: Consumables

3.5, 6, 10 cm cell culture dish	Sarstedt

4-20% Mini-Protean TGX Precast Gel	Bio-Rad
6-, 24- and 96-well plates	Sarstedt
Corning 96-Well Black Microplate	Sigma
Cover glasses	VWR
Cryovials	Sarstedt
Membrane high-bond ECL nitrocellulose	Amersham
MicroAmp Fast Optical 96-Well Reaction Plate	Thermofisher
Microscope slides	VWR
Micro tubes (0.5, 1.5, 2 ml)	Sarstedt
Mini Transblot filter paper	Bio-Rad
Pipet tips (10, 20, 200, 1000 µl)	Sarstedt
Serological pipets (1, 2, 5, 10, 25, 50 ml)	Sarstedt
Tubes (15, 50 ml)	Sarstedt

5.5 Kits

Table 24: Kits

20S Proteasome Assay	Cayman Chemicals
Autophagy/Cytotoxicity Dual Staining	Cayman Chemicals
CellTiter-Glo Luminescent Cell Viability Assay	Promega
CellTox Green Cytotoxicity Assay	Promega
Clarity Western ECL substrate	BioRad
DCFDA – Cellular ROS Detection Assay	Abcam

Muse Cell Cycle Assay Kit	MerckMillipore
Seahorse XF Cell Mito Stress Kit	Agilent
Omniscript RT Kit	Qiagen
QIAshredder Kit	Qiagen

6 LITERATURE

Abella, Vanessa; Scotece, Morena; Conde, Javier; Pino, Jesús; Gonzalez-Gay, Miguel Angel; Gómez-Reino, Juan J. et al. (2017): Leptin in the interplay of inflammation, metabolism and immune system disorders. In: *Nature reviews. Rheumatology* 13 (2), S. 100–109. DOI: 10.1038/nrrheum.2016.209.

Abke, Sabine; Neumeier, Markus; Weigert, Johanna; Wehrwein, Gabriele; Eggenhofer, Elke; Schäffler, Andreas et al. (2006): Adiponectin-induced secretion of interleukin-6 (IL-6), monocyte chemotactic protein-1 (MCP-1, CCL2) and interleukin-8 (IL-8, CXCL8) is impaired in monocytes from patients with type I diabetes. In: *Cardiovascular diabetology* 5, S. 17. DOI: 10.1186/1475-2840-5-17.

Adam, Stephen A.; Butin-Israeli, Veronika; Cleland, Megan M.; Shimi, Takeshi; Goldman, Robert D. (2013): Disruption of lamin B1 and lamin B2 processing and localization by farnesyltransferase inhibitors. In: *Nucleus (Austin, Tex.)* 4 (2), S. 142–150. DOI: 10.4161/nucl.24089.

Adam, Stephen A.; Goldman, Robert D. (2012): Insights into the differences between the A- and B-type nuclear lamins. In: *Advances in biological regulation* 52 (1), S. 108–113. DOI: 10.1016/j.advenzreg.2011.11.001.

Adams, J. (2003): The proteasome: structure, function, and role in the cell. In: *Cancer Treatment Reviews* 29, S. 3–9. DOI: 10.1016/S0305-7372(03)00081-1.

Aebi, U.; Cohn, J.; Buhle, L.; Gerace, L. (1986): The nuclear lamina is a meshwork of intermediate-type filaments. In: *Nature* 323 (6088), S. 560–564. DOI: 10.1038/323560a0.

Aliper, Alexander M.; Csoka, Antonei Benjamin; Buzdin, Anton; Jetka, Tomasz; Roumiantsev, Sergey; Moskalev, Alexy; Zhavoronkov, Alex (2015): Signaling pathway activation drift during aging: Hutchinson-Gilford Progeria Syndrome fibroblasts are comparable to normal middle-age and old-age cells. In: *Aging* 7 (1), S. 26–37. DOI: 10.18632/aging.100717.

Alli, Rajshekhar; Nguyen, Phuong; Boyd, Kelli; Sundberg, John P.; Geiger, Terrence L. (2012): A mouse model of clonal CD8+ T lymphocyte-mediated alopecia areata progressing to alopecia universalis. In: *Journal of immunology (Baltimore, Md. : 1950)* 188 (1), S. 477–486. DOI: 10.4049/jimmunol.1100657.

Al-Salama, Zaina T.; Scott, Lesley J. (2018): Baricitinib: A Review in Rheumatoid Arthritis. In: *Drugs* 78 (7), S. 761–772. DOI: 10.1007/s40265-018-0908-4.

Alzolibani, Abdullateef A.; Zari, Shadi; Ahmed, Ahmed A. (2012): Epidemiologic and genetic characteristics of alopecia areata (part 2). In: *Acta dermatovenerologica Alpina, Pannonica, et Adriatica* 21 (1), S. 15–19.

Aman, Yahyah; Schmauck-Medina, Tomas; Hansen, Malene; Morimoto, Richard I.; Simon, Anna Katharina; Bjedov, Ivana et al. (2021): Autophagy in healthy aging and disease. In: *Nat Aging* 1 (8), S. 634–650. DOI: 10.1038/s43587-021-00098-4.

Andrés, Vicente; González, José M. (2009): Role of A-type lamins in signaling, transcription, and chromatin organization. In: *The Journal of cell biology* 187 (7), S. 945–957. DOI: 10.1083/jcb.200904124.

Arca, Ercan; Muşabak, Ugur; Akar, Ahmet; Erbil, A. Hakan; Taştan, H. Bülent (2004): Interferon-gamma in alopecia areata. In: *European journal of dermatology : EJD* 14 (1), S. 33–36.

Arnold, Rouven; Vehns, Elena; Randl, Hannah; Djabali, Karima (2021): Baricitinib, a JAK-STAT Inhibitor, Reduces the Cellular Toxicity of the Farnesyltransferase Inhibitor Lonafarnib in Progeria Cells. In: *International journal of molecular sciences* 22 (14). DOI: 10.3390/ijms22147474.

Ashar, H. R.; James, L.; Gray, K.; Carr, D.; Black, S.; Armstrong, L. et al. (2000): Farnesyl transferase inhibitors block the farnesylation of CENP-E and CENP-F and alter the association of CENP-E with the microtubules. In: *The Journal of biological chemistry* 275 (39), S. 30451–30457. DOI: 10.1074/jbc.M003469200.

Baker, P. B.; Baba, N.; Boesel, C. P. (1981): Cardiovascular abnormalities in progeria. Case report and review of the literature. In: *Archives of pathology & laboratory medicine* 105 (7), S. 384–386.

Ballanti, Eleonora; Perricone, Carlo; Di Muzio, Gioia; Kroegler, Barbara; Chimenti, Maria Sole; Graceffa, Dario; Perricone, Roberto (2011): Role of the complement system in rheumatoid arthritis and psoriatic arthritis: relationship with anti-TNF inhibitors. In: *Autoimmunity reviews* 10 (10), S. 617–623. DOI: 10.1016/j.autrev.2011.04.012.

Banerjee, Shubhasree; Biehl, Ann; Gadina, Massimo; Hasni, Sarfaraz; Schwartz, Daniella M. (2017): JAK-STAT Signaling as a Target for Inflammatory and Autoimmune Diseases: Current and Future Prospects. In: *Drugs* 77 (5), S. 521–546. DOI: 10.1007/s40265-017-0701-9.

Barahmani, N.; Lopez, A.; Babu, D.; Hernandez, M.; Donley, S. E.; Duvic, M. (2010): Serum T helper 1 cytokine levels are greater in patients with alopecia areata regardless of severity or atopy. In: *Clinical and experimental dermatology* 35 (4), S. 409–416. DOI: 10.1111/j.1365-2230.2009.03523.x.

Barber, Glen N. (2015): STING: infection, inflammation and cancer. In: *Nature reviews. Immunology* 15 (12), S. 760–770. DOI: 10.1038/nri3921.

Bavik, Claes; Coleman, Ilsa; Dean, James P.; Knudsen, Beatrice; Plymate, Steven; Nelson, Peter S. (2006): The gene expression program of prostate fibroblast senescence modulates neoplastic epithelial cell proliferation through paracrine mechanisms. In: *Cancer research* 66 (2), S. 794–802. DOI: 10.1158/0008-5472.CAN-05-1716.

Bektas, Arsun; Schurman, Shepherd H.; Sen, Ranjan; Ferrucci, Luigi (2018): Aging, inflammation and the environment. In: *Experimental gerontology* 105, S. 10–18. DOI: 10.1016/j.exger.2017.12.015.

Bergfeld, Wilma F. (2013): Growth hormone deficiency in a young patient with alopecia areata. In: *The journal of investigative dermatology. Symposium proceedings* 16 (1), S54-5. DOI: 10.1038/jidsymp.2013.21.

Bergo, Martin O.; Gavino, Bryant; Ross, Jed; Schmidt, Walter K.; Hong, Christine; Kendall, Lonnie V. et al. (2002): Zmpste24 deficiency in mice causes spontaneous bone fractures, muscle weakness, and a prelamin A processing defect. In: *Proceedings of the National Academy of Sciences of the United States of America* 99 (20), S. 13049–13054. DOI: 10.1073/pnas.192460799.

Bikkul, Mehmet U.; Clements, Craig S.; Godwin, Lauren S.; Goldberg, Martin W.; Kill, Ian R.; Bridger, Joanna M. (2018): Farnesyltransferase inhibitor and rapamycin correct aberrant genome organisation and decrease DNA damage respectively, in Hutchinson-Gilford progeria syndrome fibroblasts. In: *Biogerontology* 19 (6), S. 579–602. DOI: 10.1007/s10522-018-9758-4.

Bittles, A. H.; Harper, N. (1984): Increased glycolysis in ageing cultured human diploid fibroblasts. In: *Bioscience reports* 4 (9), S. 751–756. DOI: 10.1007/bf01128816.

Blondel, Sophie; Jaskowiak, Anne-Laure; Egesipe, Anne-Laure; Le Corf, Amelie; Navarro, Claire; Cordette, Véronique et al. (2014): Induced pluripotent stem cells reveal functional differences between drugs currently investigated in patients with hutchinson-gilford progeria syndrome. In: *Stem cells translational medicine* 3 (4), S. 510–519. DOI: 10.5966/sctm.2013-0168.

Bolick, S. C. E.; Landowski, T. H.; Boulware, D.; Oshiro, M. M.; Ohkanda, J.; Hamilton, A. D. et al. (2003): The farnesyl transferase inhibitor, FTI-277, inhibits growth and induces apoptosis in drug-resistant myeloma tumor cells. In: *Leukemia* 17 (2), S. 451–457. DOI: 10.1038/sj.leu.2402832.

Boucher, Jeremie; Softic, Samir; El Ouaamari, Abdelfattah; Krumpoch, Megan T.; Kleinridders, Andre; Kulkarni, Rohit N. et al. (2016): Differential Roles of Insulin and IGF-1 Receptors in Adipose Tissue Development and Function. In: *Diabetes* 65 (8), S. 2201–2213. DOI: 10.2337/db16-0212.

Brack, Andrew S.; Conboy, Michael J.; Roy, Sudeep; Lee, Mark; Kuo, Calvin J.; Keller, Charles; Rando, Thomas A. (2007): Increased Wnt signaling during aging alters muscle stem cell fate and increases fibrosis. In: *Science (New York, N.Y.)* 317 (5839), S. 807–810. DOI: 10.1126/science.1144090.

Bratic, Ana; Larsson, Nils-Göran (2013): The role of mitochondria in aging. In: *The Journal of clinical investigation* 123 (3), S. 951–957. DOI: 10.1172/JCI64125.

Brennan, F. M.; Chantry, D.; Jackson, A.; Maini, R.; Feldmann, M. (1989): Inhibitory effect of TNF alpha antibodies on synovial cell interleukin-1 production in rheumatoid arthritis. In: *Lancet (London, England)* 2 (8657), S. 244–247. DOI: 10.1016/s0140-6736(89)90430-3.

Bruunsgaard, H.; Skinhøj, P.; Pedersen, A. N.; Schroll, M.; Pedersen, B. K. (2000): Ageing, tumour necrosis factor-alpha (TNF-alpha) and atherosclerosis. In: *Clinical and experimental immunology* 121 (2), S. 255–260. DOI: 10.1046/j.1365-2249.2000.01281.x.

Brydun, Andrei; Watari, Yuichiro; Yamamoto, Yoshiyuki; Okuhara, Koichiro; Teragawa, Hiroki; Kono, Fujiko et al. (2007): Reduced expression of heme oxygenase-1 in patients with coronary atherosclerosis. In: *Hypertension research : official journal of the Japanese Society of Hypertension* 30 (4), S. 341–348. DOI: 10.1291/hypres.30.341.

Buono, Chiara; Come, Carolyn E.; Witztum, Joseph L.; Maguire, Graham F.; Connelly, Philip W.; Carroll, Michael; Lichtman, Andrew H. (2002): Influence of C3 deficiency on atherosclerosis. In: *Circulation* 105 (25), S. 3025–3031. DOI: 10.1161/01.cir.0000019584.04929.83.

Butt, Christopher; Gladman, Dafna; Rahman, Proton (2006): PPAR-gamma gene polymorphisms and psoriatic arthritis. In: *The Journal of rheumatology* 33 (8), S. 1631–1633.

Campisi, Judith (2013): Aging, cellular senescence, and cancer. In: *Annual review of physiology* 75, S. 685–705. DOI: 10.1146/annurev-physiol-030212-183653.

Campisi, Judith; Andersen, Julie K.; Kapahi, Pankaj; Melov, Simon (2011): Cellular senescence: a link between cancer and age-related degenerative disease? In: *Seminars in cancer biology* 21 (6), S. 354–359. DOI: 10.1016/j.semcancer.2011.09.001.

Campisi, Judith; Di d'Adda Fagagna, Fabrizio (2007): Cellular senescence: when bad things happen to good cells. In: *Nature reviews. Molecular cell biology* 8 (9), S. 729–740. DOI: 10.1038/nrm2233.

Capell, Brian C.; Collins, Francis S. (2006): Human laminopathies: nuclei gone genetically awry. In: *Nature reviews. Genetics* 7 (12), S. 940–952. DOI: 10.1038/nrg1906.

Capell, Brian C.; Erdos, Michael R.; Madigan, James P.; Fiordalisi, James J.; Varga, Renee; Conneely, Karen N. et al. (2005): Inhibiting farnesylation of progerin prevents the characteristic nuclear blebbing of Hutchinson-Gilford progeria syndrome. In: *Proceedings of the National Academy of Sciences of the United States of America* 102 (36), S. 12879–12884. DOI: 10.1073/pnas.0506001102.

Capell, Brian C.; Olive, Michelle; Erdos, Michael R.; Cao, Kan; Faddah, Dina A.; Tavarez, Urraca L. et al. (2008): A farnesyltransferase inhibitor prevents both the onset and late progression of cardiovascular disease in a progeria mouse model. In: *Proceedings of the National Academy of Sciences of the United States of America* 105 (41), S. 15902–15907. DOI: 10.1073/pnas.0807840105.

Capobianchi, Maria Rosaria; Uleri, Elena; Caglioti, Claudia; Dolei, Antonina (2015): Type I IFN family members: similarity, differences and interaction. In: *Cytokine & growth factor reviews* 26 (2), S. 103–111. DOI: 10.1016/j.cytogfr.2014.10.011.

Carrero, Dido; Soria-Valles, Clara; López-Otín, Carlos (2016): Hallmarks of progeroid syndromes: lessons from mice and reprogrammed cells. In: *Disease models & mechanisms* 9 (7), S. 719–735. DOI: 10.1242/dmm.024711.

Castelar, L.; Silva, M. M.; Castelli, E. C.; Deghaide, N. H. S.; Mendes-Junior, C. T.; Machado, A. A. et al. (2010): Interleukin-18 and interferon-gamma polymorphisms in Brazilian human immunodeficiency virus-1-infected patients presenting with lipodystrophy syndrome. In: *Tissue antigens* 76 (2), S. 126–130. DOI: 10.1111/j.1399-0039.2010.01471.x.

Chapman, James; Fielder, Edward; Passos, João F. (2019): Mitochondrial dysfunction and cell senescence: deciphering a complex relationship. In: *FEBS letters* 593 (13), S. 1566–1579. DOI: 10.1002/1873-3468.13498.

Chen, Chia-Yen; Chi, Ya-Hui; Mutalif, Rafidah Abdul; Starost, Matthew F.; Myers, Timothy G.; Anderson, Stasia A. et al. (2012): Accumulation of the inner nuclear envelope protein Sun1 is pathogenic in progeric and dystrophic laminopathies. In: *Cell* 149 (3), S. 565–577. DOI: 10.1016/j.cell.2012.01.059.

Cheng, Tao; Sun, Xue; Wu, Jian; Wang, Mingjun; Eisenberg, Robert A.; Chen, Zhiwei (2016): Increased serum levels of tumor necrosis factor receptor-associated factor 1 (TRAF1) correlate with disease activity and autoantibodies in rheumatoid arthritis. In: *Clinica chimica acta; international journal of clinical chemistry* 462, S. 103–106. DOI: 10.1016/j.cca.2016.08.021.

Chovatiya, Raj; Medzhitov, Ruslan (2014): Stress, inflammation, and defense of homeostasis. In: *Molecular cell* 54 (2), S. 281–288. DOI: 10.1016/j.molcel.2014.03.030.

Clouthier, D. E.; Comerford, S. A.; Hammer, R. E. (1997): Hepatic fibrosis, glomerulosclerosis, and a lipodystrophy-like syndrome in PEPCK-TGF-beta1 transgenic mice. In: *The Journal of clinical investigation* 100 (11), S. 2697–2713. DOI: 10.1172/JCI119815.

Constantinescu, Dan; Csoka, Antonei B.; Navara, Christopher S.; Schatten, Gerald P. (2010): Defective DSB repair correlates with abnormal nuclear morphology and is improved with FTI treatment in Hutchinson-Gilford progeria syndrome fibroblasts. In: *Experimental cell research* 316 (17), S. 2747–2759. DOI: 10.1016/j.yexcr.2010.05.015.

Coppé, Jean-Philippe; Desprez, Pierre-Yves; Krtolica, Ana; Campisi, Judith (2010): The senescence-associated secretory phenotype: the dark side of tumor suppression. In: *Annual review of pathology* 5, S. 99–118. DOI: 10.1146/annurev-pathol-121808-102144.

Coppé, Jean-Philippe; Kauser, Katalin; Campisi, Judith; Beauséjour, Christian M. (2006): Secretion of vascular endothelial growth factor by primary human fibroblasts at senescence. In: *The Journal of biological chemistry* 281 (40), S. 29568–29574. DOI: 10.1074/jbc.M603307200.

Corcoy, R.; Aris, A.; Leiva, A. de (1989): Fertility in a case of progeria. In: *The American journal of the medical sciences* 297 (6), S. 383–384. DOI: 10.1097/00000441-198906000-00010.

Coutinho, Henrique Douglas M.; Falcão-Silva, Vivyanne S.; Gonçalves, Gregório Fernandes; da Nóbrega, Raphael Batista (2009): Molecular ageing in progeroid syndromes: Hutchinson-Gilford progeria syndrome as a model. In: *Immunity & ageing : I & A* 6, S. 4. DOI: 10.1186/1742-4933-6-4.

Davies, B. S. J.; Barnes, R. H.; Tu, Y.; Ren, S.; Andres, D. A.; Spielmann, H. P. et al. (2010): An accumulation of non-farnesylated prelamin A causes cardiomyopathy but not progeria. In: *Human molecular genetics* 19 (13), S. 2682–2694. DOI: 10.1093/hmg/ddq158.

Degeorge, Katharine C.; Degeorge, Brent R.; Testa, James S.; Rothstein, Jay L. (2008): Inhibition of oncogene-induced inflammatory chemokines using a farnesyltransferase inhibitor. In: *Journal of inflammation (London, England)* 5, S. 3. DOI: 10.1186/1476-9255-5-3.

Dhillon, Sohita (2021): Lonafarnib: First Approval. In: *Drugs* 81 (2), S. 283–289. DOI: 10.1007/s40265-020-01464-z.

Dickinson, Mary E.; Flenniken, Ann M.; Ji, Xiao; Teboul, Lydia; Wong, Michael D.; White, Jacqueline K. et al. (2016): High-throughput discovery of novel developmental phenotypes. In: *Nature* 537 (7621), S. 508–514. DOI: 10.1038/nature19356.

Dimri, G. P.; Lee, X.; Basile, G.; Acosta, M.; Scott, G.; Roskelley, C. et al. (1995): A biomarker that identifies senescent human cells in culture and in aging skin in vivo. In: *Proceedings of the National Academy of Sciences of the United States of America* 92 (20), S. 9363–9367. DOI: 10.1073/pnas.92.20.9363.

Dinh, Quynh N.; Chrissobolis, Sophocles; Diep, Henry; Chan, Christopher T.; Ferens, Dorota; Drummond, Grant R.; Sobey, Christopher G. (2017): Advanced atherosclerosis is associated with inflammation, vascular dysfunction and oxidative stress, but not hypertension. In: *Pharmacological research* 116, S. 70–76. DOI: 10.1016/j.phrs.2016.12.032.

Dittmer, Travis A.; Misteli, Tom (2011): The lamin protein family. In: *Genome biology* 12 (5), S. 222. DOI: 10.1186/gb-2011-12-5-222.

Dong, Shuanghai; Xia, Tian; Wang, Lei; Zhao, Qinghua; Tian, Jiwei (2016): Investigation of candidate genes for osteoarthritis based on gene expression profiles. In: *Acta orthopaedica et traumatologica turcica* 50 (6), S. 686–690. DOI: 10.1016/j.aott.2016.04.002.

Dorado, Beatriz; Andrés, Vicente (2017): A-type lamins and cardiovascular disease in premature aging syndromes. In: *Current opinion in cell biology* 46, S. 17–25. DOI: 10.1016/j.ceb.2016.12.005.

Dorado, Beatriz; Pløen, Gro Grunnet; Barettino, Ana; Macías, Alvaro; Gonzalo, Pilar; Andrés-Manzano, María Jesús et al. (2019): Generation and characterization of a novel knockin minipig model of Hutchinson-Gilford progeria syndrome. In: *Cell discovery* 5, S. 16. DOI: 10.1038/s41421-019-0084-z.

Dou, Zhixun; Ghosh, Kanad; Vizioli, Maria Grazia; Zhu, Jiajun; Sen, Payel; Wangensteen, Kirk J. et al. (2017): Cytoplasmic chromatin triggers inflammation in senescence and cancer. In: *Nature* 550 (7676), S. 402–406. DOI: 10.1038/nature24050.

Dragović, Gordana; Dimitrijević, Božana; Khawla, Al Musalhi; Soldatović, Ivan; Andjić, Mladen; Jevtović, Djordje; Nair, Devaki (2017): Lower levels of IL-4 and IL-10 influence lipodystrophy in HIV/AIDS patients under antiretroviral therapy. In: *Experimental and molecular pathology* 102 (2), S. 210–214. DOI: 10.1016/j.yexmp.2017.02.001.

Elzi, David J.; Song, Meihua; Hakala, Kevin; Weintraub, Susan T.; Shiio, Yuzuru (2012): Wnt antagonist SFRP1 functions as a secreted mediator of senescence. In: *Molecular and cellular biology* 32 (21), S. 4388–4399. DOI: 10.1128/MCB.06023-11.

Eriksson, Maria; Brown, W. Ted; Gordon, Leslie B.; Glynn, Michael W.; Singer, Joel; Scott, Laura et al. (2003): Recurrent de novo point mutations in lamin A cause Hutchinson-Gilford progeria syndrome. In: *Nature* 423 (6937), S. 293–298. DOI: 10.1038/nature01629.

Essaghir, Ahmed; Toffalini, Federica; Knoops, Laurent; Kallin, Anders; van Helden, Jacques; Demoulin, Jean-Baptiste (2010): Transcription factor regulation can be accurately predicted from the presence of target gene signatures in microarray gene expression data. In: *Nucleic acids research* 38 (11), e120. DOI: 10.1093/nar/gkq149.

Faget, Douglas V.; Ren, Qihao; Stewart, Sheila A. (2019): Unmasking senescence: context-dependent effects of SASP in cancer. In: *Nature reviews. Cancer* 19 (8), S. 439–453. DOI: 10.1038/s41568-019-0156-2.

Fairhurst, D. A.; Mitra, A.; MacDonald-Hull, S. (2009): Direct Immunofluorescence studies of patients with alopecia areata in affected and clinically normal areas of scalp. In: *Journal of the European Academy of Dermatology and Venereology : JEADV* 23 (3), S. 347–348. DOI: 10.1111/j.1468-3083.2008.02853.x.

Farr, Joshua N.; Xu, Ming; Weivoda, Megan M.; Monroe, David G.; Fraser, Daniel G.; Onken, Jennifer L. et al. (2017): Targeting cellular senescence prevents age-related bone loss in mice. In: *Nature medicine* 23 (9), S. 1072–1079. DOI: 10.1038/nm.4385.

Favalli, Ennio G.; Biggioggero, Martina; Maioli, Gabriella; Caporali, Roberto (2020): Baricitinib for COVID-19: a suitable treatment? In: *The Lancet Infectious Diseases* 20 (9), S. 1012–1013. DOI: 10.1016/S1473-3099(20)30262-0.

Fong, Loren G.; Frost, David; Meta, Margarita; Qiao, Xin; Yang, Shao H.; Coffinier, Catherine; Young, Stephen G. (2006): A protein farnesyltransferase inhibitor ameliorates disease in a mouse model of progeria. In: *Science (New York, N.Y.)* 311 (5767), S. 1621–1623. DOI: 10.1126/science.1124875.

Fong, Loren G.; Ng, Jennifer K.; Meta, Margarita; Coté, Nathan; Yang, Shao H.; Stewart, Colin L. et al. (2004): Heterozygosity for Lmna deficiency eliminates the progeria-like phenotypes in Zmpste24-deficient mice. In: *Proceedings of the National Academy of Sciences of the United States of America* 101 (52), S. 18111–18116. DOI: 10.1073/pnas.0408558102.

Fragoulis, George E.; McInnes, Iain B.; Siebert, Stefan (2019): JAK-inhibitors. New players in the field of immune-mediated diseases, beyond rheumatoid arthritis. In: *Rheumatology (Oxford, England)* 58 (Suppl 1), i43-i54. DOI: 10.1093/rheumatology/key276.

Franceschi, Claudio; Campisi, Judith (2014): Chronic inflammation (inflammaging) and its potential contribution to age-associated diseases. In: *The journals of gerontology. Series A, Biological sciences and medical sciences* 69 Suppl 1, S4-9. DOI: 10.1093/gerona/glu057.

Frasca, Daniela; Blomberg, Bonnie B. (2016): Inflammaging decreases adaptive and innate immune responses in mice and humans. In: *Biogerontology* 17 (1), S. 7–19. DOI: 10.1007/s10522-015-9578-8.

Freund, Adam; Laberge, Remi-Martin; Demaria, Marco; Campisi, Judith (2012): Lamin B1 loss is a senescence-associated biomarker. In: *Molecular biology of the cell* 23 (11), S. 2066–2075. DOI: 10.1091/mbc.e11-10-0884.

Fridman, Jordan S.; Scherle, Peggy A.; Collins, Robert; Burn, Timothy C.; Li, Yanlong; Li, Jun et al. (2010): Selective inhibition of JAK1 and JAK2 is efficacious in rodent models of arthritis: preclinical characterization of INCB028050. In: *Journal of immunology (Baltimore, Md. : 1950)* 184 (9), S. 5298–5307. DOI: 10.4049/jimmunol.0902819.

Fulop, Tamas; Witkowski, Jacek M.; Olivieri, Fabiola; Larbi, Anis (2018): The integration of inflammaging in age-related diseases. In: *Seminars in immunology* 40, S. 17–35. DOI: 10.1016/j.smim.2018.09.003.

Gabriel, Diana; Gordon, Leslie B.; Djabali, Karima (2016): Temsirolimus Partially Rescues the Hutchinson-Gilford Progeria Cellular Phenotype. In: *PloS one* 11 (12), e0168988. DOI: 10.1371/journal.pone.0168988.

Gabriel, Diana; Roedl, Daniela; Gordon, Leslie B.; Djabali, Karima (2015): Sulforaphane enhances progerin clearance in Hutchinson-Gilford progeria fibroblasts. In: *Aging cell* 14 (1), S. 78–91. DOI: 10.1111/acel.12300.

Gabriel, Diana; Shafry, Dinah Dorith; Gordon, Leslie B.; Djabali, Karima (2017): Intermittent treatment with farnesyltransferase inhibitor and sulforaphane improves cellular homeostasis in Hutchinson-Gilford progeria fibroblasts. In: *Oncotarget* 8 (39), S. 64809–64826. DOI: 10.18632/oncotarget.19363.

Gallego-Escuredo, José M.; Villarroya, Joan; Domingo, Pere; Targarona, Eduard M.; Alegre, Marta; Domingo, Joan C. et al. (2013): Differentially altered molecular signature of visceral adipose tissue in HIV-1-associated lipodystrophy. In: *Journal of acquired immune deficiency syndromes (1999)* 64 (2), S. 142–148. DOI: 10.1097/QAI.0b013e31829bdb67.

Gamerdinger, Martin; Hajieva, Parvana; Kaya, A. Murat; Wolfrum, Uwe; Hartl, F. Ulrich; Behl, Christian (2009): Protein quality control during aging involves recruitment of the macroautophagy pathway by BAG3. In: *The EMBO journal* 28 (7), S. 889–901. DOI: 10.1038/emboj.2009.29.

Garg, Nidhi; Krishan, Pawan; Syngle, Ashit (2016): Atherosclerosis in Psoriatic Arthritis: A Multiparametric Analysis Using Imaging Technique and Laboratory Markers of Inflammation and Vascular Function. In: *The International journal of angiology : official publication of the International College of Angiology, Inc* 25 (4), S. 222–228. DOI: 10.1055/s-0036-1584918.

Gaspar, Neide Kalil (2016): DHEA and frontal fibrosing alopecia: molecular and physiopathological mechanisms. In: *Anais brasileiros de dermatologia* 91 (6), S. 776–780. DOI: 10.1590/abd1806-4841.20165029.

Ghanemi, Abdelaziz (2015): Cell cultures in drug development: Applications, challenges and limitations. In: *Saudi pharmaceutical journal : SPJ : the official publication of the Saudi Pharmaceutical Society* 23 (4), S. 453–454. DOI: 10.1016/j.jsps.2014.04.002.

Giaginis, Costas; Giagini, Athina; Theocharis, Stamatios (2009): Peroxisome proliferator-activated receptor-gamma (PPAR-gamma) ligands as potential therapeutic agents to treat arthritis. In: *Pharmacological research* 60 (3), S. 160–169. DOI: 10.1016/j.phrs.2009.02.005.

Gilford, H. (1904): Ateleiosis and progeria : continuous youth and premature old age. In: *Brit Med J* 2, S. 914–918. Online verfügbar unter https://ci.nii.ac.jp/naid/10011594841/.

Gilhar, Amos; Landau, Marina; Assy, Bedia; Ullmann, Yehuda; Shalaginov, Raya; Serafimovich, Sima; Kalish, Richard S. (2003): Transfer of alopecia areata in the human scalp graft/Prkdc(scid) (SCID) mouse system is characterized by a TH1 response. In: *Clinical immunology (Orlando, Fla.)* 106 (3), S. 181–187. DOI: 10.1016/s1521-6616(02)00042-6.

Glück, Selene; Guey, Baptiste; Gulen, Muhammet Fatih; Wolter, Katharina; Kang, Tae-Won; Schmacke, Niklas Arndt et al. (2017): Innate immune sensing of cytosolic chromatin fragments through cGAS promotes senescence. In: *Nature cell biology* 19 (9), S. 1061–1070. DOI: 10.1038/ncb3586.

Glynn, Michael W.; Glover, Thomas W. (2005): Incomplete processing of mutant lamin A in Hutchinson-Gilford progeria leads to nuclear abnormalities, which are reversed by farnesyltransferase inhibition. In: *Human molecular genetics* 14 (20), S. 2959–2969. DOI: 10.1093/hmg/ddi326.

Goldman, Robert D.; Shumaker, Dale K.; Erdos, Michael R.; Eriksson, Maria; Goldman, Anne E.; Gordon, Leslie B. et al. (2004): Accumulation of mutant lamin A causes progressive changes in nuclear architecture in Hutchinson-Gilford progeria syndrome. In: *Proceedings of the National Academy of Sciences of the United States of America* 101 (24), S. 8963–8968. DOI: 10.1073/pnas.0402943101.

Gordon, Leslie B.; Kleinman, Monica E.; Miller, David T.; Neuberg, Donna S.; Giobbie-Hurder, Anita; Gerhard-Herman, Marie et al. (2012): Clinical trial of a farnesyltransferase inhibitor in children with Hutchinson-Gilford progeria syndrome. In: *Proceedings of the National Academy of Sciences of the United States of America* 109 (41), S. 16666–16671. DOI: 10.1073/pnas.1202529109.

Gordon, Leslie B.; Massaro, Joe; D'Agostino, Ralph B.; Campbell, Susan E.; Brazier, Joan; Brown, W. Ted et al. (2014a): Impact of farnesylation inhibitors on survival in Hutchinson-Gilford progeria syndrome. In: *Circulation* 130 (1), S. 27–34. DOI: 10.1161/CIRCULATIONAHA.113.008285.

Gordon, Leslie B.; Rothman, Frank G.; López-Otín, Carlos; Misteli, Tom (2014b): Progeria: a paradigm for translational medicine. In: *Cell* 156 (3), S. 400–407. DOI: 10.1016/j.cell.2013.12.028.

Gordon, Leslie B.; Shappell, Heather; Massaro, Joe; D'Agostino, Ralph B.; Brazier, Joan; Campbell, Susan E. et al. (2018): Association of Lonafarnib Treatment vs No Treatment With Mortality Rate in Patients With Hutchinson-Gilford Progeria Syndrome. In: *JAMA* 319 (16), S. 1687–1695. DOI: 10.1001/jama.2018.3264.

Gracie, J. A.; Forsey, R. J.; Chan, W. L.; Gilmour, A.; Leung, B. P.; Greer, M. R. et al. (1999): A proinflammatory role for IL-18 in rheumatoid arthritis. In: *The Journal of clinical investigation* 104 (10), S. 1393–1401. DOI: 10.1172/JCI7317.

Gregoriou, Stamatis; Papafragkaki, Dafni; Kontochristopoulos, George; Rallis, Eustathios; Kalogeromitros, Dimitrios; Rigopoulos, Dimitris (2010): Cytokines and other mediators in alopecia areata. In: *Mediators of inflammation* 2010, S. 928030. DOI: 10.1155/2010/928030.

Griveau, Audrey; Wiel, Clotilde; Ziegler, Dorian V.; Bergo, Martin O.; Bernard, David (2020): The JAK1/2 inhibitor ruxolitinib delays premature aging phenotypes. In: *Aging cell* 19 (4), e13122. DOI: 10.1111/acel.13122.

Gundry, Michael; Vijg, Jan (2012): Direct mutation analysis by high-throughput sequencing: from germline to low-abundant, somatic variants. In: *Mutation research* 729 (1-2), S. 1–15. DOI: 10.1016/j.mrfmmm.2011.10.001.

Gupta, A. K.; Ellis, C. N.; Cooper, K. D.; Nickoloff, B. J.; Ho, V. C.; Chan, L. S. et al. (1990): Oral cyclosporine for the treatment of alopecia areata. A clinical and immunohistochemical analysis. In: *Journal of the American Academy of Dermatology* 22 (2 Pt 1), S. 242–250. DOI: 10.1016/0190-9622(90)70032-d.

Han, Heonjong; Cho, Jae-Won; Lee, Sangyoung; Yun, Ayoung; Kim, Hyojin; Bae, Dasom et al. (2018): TRRUST v2: an expanded reference database of human and mouse transcriptional regulatory interactions. In: *Nucleic acids research* 46 (D1), D380-D386. DOI: 10.1093/nar/gkx1013.

Harhouri, Karim; Frankel, Diane; Bartoli, Catherine; Roll, Patrice; Sandre-Giovannoli, Annachiara de; Lévy, Nicolas (2018): An overview of treatment strategies for Hutchinson-Gilford Progeria syndrome. In: *Nucleus (Austin, Tex.)* 9 (1), S. 246–257. DOI: 10.1080/19491034.2018.1460045.

Haringman, Jasper J.; Gerlag, Danielle M.; Smeets, Tom J. M.; Baeten, Dominique; van den Bosch, Filip; Bresnihan, Barry et al. (2006): A randomized controlled trial with an anti-CCL2 (anti-monocyte chemotactic protein 1) monoclonal antibody in patients with rheumatoid arthritis. In: *Arthritis and rheumatism* 54 (8), S. 2387–2392. DOI: 10.1002/art.21975.

Harries, Matthew J.; Paus, Ralf (2009): Scarring alopecia and the PPAR-gamma connection. In: *The Journal of investigative dermatology* 129 (5), S. 1066–1070. DOI: 10.1038/jid.2008.425.

Harrington, J. R. (2000): The role of MCP-1 in atherosclerosis. In: *Stem cells (Dayton, Ohio)* 18 (1), S. 65–66. DOI: 10.1634/stemcells.18-1-65.

Hartman, Joshua; Frishman, William H. (2014): Inflammation and atherosclerosis: a review of the role of interleukin-6 in the development of atherosclerosis and the potential for targeted drug therapy. In: *Cardiology in review* 22 (3), S. 147–151. DOI: 10.1097/CRD.0000000000000021.

Hayden, Matthew S.; Ghosh, Sankar (2008): Shared principles in NF-kappaB signaling. In: *Cell* 132 (3), S. 344–362. DOI: 10.1016/j.cell.2008.01.020.

Hayflick, L.; Moorhead, P. S. (1961): The serial cultivation of human diploid cell strains. In: *Experimental cell research* 25 (3), S. 585–621. DOI: 10.1016/0014-4827(61)90192-6.

He, G.; Andersen, O.; Haugaard, S. B.; Lihn, A. S.; Pedersen, S. B.; Madsbad, S.; Richelsen, B. (2005): Plasminogen activator inhibitor type 1 (PAI-1) in plasma and adipose tissue in HIV-associated lipodystrophy syndrome. Implications of adipokines. In: *European journal of clinical investigation* 35 (9), S. 583–590. DOI: 10.1111/j.1365-2362.2005.01547.x.

Hennekam, Raoul C. M. (2006): Hutchinson-Gilford progeria syndrome: review of the phenotype. In: *American journal of medical genetics. Part A* 140 (23), S. 2603–2624. DOI: 10.1002/ajmg.a.31346.

Hernandez-Segura, Alejandra; Jong, Tristan V. de; Melov, Simon; Guryev, Victor; Campisi, Judith; Demaria, Marco (2017): Unmasking Transcriptional Heterogeneity in Senescent Cells. In: *Current biology : CB* 27 (17), 2652-2660.e4. DOI: 10.1016/j.cub.2017.07.033.

Higashi, Yusuke; Sukhanov, Sergiy; Anwar, Asif; Shai, Shaw-Yung; Delafontaine, Patrice (2012): Aging, atherosclerosis, and IGF-1. In: *The journals of gerontology. Series A, Biological sciences and medical sciences* 67 (6), S. 626–639. DOI: 10.1093/gerona/gls102.

Hong, Seok-Beom; Jin, Sheng-Yu; Park, Hae-Jeong; Jung, Joo-Ho; Sim, Woo-Young (2006): Analysis of the monocyte chemoattractant protein 1 -2518 promoter polymorphism in Korean patients with alopecia areata. In: *Journal of Korean medical science* 21 (1), S. 90–94. DOI: 10.3346/jkms.2006.21.1.90.

Howard, A. N.; Thurnham, D. I. (2017): Lutein and atherosclerosis: Belfast versus Toulouse revisited. In: *Medical hypotheses* 98, S. 63–68. DOI: 10.1016/j.mehy.2016.10.030.

Hui, W.; Rowan, A. D.; Cawston, T. (2001): Modulation of the expression of matrix metalloproteinase and tissue inhibitors of metalloproteinases by TGF-beta1 and IGF-1 in primary human articular and bovine nasal chondrocytes stimulated with TNF-alpha. In: *Cytokine* 16 (1), S. 31–35. DOI: 10.1006/cyto.2001.0950.

Hussein, Deema; Taylor, Stephen S. (2002): Farnesylation of Cenp-F is required for G2/M progression and degradation after mitosis. In: *Journal of cell science* 115 (Pt 17), S. 3403–3414.

Hutchinson, J. (1886): Case of congenital absence of hair, with atrophic condition of the skin and its appendages, in a boy whose mother had been almost wholly bald from alopecia areata from the age of six. In: *Lancet*, S. 923. Online verfügbar unter https://ci.nii.ac.jp/naid/10011594842/.

Iannello, Alexandre; Samarani, Suzanne; Debbeche, Olfa; Boulassel, Mohamed-Rachid; Tremblay, Cécile; Toma, Emil et al. (2010): Potential role of IL-18 in the immunopathogenesis of AIDS, HIV-associated lipodystrophy and related clinical conditions. In: *Current HIV research* 8 (2), S. 147–164. DOI: 10.2174/157016210790442713.

Inglese, J.; Glickman, J. F.; Lorenz, W.; Caron, M. G.; Lefkowitz, R. J. (1992): Isoprenylation of a protein kinase. Requirement of farnesylation/alpha-carboxyl methylation for full enzymatic activity of rhodopsin kinase. In: *The Journal of biological chemistry* 267 (3), S. 1422–1425.

Itahana, Koji; Campisi, Judith; Dimri, Goberdhan P. (2007): Methods to detect biomarkers of cellular senescence: the senescence-associated beta-galactosidase assay. In: *Methods in molecular biology (Clifton, N.J.)* 371, S. 21–31. DOI: 10.1007/978-1-59745-361-5_3.

Ivanov, Andre; Pawlikowski, Jeff; Manoharan, Indrani; van Tuyn, John; Nelson, David M.; Rai, Taranjit Singh et al. (2013): Lysosome-mediated processing of chromatin in senescence. In: *The Journal of cell biology* 202 (1), S. 129–143. DOI: 10.1083/jcb.201212110.

Jabbari, Ali; Dai, Zhenpeng; Xing, Luzhou; Cerise, Jane E.; Ramot, Yuval; Berkun, Yackov et al. (2015): Reversal of Alopecia Areata Following Treatment With the JAK1/2 Inhibitor Baricitinib. In: *EBioMedicine* 2 (4), S. 351–355. DOI: 10.1016/j.ebiom.2015.02.015.

Jansen, Joyce; Delaere, Lien; Spielberg, Leigh; Leys, Anita (2013): Long-term fundus changes in acquired partial lipodystrophy. In: *BMJ case reports* 2013. DOI: 10.1136/bcr-2013-201218.

Jia, Guanghong; Cheng, Gang; Gangahar, Deepak M.; Agrawal, Devendra K. (2006): Insulin-like growth factor-1 and TNF-alpha regulate autophagy through c-jun N-terminal kinase and Akt pathways in human atherosclerotic vascular smooth cells. In: *Immunology and cell biology* 84 (5), S. 448–454. DOI: 10.1111/j.1440-1711.2006.01454.x.

Jiang, C.; Ting, A. T.; Seed, B. (1998): PPAR-gamma agonists inhibit production of monocyte inflammatory cytokines. In: *Nature* 391 (6662), S. 82–86. DOI: 10.1038/34184.

Jin, Shengkan; White, Eileen (2008): Tumor suppression by autophagy through the management of metabolic stress. In: *Autophagy* 4 (5), S. 563–566.

Kanameishi, S.; Nakamizo, S.; Endo, Y.; Fujisawa, A.; Dainichi, T.; Tanaka, T. et al. (2017): High level of serum human interleukin-18 in a patient with pyogenic arthritis, pyoderma gangrenosum and acne syndrome. In: *Journal of the European Academy of Dermatology and Venereology : JEADV* 31 (2), e115-e116. DOI: 10.1111/jdv.13856.

Kannisto, Katja; Sutinen, Jussi; Korsheninnikova, Elena; Fisher, Rachel M.; Ehrenborg, Ewa; Gertow, Karl et al. (2003): Expression of adipogenic transcription factors, peroxisome proliferator-activated receptor gamma co-activator 1, IL-6 and CD45 in subcutaneous adipose tissue in lipodystrophy associated with highly active antiretroviral therapy. In: *AIDS (London, England)* 17 (12), S. 1753–1762. DOI: 10.1097/00002030-200308150-00004.

Kasumagic-Halilovic, Emina; Prohic, Asja; Cavaljuga, Semra (2011): Tumor necrosis factor-alpha in patients with alopecia areata. In: *Indian journal of dermatology* 56 (5), S. 494–496. DOI: 10.4103/0019-5154.87124.

Kauppinen, Anu; Suuronen, Tiina; Ojala, Johanna; Kaarniranta, Kai; Salminen, Antero (2013): Antagonistic crosstalk between NF-κB and SIRT1 in the regulation of inflammation and metabolic disorders. In: *Cellular signalling* 25 (10), S. 1939–1948. DOI: 10.1016/j.cellsig.2013.06.007.

Kieran, Mark W.; Packer, Roger J.; Onar, Arzu; Blaney, Susan M.; Phillips, Peter; Pollack, Ian F. et al. (2007): Phase I and pharmacokinetic study of the oral farnesyltransferase inhibitor lonafarnib administered twice daily to pediatric patients with advanced central nervous system tumors using a modified continuous reassessment method: a Pediatric Brain Tumor Consortium Study. In: *Journal of clinical oncology : official journal of the American Society of Clinical Oncology* 25 (21), S. 3137–3143. DOI: 10.1200/JCO.2006.09.4243.

Kim, Go Woon; Lee, Na Ra; Pi, Ryo Han; Lim, Yee Seul; Lee, Yu Mi; Lee, Jong Min et al. (2015a): IL-6 inhibitors for treatment of rheumatoid arthritis: past, present, and future. In: *Archives of pharmacal research* 38 (5), S. 575–584. DOI: 10.1007/s12272-015-0569-8.

Kim, Kyoung-Woon; Kim, Bo-Mi; Moon, Hee-Won; Lee, Sang-Heon; Kim, Hae-Rim (2015b): Role of C-reactive protein in osteoclastogenesis in rheumatoid arthritis. In: *Arthritis research & therapy* 17, S. 41. DOI: 10.1186/s13075-015-0563-z.

Kitagawa, Kazuo; Matsumoto, Masayasu; Sasaki, Tsutomu; Hashimoto, Hiroyuki; Kuwabara, Keisuke; Ohtsuki, Toshiho; Hori, Masatsugu (2002): Involvement of ICAM-1 in the progression of atherosclerosis in APOE-knockout mice. In: *Atherosclerosis* 160 (2), S. 305–310. DOI: 10.1016/s0021-9150(01)00587-1.

Kizilay Mancini, Özge; Lora, Maximilien; Shum-Tim, Dominique; Nadeau, Stephanie; Rodier, Francis; Colmegna, Inés (2017): A Proinflammatory Secretome Mediates the Impaired Immunopotency of Human Mesenchymal Stromal Cells in Elderly Patients with Atherosclerosis. In: *Stem cells translational medicine* 6 (4), S. 1132–1140. DOI: 10.1002/sctm.16-0221.

Klass, Michael R. (1983): A method for the isolation of longevity mutants in the nematode Caenorhabditis elegans and initial results. In: *Mechanisms of Ageing and Development* 22 (3-4), S. 279–286. DOI: 10.1016/0047-6374(83)90082-9.

Kleinbongard, Petra; Heusch, Gerd; Schulz, Rainer (2010): TNFalpha in atherosclerosis, myocardial ischemia/reperfusion and heart failure. In: *Pharmacology & therapeutics* 127 (3), S. 295–314. DOI: 10.1016/j.pharmthera.2010.05.002.

Koenen, Rory R.; Weber, Christian (2010): Therapeutic targeting of chemokine interactions in atherosclerosis. In: *Nature reviews. Drug discovery* 9 (2), S. 141–153. DOI: 10.1038/nrd3048.

Kontis, Vasilis; Bennett, James E.; Mathers, Colin D.; Li, Guangquan; Foreman, Kyle; Ezzati, Majid (2017): Future life expectancy in 35 industrialised countries: projections with a Bayesian model ensemble. In: *The Lancet* 389 (10076), S. 1323–1335. DOI: 10.1016/S0140-6736(16)32381-9.

Krtolica, Ana; Larocque, Nick; Genbacev, Olga; Ilic, Dusko; Coppe, Jean-Philippe; Patil, Christopher K. et al. (2011): GROα regulates human embryonic stem cell self-renewal or adoption of a neuronal fate. In: *Differentiation; research in biological diversity* 81 (4), S. 222–232. DOI: 10.1016/j.diff.2011.01.001.

Kulkarni, Sai; Punia, Rajpal Singh; Kundu, Reetu; Thami, Gurvinder Pal; Mohan, Harsh (2014): Direct immunofluorescence pattern and histopathological staging in alopecia areata. In: *International journal of trichology* 6 (4), S. 164–167. DOI: 10.4103/0974-7753.142859.

Kumar, Ashok; Takada, Yasunari; Boriek, Aladin M.; Aggarwal, Bharat B. (2004): Nuclear factor-kappaB: its role in health and disease. In: *Journal of molecular medicine (Berlin, Germany)* 82 (7), S. 434–448. DOI: 10.1007/s00109-004-0555-y.

Kumari, Ruchi; Jat, Parmjit (2021): Mechanisms of Cellular Senescence: Cell Cycle Arrest and Senescence Associated Secretory Phenotype. In: *Frontiers in cell and developmental biology* 9, S. 645593. DOI: 10.3389/fcell.2021.645593.

Laberge, Remi-Martin; Awad, Pierre; Campisi, Judith; Desprez, Pierre-Yves (2012): Epithelial-mesenchymal transition induced by senescent fibroblasts. In: *Cancer microenvironment : official journal of the International Cancer Microenvironment Society* 5 (1), S. 39–44. DOI: 10.1007/s12307-011-0069-4.

Lai, Wing-Fu; Wong, Wing-Tak (2020): Progress and trends in the development of therapies for Hutchinson-Gilford progeria syndrome. In: *Aging cell* 19 (7), e13175. DOI: 10.1111/acel.13175.

Lan, Yuk Yuen; Heather, James M.; Eisenhaure, Thomas; Garris, Christopher Stuart; Lieb, David; Raychowdhury, Raktima; Hacohen, Nir (2019): Extranuclear DNA accumulates in aged cells and contributes to senescence and inflammation. In: *Aging cell* 18 (2), e12901. DOI: 10.1111/acel.12901.

Laviades, C.; Varo, N.; Díez, J. (2000): Transforming growth factor beta in hypertensives with cardiorenal damage. In: *Hypertension (Dallas, Tex. : 1979)* 36 (4), S. 517–522. DOI: 10.1161/01.hyp.36.4.517.

Lee, Bo Yun; Han, Jung A.; Im, Jun Sub; Morrone, Amelia; Johung, Kimberly; Goodwin, Edward C. et al. (2006): Senescence-associated beta-galactosidase is lysosomal beta-galactosidase. In: *Aging cell* 5 (2), S. 187–195. DOI: 10.1111/j.1474-9726.2006.00199.x.

Lee, Deborah; Hong, Soon-Kwon; Park, Sung-Wook; Hur, Dae-Young; Shon, Ji-Hong; Shin, Jae-Gook et al. (2010): Serum levels of IL-18 and sIL-2R in patients with alopecia areata receiving combined therapy with oral cyclosporine and steroids. In: *Experimental dermatology* 19 (2), S. 145–147. DOI: 10.1111/j.1600-0625.2009.00937.x.

Lee, Ji Hyun; Cho, Dae Ho; Park, Hyun Jeong (2015): IL-18 and Cutaneous Inflammatory Diseases. In: *International journal of molecular sciences* 16 (12), S. 29357–29369. DOI: 10.3390/ijms161226172.

Lee, Seung Hoon; Kwon, Ji Ye; Kim, Se-Young; Jung, KyoungAh; Cho, Mi-La (2017): Interferon-gamma regulates inflammatory cell death by targeting necroptosis in experimental autoimmune arthritis. In: *Scientific reports* 7 (1), S. 10133. DOI: 10.1038/s41598-017-09767-0.

Lee, Yong Woo; Hirani, Anjali A. (2006): Role of interleukin-4 in atherosclerosis. In: *Archives of pharmacal research* 29 (1), S. 1–15. DOI: 10.1007/BF02977462.

Leung, Vivien; Chiu, Ya-Lin; Kotler, Donald P.; Albu, Jeanine; Zhu, Yuan-Shan; Ham, Kirsis et al. (2016): Effect of Recombinant Human Growth Hormone and Rosiglitazone for HIV-Associated Abdominal Fat Accumulation on Adiponectin and other Markers of Inflammation. In: *HIV clinical trials* 17 (2), S. 55–62. DOI: 10.1080/15284336.2015.1126424.

Liberti, Maria V.; Locasale, Jason W. (2016): The Warburg Effect: How Does it Benefit Cancer Cells? In: *Trends in biochemical sciences* 41 (3), S. 211–218. DOI: 10.1016/j.tibs.2015.12.001.

Lichtenstein, Kenneth A. (2005): Redefining lipodystrophy syndrome: risks and impact on clinical decision making. In: *Journal of acquired immune deficiency syndromes (1999)* 39 (4), S. 395–400. DOI: 10.1097/01.qai.0000167478.28051.3a.

Lindegaard, Birgitte; Hansen, Ann-Brit Eg; Pilegaard, Henriette; Keller, Pernille; Gerstoft, Jan; Pedersen, Bente Klarlund (2004): Adipose tissue expression of IL-18 and HIV-associated lipodystrophy. In: *AIDS (London, England)* 18 (14), S. 1956–1958. DOI: 10.1097/00002030-200409240-00013.

Liu, Baohua; Wang, Jianming; Chan, Kui Ming; Tjia, Wai Mui; Deng, Wen; Guan, Xinyuan et al. (2005): Genomic instability in laminopathy-based premature aging. In: *Nature medicine* 11 (7), S. 780–785. DOI: 10.1038/nm1266.

Liu, Chang; Arnold, Rouven; Henriques, Gonçalo; Djabali, Karima (2019): Inhibition of JAK-STAT Signaling with Baricitinib Reduces Inflammation and Improves Cellular Homeostasis in Progeria Cells. In: *Cells* 8 (10). DOI: 10.3390/cells8101276.

Liu, Yin; Ramot, Yuval; Torrelo, Antonio; Paller, Amy S.; Si, Nuo; Babay, Sofia et al. (2012): Mutations in proteasome subunit β type 8 cause chronic atypical neutrophilic dermatosis with lipodystrophy and elevated temperature with evidence of genetic and phenotypic heterogeneity. In: *Arthritis and rheumatism* 64 (3), S. 895–907. DOI: 10.1002/art.33368.

Liu, Yiyong; Rusinol, Antonio; Sinensky, Michael; Wang, Youjie; Zou, Yue (2006): DNA damage responses in progeroid syndromes arise from defective maturation of prelamin A. In: *Journal of cell science* 119 (Pt 22), S. 4644–4649. DOI: 10.1242/jcs.03263.

Lomashvili, Koba A.; Narisawa, Sonoko; Millán, Jose L.; O'Neill, W. Charles (2014): Vascular calcification is dependent on plasma levels of pyrophosphate. In: *Kidney international* 85 (6), S. 1351–1356. DOI: 10.1038/ki.2013.521.

Loonam, Cathriona R.; O'Dell, Sandra D.; Sharp, Paul A.; Mullen, Anne (2016): Microarray Analysis Reveals Altered Lipid and Glucose Metabolism Genes in Differentiated, Ritonavir-Treated 3T3-L1 Adipocytes. In: *Current HIV research* 14 (1), S. 37–46. DOI: 10.2174/1570162x13666150806110238.

Lopez-Mejia, Isabel C.; Toledo, Marion de; Chavey, Carine; Lapasset, Laure; Cavelier, Patricia; Lopez-Herrera, Celia et al. (2014): Antagonistic functions of LMNA isoforms in energy expenditure and lifespan. In: *EMBO reports* 15 (5), S. 529–539. DOI: 10.1002/embr.201338126.

López-Otín, Carlos; Blasco, Maria A.; Partridge, Linda; Serrano, Manuel; Kroemer, Guido (2013): The hallmarks of aging. In: *Cell* 153 (6), S. 1194–1217. DOI: 10.1016/j.cell.2013.05.039.

Lu, Gui-Qing; Wu, Zhi-Bo; Chu, Xiao-Yan; Bi, Zhi-Gang; Fan, Wei-Xin (2016): An investigation of crosstalk between Wnt/β-catenin and transforming growth factor-β signaling in androgenetic alopecia. In: *Medicine* 95 (30), e4297. DOI: 10.1097/MD.0000000000004297.

Lufei, Chengchen; Ma, Jing; Huang, Guochang; Zhang, Tong; Novotny-Diermayr, Veronica; Ong, Chin Thing; Cao, Xinmin (2003): GRIM-19, a death-regulatory gene product, suppresses Stat3 activity via functional interaction. In: *The EMBO journal* 22 (6), S. 1325–1335. DOI: 10.1093/emboj/cdg135.

Magalhães, João Pedro de; Finch, Caleb E.; Janssens, Georges (2010): Next-generation sequencing in aging research: emerging applications, problems, pitfalls and possible solutions. In: *Ageing research reviews* 9 (3), S. 315–323. DOI: 10.1016/j.arr.2009.10.006.

Mahajan, Supriya D.; Gaekwad, Asmita; Pawar, Jyoti; Tripathy, Srikanth; Ghate, Manisha; Bhattacharya, Jayanta et al. (2015): Cardiac morbidity in an HIV-1 lipodystrophy patient cohort expressing the TNF-α-238 G/A single nucleotide gene polymorphism. In: *Current HIV research* 13 (2), S. 98–108. DOI: 10.2174/1570162x12666141202125016.

Mahamid, Mahmud; Abu-Elhija, Omar; Samamra, Mosab; Mahamid, Ammad; Nseir, William (2014): Association between vitamin D levels and alopecia areata. In: *The Israel Medical Association journal : IMAJ* 16 (6), S. 367–370.

Mallampalli, Monica P.; Huyer, Gregory; Bendale, Pravin; Gelb, Michael H.; Michaelis, Susan (2005): Inhibiting farnesylation reverses the nuclear morphology defect in a HeLa cell model for Hutchinson-Gilford progeria syndrome. In: *Proceedings of the National Academy of Sciences of the United States of America* 102 (40), S. 14416–14421. DOI: 10.1073/pnas.0503712102.

Manente, Lucrezia; Lucariello, Angela; Costanzo, Carmelina; Viglietti, Rosaria; Parrella, Giovanni; Parrella, Roberto et al. (2012): Suppression of pre adipocyte differentiation and promotion of adipocyte death by anti-HIV drugs. In: *In vivo (Athens, Greece)* 26 (2), S. 287–291.

Manivel, Vivek Anand; Sohrabian, Azita; Rönnelid, Johan (2016): Granulocyte-augmented chemokine production induced by type II collagen containing immune complexes is mediated via TLR4 in rheumatoid arthritis patients. In: *European journal of immunology* 46 (12), S. 2822–2834. DOI: 10.1002/eji.201646496.

Marbach, Daniel; Lamparter, David; Quon, Gerald; Kellis, Manolis; Kutalik, Zoltán; Bergmann, Sven (2016): Tissue-specific regulatory circuits reveal variable modular perturbations across complex diseases. In: *Nature methods* 13 (4), S. 366–370. DOI: 10.1038/nmeth.3799.

Marzolla, Vincenzo; Armani, Andrea; Mammi, Caterina; Moss, Mary E.; Pagliarini, Vittoria; Pontecorvo, Laura et al. (2017): Essential role of ICAM-1 in aldosterone-induced atherosclerosis. In: *International journal of cardiology* 232, S. 233–242. DOI: 10.1016/j.ijcard.2017.01.013.

Mazzocca, Antonio; Giusti, Sabrina; Hamilton, Andrew D.; Sebti, Said M.; Pantaleo, Pietro; Carloni, Vinicio (2003): Growth inhibition by the farnesyltransferase inhibitor FTI-277 involves Bcl-2 expression and defective association with Raf-1 in liver cancer cell lines. In: *Molecular pharmacology* 63 (1), S. 159–166. DOI: 10.1124/mol.63.1.159.

McClintock, Dayle; Ratner, Desiree; Lokuge, Meepa; Owens, David M.; Gordon, Leslie B.; Collins, Francis S.; Djabali, Karima (2007): The mutant form of lamin A that causes Hutchinson-Gilford progeria is a biomarker of cellular aging in human skin. In: *PloS one* 2 (12), e1269. DOI: 10.1371/journal.pone.0001269.

McLaren, James E.; Ramji, Dipak P. (2009): Interferon gamma: a master regulator of atherosclerosis. In: *Cytokine & growth factor reviews* 20 (2), S. 125–135. DOI: 10.1016/j.cytogfr.2008.11.003.

Meiler, Svenja; Lutgens, Esther; Weber, Christian; Gerdes, Norbert (2016): Atherosclerosis: cell biology and lipoproteins-focus on interleukin-18 signaling, chemotactic heteromers, and microRNAs. In: *Current opinion in lipidology* 27 (3), S. 308–309. DOI: 10.1097/MOL.0000000000000305.

Melendez, Mark M.; McNurlan, Margaret A.; Mynarcik, Dennis C.; Khan, Shilpi; Gelato, Marie C. (2008): Endothelial adhesion molecules are associated with inflammation in subjects with HIV disease. In: *Clinical infectious diseases : an official publication of the Infectious Diseases Society of America* 46 (5), S. 775–780. DOI: 10.1086/527563.

Mewar, Devesh; Wilson, Anthony G. (2011): Treatment of rheumatoid arthritis with tumour necrosis factor inhibitors. In: *British journal of pharmacology* 162 (4), S. 785–791. DOI: 10.1111/j.1476-5381.2010.01099.x.

Meyer, Sara C.; Levine, Ross L. (2014): Molecular pathways: molecular basis for sensitivity and resistance to JAK kinase inhibitors. In: *Clinical cancer research : an official journal of the American Association for Cancer Research* 20 (8), S. 2051–2059. DOI: 10.1158/1078-0432.CCR-13-0279.

Miehle, Konstanze; Ebert, Thomas; Kralisch, Susan; Hoffmann, Annett; Kratzsch, Jürgen; Schlögl, Haiko et al. (2016): Progranulin is increased in human and murine lipodystrophy. In: *Diabetes research and clinical practice* 120, S. 1–7. DOI: 10.1016/j.diabres.2016.07.017.

Misiakos, E. P.; Kouraklis, G.; Agapitos, E.; Perrea, D.; Karatzas, G.; Boudoulas, H.; Karayannakos, P. E. (2001): Expression of PDGF-A, TGFb and VCAM-1 during the developmental stages of experimental atherosclerosis. In: *European surgical research. Europaische chirurgische Forschung. Recherches chirurgicales europeennes* 33 (4), S. 264–269. DOI: 10.1159/000049716.

Missiou, Anna; Köstlin, Natascha; Varo, Nerea; Rudolf, Philipp; Aichele, Peter; Ernst, Sandra et al. (2010): Tumor necrosis factor receptor-associated factor 1 (TRAF1) deficiency attenuates atherosclerosis in mice by impairing monocyte recruitment to the vessel wall. In: *Circulation* 121 (18), S. 2033–2044. DOI: 10.1161/CIRCULATIONAHA.109.895037.

Moelants, Eva A. V.; Mortier, Anneleen; van Damme, Jo; Proost, Paul (2013): Regulation of TNF-α with a focus on rheumatoid arthritis. In: *Immunology and cell biology* 91 (6), S. 393–401. DOI: 10.1038/icb.2013.15.

Montecucco, Alessandra; Zanetta, Francesca; Biamonti, Giuseppe (2015): Molecular mechanisms of etoposide. In: *EXCLI journal* 14, S. 95–108. DOI: 10.17179/excli2015-561.

Motegi, Sei-ichiro; Yokoyama, Yoko; Uchiyama, Akihiko; Ogino, Sachiko; Takeuchi, Yuko; Yamada, Kazuya et al. (2014): First Japanese case of atypical progeroid syndrome/atypical Werner syndrome with heterozygous LMNA mutation. In: *The Journal of dermatology* 41 (12), S. 1047–1052. DOI: 10.1111/1346-8138.12657.

Mozzini, Chiara (2020): Progeria, atherosclerosis and clonal hematopoiesis: links and future perspectives. In: *Mechanisms of Ageing and Development* 192, S. 111365. DOI: 10.1016/j.mad.2020.111365.

Müller-Ladner, Ulf; Pap, Thomas; Gay, Renate E.; Neidhart, Michel; Gay, Steffen (2005): Mechanisms of disease: the molecular and cellular basis of joint destruction in rheumatoid arthritis. In: *Nature clinical practice. Rheumatology* 1 (2), S. 102–110. DOI: 10.1038/ncprheum0047.

Muñoz-Espín, Daniel; Serrano, Manuel (2014): Cellular senescence: from physiology to pathology. In: *Nature reviews. Molecular cell biology* 15 (7), S. 482–496. DOI: 10.1038/nrm3823.

Nacarelli, Timothy; Azar, Ashley; Altinok, Oya; Orynbayeva, Zulfiya; Sell, Christian (2018): Rapamycin increases oxidative metabolism and enhances metabolic flexibility in human cardiac fibroblasts. In: *GeroScience*. DOI: 10.1007/s11357-018-0030-2.

Neurohr, Gabriel E.; Terry, Rachel L.; Lengefeld, Jette; Bonney, Megan; Brittingham, Gregory P.; Moretto, Fabien et al. (2019): Excessive Cell Growth Causes Cytoplasm Dilution And Contributes to Senescence. In: *Cell* 176 (5), 1083-1097.e18. DOI: 10.1016/j.cell.2019.01.018.

Nissan, Xavier; Blondel, Sophie; Navarro, Claire; Maury, Yves; Denis, Cécile; Girard, Mathilde et al. (2012): Unique preservation of neural cells in Hutchinson- Gilford progeria syndrome is due to the expression of the neural-specific miR-9 microRNA. In: *Cell reports* 2 (1), S. 1–9. DOI: 10.1016/j.celrep.2012.05.015.

Niu, Qian; Cai, Bei; Huang, Zhuo-chun; Shi, Yun-ying; Wang, Lan-lan (2012): Disturbed Th17/Treg balance in patients with rheumatoid arthritis. In: *Rheumatology international* 32 (9), S. 2731–2736. DOI: 10.1007/s00296-011-1984-x.

Noda, Asao; Mishima, Shuji; Hirai, Yuko; Hamasaki, Kanya; Landes, Reid D.; Mitani, Hiroshi et al. (2015): Progerin, the protein responsible for the Hutchinson-Gilford progeria syndrome, increases the unrepaired DNA damages following exposure to ionizing radiation. In: *Genes and environment : the official journal of the Japanese Environmental Mutagen Society* 37, S. 13. DOI: 10.1186/s41021-015-0018-4.

Novakova, Z.; Hubackova, S.; Kosar, M.; Janderova-Rossmeislova, L.; Dobrovolna, J.; Vasicova, P. et al. (2010): Cytokine expression and signaling in drug-induced cellular senescence. In: *Oncogene* 29 (2), S. 273–284. DOI: 10.1038/onc.2009.318.

Novelli, Giuseppe; Muchir, Antoine; Sangiuolo, Federica; Helbling-Leclerc, Anne; D'Apice, Maria Rosaria; Massart, Catherine et al. (2002): Mandibuloacral dysplasia is caused by a mutation in LMNA-encoding lamin A/C. In: *American journal of human genetics* 71 (2), S. 426–431. DOI: 10.1086/341908.

Okazaki, Shuhei; Sakaguchi, Manabu; Miwa, Kaori; Furukado, Shigetaka; Yamagami, Hiroshi; Yagita, Yoshiki et al. (2014): Association of interleukin-6 with the progression of carotid atherosclerosis: a 9-year follow-up study. In: *Stroke* 45 (10), S. 2924–2929. DOI: 10.1161/STROKEAHA.114.005991.

Oliveira Pinto, Luzia Maria de; Garcia, Sylvie; Lecoeur, Hervé; Rapp, Christophe; Gougeon, Marie-Lise (2002): Increased sensitivity of T lymphocytes to tumor necrosis factor receptor 1 (TNFR1)- and TNFR2-mediated apoptosis in HIV infection: relation to expression of Bcl-2 and active caspase-8 and caspase-3. In: *Blood* 99 (5), S. 1666–1675. DOI: 10.1182/blood.v99.5.1666.

Osorio, F. G.; Soria-Valles, C.; Santiago-Fernández, O.; Freije, J. M. P.; López-Otín, C. (2016): NF-κB signaling as a driver of ageing. In: *International review of cell and molecular biology* 326, S. 133–174. DOI: 10.1016/bs.ircmb.2016.04.003.

Osorio, Fernando G.; Bárcena, Clea; Soria-Valles, Clara; Ramsay, Andrew J.; Carlos, Félix de; Cobo, Juan et al. (2012): Nuclear lamina defects cause ATM-dependent NF-κB activation and link accelerated aging to a systemic inflammatory response. In: *Genes & development* 26 (20), S. 2311–2324. DOI: 10.1101/gad.197954.112.

Osorio, Fernando G.; Navarro, Claire L.; Cadiñanos, Juan; López-Mejía, Isabel C.; Quirós, Pedro M.; Bartoli, Catherine et al. (2011): Splicing-directed therapy in a new mouse model of human accelerated aging. In: *Science translational medicine* 3 (106), 106ra107. DOI: 10.1126/scitranslmed.3002847.

Paffen, Elaine; DeMaat, Moniek P. M. (2006): C-reactive protein in atherosclerosis: A causal factor? In: *Cardiovascular research* 71 (1), S. 30–39. DOI: 10.1016/j.cardiores.2006.03.004.

Pandey, Rahul; Bakay, Marina; Strenkowski, Bryan P.; Hain, Heather S.; Hakonarson, Hakon (2021): JAK/STAT inhibitor therapy partially rescues the lipodystrophic autoimmune phenotype in Clec16a KO mice. In: *Scientific reports* 11 (1), S. 7372. DOI: 10.1038/s41598-021-86493-8.

Paramel Varghese, Geena; Folkersen, Lasse; Strawbridge, Rona J.; Halvorsen, Bente; Yndestad, Arne; Ranheim, Trine et al. (2016): NLRP3 Inflammasome Expression and Activation in Human Atherosclerosis. In: *Journal of the American Heart Association* 5 (5). DOI: 10.1161/JAHA.115.003031.

Pasolli, Edoardo; Schiffer, Lucas; Manghi, Paolo; Renson, Audrey; Obenchain, Valerie; Truong, Duy Tin et al. (2017): Accessible, curated metagenomic data through ExperimentHub. In: *Nature methods* 14 (11), S. 1023–1024. DOI: 10.1038/nmeth.4468.

Payne, Gregory A.; Tune, Johnathan D.; Knudson, Jarrod D. (2014): Leptin-induced endothelial dysfunction: a target for therapeutic interventions. In: *Current pharmaceutical design* 20 (4), S. 603–608. DOI: 10.2174/13816128113199990017.

Paz-Filho, Gilberto; Mastronardi, Claudio A.; Licinio, Julio (2015): Leptin treatment: Facts and expectations. In: *Metabolism* 64 (1), S. 146–156. DOI: 10.1016/j.metabol.2014.07.014.

Pendás, Alberto M.; Zhou, Zhongjun; Cadiñanos, Juan; Freije, José M. P.; Wang, Jianming; Hultenby, Kjell et al. (2002): Defective prelamin A processing and muscular and adipocyte alterations in Zmpste24 metalloproteinase-deficient mice. In: *Nature genetics* 31 (1), S. 94–99. DOI: 10.1038/ng871.

Peth, Andreas; Nathan, James A.; Goldberg, Alfred L. (2013): The ATP costs and time required to degrade ubiquitinated proteins by the 26 S proteasome. In: *The Journal of biological chemistry* 288 (40), S. 29215–29222. DOI: 10.1074/jbc.M113.482570.

Pfaffl, M. W. (2001): A new mathematical model for relative quantification in real-time RT-PCR. In: *Nucleic acids research* 29 (9), e45. DOI: 10.1093/nar/29.9.e45.

Philpott, M. P.; Sanders, D. A.; Bowen, J.; Kealey, T. (1996): Effects of interleukins, colony-stimulating factor and tumour necrosis factor on human hair follicle growth in vitro: a possible role for interleukin-1 and tumour necrosis factor-alpha in alopecia areata. In: *The British journal of dermatology* 135 (6), S. 942–948. DOI: 10.1046/j.1365-2133.1996.d01-1099.x.

Piekarowicz, Katarzyna; Machowska, Magdalena; Dzianisava, Volha; Rzepecki, Ryszard (2019): Hutchinson-Gilford Progeria Syndrome-Current Status and Prospects for Gene Therapy Treatment. In: *Cells* 8 (2). DOI: 10.3390/cells8020088.

Plesković, Aleš; Letonja, Marija Šantl; Vujkovac, Andreja Cokan; Nikolajević Starčević, Jovana; Gazdikova, Katarina; Caprnda, Martin et al. (2017): C-reactive protein as a marker of progression of carotid atherosclerosis in subjects with type 2 diabetes mellitus. In: *VASA. Zeitschrift fur Gefasskrankheiten* 46 (3), S. 187–192. DOI: 10.1024/0301-1526/a000614.

Pricola, Katie L.; Kuhn, Nastaran Z.; Haleem-Smith, Hana; Song, Yingjie; Tuan, Rocky S. (2009): Interleukin-6 maintains bone marrow-derived mesenchymal stem cell stemness by an ERK1/2-dependent mechanism. In: *Journal of cellular biochemistry* 108 (3), S. 577–588. DOI: 10.1002/jcb.22289.

Prins, J. B.; Niesler, C. U.; Winterford, C. M.; Bright, N. A.; Siddle, K.; O'Rahilly, S. et al. (1997): Tumor necrosis factor-alpha induces apoptosis of human adipose cells. In: *Diabetes* 46 (12), S. 1939–1944. DOI: 10.2337/diab.46.12.1939.

Prokocimer, Miron; Davidovich, Maya; Nissim-Rafinia, Malka; Wiesel-Motiuk, Naama; Bar, Daniel Z.; Barkan, Rachel et al. (2009): Nuclear lamins: key regulators of nuclear structure and activities. In: *Journal of cellular and molecular medicine* 13 (6), S. 1059–1085. DOI: 10.1111/j.1582-4934.2008.00676.x.

Rani, Jyoti; Shah, A. B. Rauf; Ramachandran, Srinivasan (2015): pubmed.mineR: an R package with text-mining algorithms to analyse PubMed abstracts. In: *Journal of biosciences* 40 (4), S. 671–682. DOI: 10.1007/s12038-015-9552-2.

Rawlings, Jason S.; Rosler, Kristin M.; Harrison, Douglas A. (2004): The JAK/STAT signaling pathway. In: *Journal of cell science* 117 (Pt 8), S. 1281–1283. DOI: 10.1242/jcs.00963.

Redler, S.; Brockschmidt, F. F.; Forstbauer, L.; Giehl, K. A.; Herold, C.; Eigelshoven, S. et al. (2010): The TRAF1/C5 locus confers risk for familial and severe alopecia areata. In: *The British journal of dermatology* 162 (4), S. 866–869. DOI: 10.1111/j.1365-2133.2009.09598.x.

Rincon, Mercedes; Pereira, Felipe Valença (2018): A New Perspective: Mitochondrial Stat3 as a Regulator for Lymphocyte Function. In: *International journal of molecular sciences* 19 (6). DOI: 10.3390/ijms19061656.

Rivera-Torres, José; Acín-Perez, Rebeca; Cabezas-Sánchez, Pablo; Osorio, Fernando G.; Gonzalez-Gómez, Cristina; Megias, Diego et al. (2013): Identification of mitochondrial dysfunction in Hutchinson-Gilford progeria syndrome through use of stable isotope labeling with amino acids in cell culture. In: *Journal of proteomics* 91, S. 466–477. DOI: 10.1016/j.jprot.2013.08.008.

Rodier, Francis; Muñoz, Denise P.; Teachenor, Robert; Chu, Victoria; Le, Oanh; Bhaumik, Dipa et al. (2011): DNA-SCARS: distinct nuclear structures that sustain damage-induced senescence growth arrest and inflammatory cytokine secretion. In: *Journal of cell science* 124 (Pt 1), S. 68–81. DOI: 10.1242/jcs.071340.

Röhrl, Jennifer M.; Arnold, Rouven; Djabali, Karima (2021): Nuclear Pore Complexes Cluster in Dysmorphic Nuclei of Normal and Progeria Cells during Replicative Senescence. In: *Cells* 10 (1). DOI: 10.3390/cells10010153.

Rossi, A.; Cantisani, C.; Carlesimo, M.; Scarnò, M.; Scali, E.; Mari, E. et al. (2012): Serum concentrations of IL-2, IL-6, IL-12 and TNF-α in patients with alopecia areata. In: *International journal of immunopathology and pharmacology* 25 (3), S. 781–788. DOI: 10.1177/039463201202500327.

Rueda, Blanca; Oliver, Javier; Robledo, Gema; López-Nevot, Miguel A.; Balsa, Alejandro; Pascual-Salcedo, Dora et al. (2007): HO-1 promoter polymorphism associated with rheumatoid arthritis. In: *Arthritis and rheumatism* 56 (12), S. 3953–3958. DOI: 10.1002/art.23048.

Sabbatinelli, Jacopo; Prattichizzo, Francesco; Olivieri, Fabiola; Procopio, Antonio Domenico; Rippo, Maria Rita; Giuliani, Angelica (2019): Where Metabolism Meets Senescence: Focus on Endothelial Cells. In: *Frontiers in physiology* 10, S. 1523. DOI: 10.3389/fphys.2019.01523.

Samaras, Katherine; Gan, Seng K.; Peake, Phillip W.; Carr, Andrew; Campbell, Lesley V. (2009): Proinflammatory markers, insulin sensitivity, and cardiometabolic risk factors in treated HIV infection. In: *Obesity (Silver Spring, Md.)* 17 (1), S. 53–59. DOI: 10.1038/oby.2008.500.

Sandre-Giovannoli, Annachiara de; Bernard, Rafaëlle; Cau, Pierre; Navarro, Claire; Amiel, Jeanne; Boccaccio, Irène et al. (2003): Lamin a truncation in Hutchinson-Gilford progeria. In: *Science (New York, N.Y.)* 300 (5628), S. 2055. DOI: 10.1126/science.1084125.

Sarkar, Sumantra; Alam, Md Mahboob; Das, Gargi; Datta, Supratim (2017): Inflammatory Markers and Disease Activity in Juvenile Idiopathic Arthritis. In: *Indian journal of pediatrics* 84 (5), S. 349–356. DOI: 10.1007/s12098-017-2292-6.

Savage, David B.; Semple, Robert K.; Clatworthy, Menna R.; Lyons, Paul A.; Morgan, B. Paul; Cochran, Elaine K. et al. (2009): Complement abnormalities in acquired lipodystrophy revisited. In: *The Journal of clinical endocrinology and metabolism* 94 (1), S. 10–16. DOI: 10.1210/jc.2008-1703.

Saxena, Saurabh; Kumar, Sanjeev (2020): Pharmacotherapy to gene editing: potential therapeutic approaches for Hutchinson-Gilford progeria syndrome. In: *GeroScience* 42 (2), S. 467–494. DOI: 10.1007/s11357-020-00167-3.

Scaffidi, Paola; Misteli, Tom (2006): Lamin A-dependent nuclear defects in human aging. In: *Science (New York, N.Y.)* 312 (5776), S. 1059–1063. DOI: 10.1126/science.1127168.

Shimi, Takeshi; Butin-Israeli, Veronika; Adam, Stephen A.; Hamanaka, Robert B.; Goldman, Anne E.; Lucas, Catherine A. et al. (2011): The role of nuclear lamin B1 in cell proliferation and senescence. In: *Genes & development* 25 (24), S. 2579–2593. DOI: 10.1101/gad.179515.111.

Soler Palacios, Blanca; Estrada-Capetillo, Lizbeth; Izquierdo, Elena; Criado, Gabriel; Nieto, Concha; Municio, Cristina et al. (2015): Macrophages from the synovium of active rheumatoid arthritis exhibit an activin A-dependent pro-inflammatory profile. In: *The Journal of pathology* 235 (3), S. 515–526. DOI: 10.1002/path.4466.

Soto-Gamez, Abel; Demaria, Marco (2017): Therapeutic interventions for aging: the case of cellular senescence. In: *Drug discovery today* 22 (5), S. 786–795. DOI: 10.1016/j.drudis.2017.01.004.

Souza Dantas Oliveira, Sandro Henrique de; Souza Aarão, Tinara Leila de; da Silva Barbosa, Leonardo; Souza Lisbôa, Paulo Guilherme; Tavares Dutra, Claudia Daniele; Margalho Sousa, Lorena et al. (2014): Immunohistochemical analysis of the expression of TNF-alpha, TGF-beta, and caspase-3 in subcutaneous tissue of patients with HIV lipodystrophy syndrome. In: *Microbial pathogenesis* 67-68, S. 41–47. DOI: 10.1016/j.micpath.2014.02.004.

Squarzoni, Stefano; Schena, Elisa; Sabatelli, Patrizia; Mattioli, Elisabetta; Capanni, Cristina; Cenni, Vittoria et al. (2021): Interleukin-6 neutralization ameliorates symptoms in prematurely aged mice. In: *Aging cell* 20 (1), e13285. DOI: 10.1111/acel.13285.

Strandgren, Charlotte; Revêchon, Gwladys; Sola-Carvajal, Agustín; Eriksson, Maria (2017): Emerging candidate treatment strategies for Hutchinson-Gilford progeria syndrome. In: *Biochemical Society transactions* 45 (6), S. 1279–1293. DOI: 10.1042/BST20170141.

Sugiura, Y.; Niimi, T.; Sato, S.; Yoshinouchi, T.; Banno, S.; Naniwa, T. et al. (2002): Transforming growth factor beta1 gene polymorphism in rheumatoid arthritis. In: *Annals of the rheumatic diseases* 61 (9), S. 826–828. DOI: 10.1136/ard.61.9.826.

Sun, Lijun; Wu, Jiaxi; Du, Fenghe; Chen, Xiang; Chen, Zhijian J. (2013): Cyclic GMP-AMP synthase is a cytosolic DNA sensor that activates the type I interferon pathway. In: *Science (New York, N.Y.)* 339 (6121), S. 786–791. DOI: 10.1126/science.1232458.

Szekanecz, Zoltán; Kim, Joon; Koch, Alisa E. (2003): Chemokines and chemokine receptors in rheumatoid arthritis. In: *Seminars in immunology* 15 (1), S. 15–21. DOI: 10.1016/s1044-5323(02)00124-0.

Szklarczyk, Damian; Gable, Annika L.; Lyon, David; Junge, Alexander; Wyder, Stefan; Huerta-Cepas, Jaime et al. (2019): STRING v11: protein-protein association networks with increased coverage, supporting functional discovery in genome-wide experimental datasets. In: *Nucleic acids research* 47 (D1), D607-D613. DOI: 10.1093/nar/gky1131.

T Virtanen, Anniina; Haikarainen, Teemu; Raivola, Juuli; Silvennoinen, Olli (2019): Selective JAKinibs: Prospects in Inflammatory and Autoimmune Diseases. In: *BioDrugs : clinical immunotherapeutics, biopharmaceuticals and gene therapy* 33 (1), S. 15–32. DOI: 10.1007/s40259-019-00333-w.

Tabas, Ira; Glass, Christopher K. (2013): Anti-inflammatory therapy in chronic disease: challenges and opportunities. In: *Science (New York, N.Y.)* 339 (6116), S. 166–172. DOI: 10.1126/science.1230720.

Tang, Liren; Bernardo, Olga; Bolduc, Chantal; Lui, Harvey; Madani, Shabnam; Shapiro, Jerry (2003): The expression of insulin-like growth factor 1 in follicular dermal papillae correlates with therapeutic

efficacy of finasteride in androgenetic alopecia. In: *Journal of the American Academy of Dermatology* 49 (2), S. 229–233. DOI: 10.1067/s0190-9622(03)00777-1.

te Poele, Robert H.; Okorokov, Andrei L.; Jardine, Lesley; Cummings, Jeffrey; Joel, Simon P. (2002): DNA damage is able to induce senescence in tumor cells in vitro and in vivo. In: *Cancer research* 62 (6), S. 1876–1883.

Tenger, Charlotta; Sundborger, Anna; Jawien, Jacek; Zhou, Xinghua (2005): IL-18 accelerates atherosclerosis accompanied by elevation of IFN-gamma and CXCL16 expression independently of T cells. In: *Arteriosclerosis, thrombosis, and vascular biology* 25 (4), S. 791–796. DOI: 10.1161/01.ATV.0000153516.02782.65.

Toth, Julia I.; Yang, Shao H.; Qiao, Xin; Beigneux, Anne P.; Gelb, Michael H.; Moulson, Casey L. et al. (2005): Blocking protein farnesyltransferase improves nuclear shape in fibroblasts from humans with progeroid syndromes. In: *Proceedings of the National Academy of Sciences of the United States of America* 102 (36), S. 12873–12878. DOI: 10.1073/pnas.0505767102.

Trifunovic, A.; Larsson, N-G (2008): Mitochondrial dysfunction as a cause of ageing. In: *Journal of internal medicine* 263 (2), S. 167–178. DOI: 10.1111/j.1365-2796.2007.01905.x.

Ullrich, Nicole J.; Gordon, Leslie B. (2015): Hutchinson-Gilford progeria syndrome. In: *Handbook of clinical neurology* 132, S. 249–264. DOI: 10.1016/B978-0-444-62702-5.00018-4.

van den Berg, W. B. (1999): The role of cytokines and growth factors in cartilage destruction in osteoarthritis and rheumatoid arthritis. In: *Zeitschrift fur Rheumatologie* 58 (3), S. 136–141. DOI: 10.1007/s003930050163.

van Deursen, Jan M. (2014): The role of senescent cells in ageing. In: *Nature* 509 (7501), S. 439–446. DOI: 10.1038/nature13193.

Verstraeten, Valerie L. R. M.; Peckham, Lana A.; Olive, Michelle; Capell, Brian C.; Collins, Francis S.; Nabel, Elizabeth G. et al. (2011): Protein farnesylation inhibitors cause donut-shaped cell nuclei attributable to a centrosome separation defect. In: *Proceedings of the National Academy of Sciences of the United States of America* 108 (12), S. 4997–5002. DOI: 10.1073/pnas.1019532108.

Victoria, B.; Cabezas-Agrícola, J. M.; González-Méndez, B.; Lattanzi, G.; Del Coco, R.; Loidi, L. et al. (2010): Reduced adipogenic gene expression in fibroblasts from a patient with type 2 congenital generalized lipodystrophy. In: *Diabetic medicine : a journal of the British Diabetic Association* 27 (10), S. 1178–1187. DOI: 10.1111/j.1464-5491.2010.03052.x.

Villa-Bellosta, Ricardo (2018): Synthesis of Extracellular Pyrophosphate Increases in Vascular Smooth Muscle Cells During Phosphate-Induced Calcification. In: *Arteriosclerosis, thrombosis, and vascular biology* 38 (9), S. 2137–2147. DOI: 10.1161/ATVBAHA.118.311444.

Villa-Bellosta, Ricardo (2019): ATP-based therapy prevents vascular calcification and extends longevity in a mouse model of Hutchinson-Gilford progeria syndrome. In: *Proceedings of the National Academy of Sciences of the United States of America* 116 (47), S. 23698–23704. DOI: 10.1073/pnas.1910972116.

Villarroya, Joan; Diaz-Delfin, Julieta; Hyink, Deborah; Domingo, Pere; Giralt, Marta; Klotman, Paul E.; Villarroya, Francesc (2010): HIV type-1 transgene expression in mice alters adipose tissue and adipokine levels: towards a rodent model of HIV type-1 lipodystrophy. In: *Antiviral therapy* 15 (7), S. 1021–1028. DOI: 10.3851/IMP1669.

Vizioli, Maria Grazia; Liu, Tianhui; Miller, Karl N.; Robertson, Neil A.; Gilroy, Kathryn; Lagnado, Anthony B. et al. (2020): Mitochondria-to-nucleus retrograde signaling drives formation of cytoplasmic chromatin and inflammation in senescence. In: *Genes & development* 34 (5-6), S. 428–445. DOI: 10.1101/gad.331272.119.

Wang, Jingyuan; Yao, Xue; Huang, Jin (2017a): New tricks for human farnesyltransferase inhibitor: cancer and beyond. In: *MedChemComm* 8 (5), S. 841–854. DOI: 10.1039/c7md00030h.

Wang, Mei; Casey, Patrick J. (2016): Protein prenylation: unique fats make their mark on biology. In: *Nature reviews. Molecular cell biology* 17 (2), S. 110–122. DOI: 10.1038/nrm.2015.11.

Wang, Rong; Yu, Zhen; Sunchu, Bharath; Shoaf, James; Dang, Ivana; Zhao, Stephanie et al. (2017b): Rapamycin inhibits the secretory phenotype of senescent cells by a Nrf2-independent mechanism. In: *Aging cell* 16 (3), S. 564–574. DOI: 10.1111/acel.12587.

Wang, Yuexia; Ostlund, Cecilia; Choi, Jason C.; Swayne, Theresa C.; Gundersen, Gregg G.; Worman, Howard J. (2012): Blocking farnesylation of the prelamin A variant in Hutchinson-Gilford progeria syndrome alters the distribution of A-type lamins. In: *Nucleus (Austin, Tex.)* 3 (5), S. 452–462. DOI: 10.4161/nucl.21675.

Wee, Kenneth; Yang, Wulin; Sugii, Shigeki; Han, Weiping (2014): Towards a mechanistic understanding of lipodystrophy and seipin functions. In: *Bioscience reports* 34 (5). DOI: 10.1042/BSR20140114.

Wei, Wei-Min; Wu, Xiao-Yan; Li, Shu-Ting; Shen, QingYu (2016): PPARG gene C161T CT/TT associated with lower blood lipid levels and ischemic stroke from large-artery atherosclerosis in a Han population in Guangdong. In: *Neurological research* 38 (7), S. 620–624. DOI: 10.1080/01616412.2016.1189056.

Wiley, Christopher D.; Velarde, Michael C.; Lecot, Pacome; Liu, Su; Sarnoski, Ethan A.; Freund, Adam et al. (2016): Mitochondrial Dysfunction Induces Senescence with a Distinct Secretory Phenotype. In: *Cell metabolism* 23 (2), S. 303–314. DOI: 10.1016/j.cmet.2015.11.011.

Wojdasiewicz, Piotr; Poniatowski, Łukasz A.; Szukiewicz, Dariusz (2014): The role of inflammatory and anti-inflammatory cytokines in the pathogenesis of osteoarthritis. In: *Mediators of inflammation* 2014, S. 561459. DOI: 10.1155/2014/561459.

Wu, Jiaxi; Sun, Lijun; Chen, Xiang; Du, Fenghe; Shi, Heping; Chen, Chuo; Chen, Zhijian J. (2013): Cyclic GMP-AMP is an endogenous second messenger in innate immune signaling by cytosolic DNA. In: *Science (New York, N.Y.)* 339 (6121), S. 826–830. DOI: 10.1126/science.1229963.

Wu, Meng-Ling; Ho, Yen-Chun; Lin, Chen-Yu; Yet, Shaw-Fang (2011): Heme oxygenase-1 in inflammation and cardiovascular disease. In: *American journal of cardiovascular disease* 1 (2), S. 150–158.

Xu, Ming; Tchkonia, Tamar; Kirkland, James L. (2016): Perspective: Targeting the JAK/STAT pathway to fight age-related dysfunction. In: *Pharmacological research* 111, S. 152–154. DOI: 10.1016/j.phrs.2016.05.015.

Xu, Ming; Tchkonia, Tamara; Ding, Husheng; Ogrodnik, Mikolaj; Lubbers, Ellen R.; Pirtskhalava, Tamar et al. (2015): JAK inhibition alleviates the cellular senescence-associated secretory phenotype and frailty in old age. In: *Proceedings of the National Academy of Sciences of the United States of America* 112 (46), E6301-10. DOI: 10.1073/pnas.1515386112.

Yang, Chao-Chun; Chung, Pei-Lun; Lin, Li-Yu; Hughes, Michael W.; Tsai, Yau-Sheng (2017): Higher plasma leptin is associated with higher risk of androgenetic alopecia in men. In: *Experimental dermatology* 26 (6), S. 524–526. DOI: 10.1111/exd.13369.

Yang, Chuen-Mao; Luo, Shue-Fen; Hsieh, Hsi-Lung; Chi, Pei-Ling; Lin, Chih-Chung; Wu, Chi-Chuan; Hsiao, Li-Der (2010): Interleukin-1beta induces ICAM-1 expression enhancing leukocyte adhesion in human rheumatoid arthritis synovial fibroblasts: involvement of ERK, JNK, AP-1, and NF-kappaB. In: *Journal of cellular physiology* 224 (2), S. 516–526. DOI: 10.1002/jcp.22153.

Yang, Gong; Rosen, Daniel G.; Zhang, Zhihong; Bast, Robert C.; Mills, Gordon B.; Colacino, Justin A. et al. (2006a): The chemokine growth-regulated oncogene 1 (Gro-1) links RAS signaling to the senescence of stromal fibroblasts and ovarian tumorigenesis. In: *Proceedings of the National Academy of Sciences of the United States of America* 103 (44), S. 16472–16477. DOI: 10.1073/pnas.0605752103.

Yang, Shao H.; Andres, Douglas A.; Spielmann, H. Peter; Young, Stephen G.; Fong, Loren G. (2008a): Progerin elicits disease phenotypes of progeria in mice whether or not it is farnesylated. In: *The Journal of clinical investigation* 118 (10), S. 3291–3300. DOI: 10.1172/JCI35876.

Yang, Shao H.; Bergo, Martin O.; Toth, Julia I.; Qiao, Xin; Hu, Yan; Sandoval, Salemiz et al. (2005): Blocking protein farnesyltransferase improves nuclear blebbing in mouse fibroblasts with a targeted Hutchinson-Gilford progeria syndrome mutation. In: *Proceedings of the National Academy of Sciences of the United States of America* 102 (29), S. 10291–10296. DOI: 10.1073/pnas.0504641102.

Yang, Shao H.; Meta, Margarita; Qiao, Xin; Frost, David; Bauch, Joy; Coffinier, Catherine et al. (2006b): A farnesyltransferase inhibitor improves disease phenotypes in mice with a Hutchinson-Gilford progeria syndrome mutation. In: *The Journal of clinical investigation* 116 (8), S. 2115–2121. DOI: 10.1172/JCI28968.

Yang, Shao H.; Qiao, Xin; Fong, Loren G.; Young, Stephen G. (2008b): Treatment with a farnesyltransferase inhibitor improves survival in mice with a Hutchinson-Gilford progeria syndrome mutation. In: *Biochimica et biophysica acta* 1781 (1-2), S. 36–39. DOI: 10.1016/j.bbalip.2007.11.003.

Yates, Bethan; Braschi, Bryony; Gray, Kristian A.; Seal, Ruth L.; Tweedie, Susan; Bruford, Elspeth A. (2017): Genenames.org: the HGNC and VGNC resources in 2017. In: *Nucleic acids research* 45 (D1), D619-D625. DOI: 10.1093/nar/gkw1033.

Yavuz, Sevgi; Acartürk, Tahsin Oğuz (2010): Acquired partial lipodystrophy with C3 hypocomplementemia and antiphospholipid and anticardiolipin antibodies. In: *Pediatric dermatology* 27 (5), S. 504–508. DOI: 10.1111/j.1525-1470.2010.01255.x.

Ye, Jian; Coulouris, George; Zaretskaya, Irena; Cutcutache, Ioana; Rozen, Steve; Madden, Thomas L. (2012): Primer-BLAST: a tool to design target-specific primers for polymerase chain reaction. In: *BMC bioinformatics* 13, S. 134. DOI: 10.1186/1471-2105-13-134.

Yu, Mei; Kissling, Sabine; Freyschmidt-Paul, Pia; Hoffmann, Rolf; Shapiro, Jerry; McElwee, Kevin J. (2008): Interleukin-6 cytokine family member oncostatin M is a hair-follicle-expressed factor with hair growth inhibitory properties. In: *Experimental dermatology* 17 (1), S. 12–19. DOI: 10.1111/j.1600-0625.2007.00643.x.

Yu, Q.; Li, Y.; Wang, Y.; Zhao, S.; Yang, P.; Chen, Y. et al. (2012): C-reactive protein levels are associated with the progression of atherosclerotic lesions in rabbits. In: *Histology and histopathology* 27 (4), S. 529–535. DOI: 10.14670/HH-27.529.

Yun, Sook Jung; Kim, Hyung-Sung; Choi, Jee Young; Lee, Jee-Bum; Kim, Seong-Jin; Won, Young Ho; Lee, Seung-Chul (2009): Decreased heme oxygenase-1 expression in the scalp of patients with alopecia areata: the pathogenic role of heme oxygenase-1. In: *Journal of dermatological science* 54 (1), S. 43–45. DOI: 10.1016/j.jdermsci.2008.11.009.

Zaghini, Anna; Sarli, Giuseppe; Barboni, Catia; Sanapo, Mara; Pellegrino, Valeria; Diana, Alessia et al. (2020): Long term breeding of the Lmna G609G progeric mouse: Characterization of homozygous and heterozygous models. In: *Experimental gerontology* 130, S. 110784. DOI: 10.1016/j.exger.2019.110784.

Zecevic, M.; Catling, A. D.; Eblen, S. T.; Renzi, L.; Hittle, J. C.; Yen, T. J. et al. (1998): Active MAP kinase in mitosis: localization at kinetochores and association with the motor protein CENP-E. In: *The Journal of cell biology* 142 (6), S. 1547–1558. DOI: 10.1083/jcb.142.6.1547.

Zhang, Da-yong; Wang, Hai-jie; Tan, Yu-zhen (2011): Wnt/β-catenin signaling induces the aging of mesenchymal stem cells through the DNA damage response and the p53/p21 pathway. In: *PloS one* 6 (6), e21397. DOI: 10.1371/journal.pone.0021397.

Zhang, Xiaoting; Zhao, Ying; Ye, Yanting; Li, Shuifeng; Qi, Shiling; Yang, Yuqing et al. (2015): Lesional infiltration of mast cells, Langerhans cells, T cells and local cytokine profiles in alopecia areata. In: *Archives of dermatological research* 307 (4), S. 319–331. DOI: 10.1007/s00403-015-1539-1.

Zirlik, Andreas; Bavendiek, Udo; Libby, Peter; MacFarlane, Lindsey; Gerdes, Norbert; Jagielska, Joanna et al. (2007): TRAF-1, -2, -3, -5, and -6 are induced in atherosclerotic plaques and differentially mediate proinflammatory functions of CD40L in endothelial cells. In: *Arteriosclerosis, thrombosis, and vascular biology* 27 (5), S. 1101–1107. DOI: 10.1161/ATVBAHA.107.140566.

Zwerina, Jochen; Tzima, Sotiria; Hayer, Silvia; Redlich, Kurt; Hoffmann, Oskar; Hanslik-Schnabel, Beatrice et al. (2005): Heme oxygenase 1 (HO-1) regulates osteoclastogenesis and bone resorption. In: *FASEB journal : official publication of the Federation of American Societies for Experimental Biology* 19 (14), S. 2011–2013. DOI: 10.1096/fj.05-4278fje.

Zwerschke, Werner; Mazurek, Sybille; Stöckl, Petra; Hütter, Eveline; Eigenbrodt, Erich; Jansen-Dürr, Pidder (2003): Metabolic analysis of senescent human fibroblasts reveals a role for AMP in cellular senescence. In: *The Biochemical journal* 376 (Pt 2), S. 403–411. DOI: 10.1042/bj20030816.